USE OF GIS AND RS FOR ASSESSING LAKE SEDIMENTATION PROCESSES

CASE STUDY
FOR NAIVASHA LAKE, KENYA

R.A.P. Rupasingha
March, 2002

USE OF GIS AND RS FOR ASSESSING LAKE SEDIMENTATION PROCESSES
Case study for Naivasha Lake, Kenya

By

R.A.P. RUPASINGHA

Thesis submitted to the International Institute for Geo-information Science and Earth Observation in partial fulfilment of the requirements for the degree of Master of Science in Water Resources and Environmental Management

Degree Assessment Board

Chairman:	Prof. A.M.J. Meijerink (Head WRES, ITC)
External Examiner:	Dr. Ir. E.O. Seyhan (Free University, Amsterdam)
Primary Supervisor:	Dr. Ir. Chris Mannaerts (WRES, ITC)
Member:	Dr. Zoltan Vekerdy (WRES, ITC)

INTERNATIONAL INSTITUTE FOR GEO-INFORMATION SCIENCE AND EARTH OBSERVATION
ENSCHEDE, THE NETHERLANDS

Disclaimer

This document describes work undertaken as part of a programme of study at the International Institute of Geo-information Science and Earth Observation. All views and opinions expressed therein remain sole responsibility of the author, and do not necessarily represent those of the institute.

ACKNOWLEDGEMENT

First and foremost I express my grateful thanks to the Panel of Lecturers, International Institute of Aerospace Survey and Earth Sciences, Enschede, The Netherlands for creating this opportunity, which enabled me to participate in this course on the Masters of Science Degree in Water Resources and Environmental Management. Also I wish to pay my gratitude to the Netherlands Fellowship Program (NFP) and the Mahaweli Authority of Sri Lanka for providing financial assistance to cover the course fee for the M.Sc course.

My special grateful thanks are also extended to my Supervisor, Dr. Ir. Chris Mannaerts who was gracious enough to spend his valuable time and ably imparted his knowledge in a professional manner. Also thanks goes to Prof. A.M.J. Meijerink (Head WRES, ITC), for his valuable guidance throughout the course. I extended my special thanks to Drs. Robert Becht and Eng. Remco Dost for giving their wholehearted support and for assisting during fieldwork, to carry out this investigation successfully. Also I should pay my gratitude to Dr. Zoltan Vekerdy (WRES, ITC) and my external examiner, Dr. Ir. E.O. Seyhan (Free University, Amsterdam) for spending their valuable time to read my thesis.

I should not forget to thank to Ms. Barbara Casentini for her support during the laboratory work. I wish to express my gratitude to the WRAP teams both in Nakuru and Nairobi, Kenya Ministry of Water Resources and Development, Sulmac, LNRA, KWS, SHELL Company and La Belle Inn for their support in providing necessary assistance during field work in Kenya.

Finally I extend my profound thanks to all my colleagues and those who had a hand either directly or indirectly for the successful completion of this project, which I consider as an experience of a lifetime.

ABSTRACT

The objective of this research is to explore the use of GIS and RS techniques for determination of the sedimentation rate of lake Naivasha. Fieldwork consisted of geo-referenced sonar bathymetric depth, turbidity and suspended sediment surveys of the lake, sediment core sampling, flow and suspended sediment analysis of river inflows. Comparisons of survey results with historic data permitted to determine the sediment accumulation and spatial distribution in the lake. Furthermore, an exploratory modelling analysis was done to correlate incoming sediment fluxes of the main rivers with the lake sedimentation.

Malewa River supplies long-term suspended sediment concentration of 0.23 kg/m^3 and 0.26 kg/m^3 from 1932-1990 and 1957-1990 respectively. Measured concentrations during the 2001 fieldwork, shows that the average suspended sediment concentration along the Malewa River is about 0.21 kg/m^3 . Long-term estimated annual average suspended sediment load of Malewa is about $42.8x10^3$ tons and 55.9 $x10^3$ tons for the periods from 1932-1990 and 1957-1990 respectively. Based on latter figure, total estimated suspended sediment load to the lake through Malewa, from 1957 to 2001 is about 2.5 $x10^6$ tons.

According to our analysis, the sediment input in lake Naivasha in the period 1957 – 2001 was 19.0 million m^3 of sediment, which, if spread evenly over the depositional area of lake bottom (89.23 km^2 at 1884 m level m.a.s.l.) would give an average thickness of 0.21 m. The total mass of sediment accumulated in the lake was estimated at $7.07x10^6$ tons for the 44 year period from 1957-2001. Out of this, 5.75 $x10^6$ tons was determined as inorganic mineral matter and 1.32 $x10^6$ tons of organic matter. A comparison of the lake sedimentation with suspended sediment fluxes of Malewa and Gilgil rivers reveals that the Malewa river wash load contributes to 35% of the lake sedimentation. This implies that 65% of the sediment mass is transported either as bed load, a fraction also by the much smaller Gilgil river, or by another active sediment source.

Considering the whole drainage basin of lake Naivasha, the estimated long-term watershed sediment yield is about 39.5 metric $tons/km^2/year$ and 48.0 $tons/km^2/year$ from 1957 to 2001 for respectively inorganic mineral and total sediment. Assuming that the active contribution for lake sedimentation is only from the hydraulically connected sub basins, i.e. Malewa and Gilgil river systems, the long-term average annual watershed sediment yield (of these watersheds) will draw around 74 $tons/km^2/year$. Between 1957 and 2001, this accounted for a 7 % reduction of the lake volume capacity (using the 1957 bathymetry and 1985 m.a.s.l. as lake reference level). For this 44-year period, the annual volume depreciation rate is about 0.0016% only. Assuming this constant depreciation rate, Naivasha lake will be reduced to its half capacity only after in 400 years. Of course, lake volume changes due to certain biogenetic (peat formation, etc.) and other processes must be also considered.

TABLE OF CONTENTS

LIST OF FIGURES

LIST OF TABLES

LIST OF APPENDICES

CHAPTER 1 – GENERAL INTRODUCTION

1.1 INTRODUCTION

1.1.1 Background and Problem Formulation

The rapid growth of population in many countries together with a generally increasing standard of living is increasing demands on surface water for irrigation, industry and urban water supply and is decreasing the quality of surface water. Lakes and rivers are an integral part of our urban environment providing transportation, drinking water, food, and recreation. Human impacts on these systems are profound, techniques of Remote Sensing and GIS can provide a means to monitor and assess these impacts.

Alluvial rivers and lakes/reservoirs frequently adjust their geometry and conveyance patterns through natural processes of sediment transport. If left uncontrolled, however, excessive scour of a streambed will induce major shifts in boundary geometry and can threaten stability of in-stream structures, such as bridges or underground utilities. Likewise, continued deposition of bed sediment will cause reduced storage capacities in stream channels and in conservation and flood control reservoirs and lakes. This decline in storage eventually eliminates the intended capacity for flow regulation and water supply, and reduces the irrigation, hydroelectric power generation, navigation and recreation benefits that are dependent on reservoir storage (Julien, 1995).

Concentrated accumulation of sediment can also reduce water quality when the transported materials have previously been exposed to and become attached to contaminants, such as those found in some agricultural lands. Reservoir sediment quality is an important environmental concern because sediment may act as both a sink and a source of water-quality constituents to the overlying water column and to biota. Once in the food chain, sediment-derived constituents may pose an even greater concern due to bioaccumulation (Keith et al., 1973).

Reservoir sediment studies have been useful in reconstructing historical trends in water quality that can be used as a measure of the effectiveness of best management practices implemented throughout the watershed. With the addition of bathymetric surveys and the inclusion of additional reservoir sediment studies also can be used to establish baselines for estimating historical loading of phosphorous and other constituents in future water quality assessments (David et al., 2001). Such sediment-derived information may be used to assist in calculating mass loadings, to determine if water quality in a basin is changing, to provide a warning of potential future water-quality problems, and to provide a baseline against which to measure the effectiveness of implemented best-management practices in a basin.

Subsequently, the methodology must attempt to overcome historical gaps between theoretical developments in optimization and practical reservoir management by incorporating GIS and RS techniques. This research proposal focuses on the assessment of lake sedimentation processes and application of GIS and RS techniques for lake/reservoir management that will provide a means for sustaining the benefits that regional water resources are capable of providing.

1.1.2 Relevance of Research

Many studies have been conducted on lake Naivasha bathymetry and the water balance studies in the lake. For example Mmbui(1998) established the lake water balance model using the earlier calculated stage-volume relationships. Ase et al., (1986) studied about the lake bathymetry and discussed the morphology of the lake as well as delta forming. But, even though in early 50's sediment loads measurements were carried out in the lake, only few studies concentrated on lake sedimentation process and sediment influx to the lake. Therefore, exploration of the use of GIS and RS techniques for assessing lake sedimentation processes will be useful for future development in this field.

1.1.3 Research Objectives

The objective of this research is to explore the use of GIS and RS techniques for determination of the sedimentation rate of lake Naivasha. Following major tasks to fulfil the objective were carried out as given below.

(a) GPS- controlled sonar bathymetric depth survey of lake Naivasha;
(b) Geo-statistical data analysis and use of different interpolation techniques to create bathymetric map;
(c) Compare with historic data in order to assess the changes in the lakebed topography due to sedimentation;
(d) Estimate the Lake Sedimentation Rate and the Sediment Yield of the catchment;
(e) Exploratory analysis of incoming river sediment fluxes to the lake to correlate with the lake sedimentation rate;
(f) Assess the possibility of use the remote sensing images for the prediction of lake depth, water quality parameters and suspended sediment concentrations.

1.1.4 Research Questions

The following questions will be answered;

- Are there any significant changes of lake bathymetric depth between 2001 and 1957?
- Is the Lake sedimentation rate significant?
- Do main river incoming sediment fluxes correlate with the lake sedimentation rate?
- Is remote sensing applicable to assess physical water quality parameters (Turbidity and suspended sediment etc.,) and what are the constraints?

1.1.5 Thesis Structure and Organization

The Thesis is comprised of seven chapters**;** Chapter (1) is the general introduction of the subject. Background theory including literature review is presented in Chapter 2.

Study area, Materials and Methods are explained in Chapter 3, including methodology followed for onsite lake measurements and sampling of input rivers. Field data collection and analysis are developed in Chapter 4, which mainly focussed on the lake bathymetric, on the onsite lake measurements and on the sampling of sediment inputs from the rivers.

Chapter 5 mainly concentrates on the explanatory analysis of river sediment fluxes and the lake sedimentation. Chapter 6 is addressed on the possibility of use of Remote Sensing techniques to assess lake sedimentation process as well as water quality parameters; finally Chapter 7 frames the conclusions.

CHAPTER 2 : BACKGROUND THEORY

2.1 LAKE SEDIMENTATION PROCESSES

The processes of erosion, entrainment, transportation and deposition of sediment are complex (Julien, 1992). Methods have not yet been developed to extrapolate existing results of fundamental research to broad, complex areas such as watersheds for prediction of the expected rate or processes of reservoir sedimentation. Although considerable basic data have been assembled and comprehensive research has been initiated in the past quarter century, much yet remains to be done before the prediction of rates and processes of reservoir sedimentation to achieve the degree of accuracy desired (Chow, 1964).

Despite extensive research effort, knowledge of erosion and sediment transport still remains incomplete, and there is no generally accepted formula to be used for an accurate solution of the sediment transport rate and watershed sediment yield. However, significant progress has been made in recent decades and approximate solutions can be obtained (Maidment, 1992).

2.2 FACTORS INFLUNCING LAKE SEDIMENTATION PROCESSES

2.2.1 Trap Efficiency of Lakes/Reservoirs

The ability of a reservoir/lake to trap and retain sediment is known as the trap efficiency, and is expressed as the percent of sediment yield (incoming sediment), which is retained in the basin (Julien, 1995). Factors influencing trap efficiency are the sediment characteristics, detention-storage time and the Nature of outlets. Sediment deposition in reservoirs varies greatly with the grain-sized distribution of particles. As stream flow enters a lake/reservoir, the cross sectional area of flow normally is increased, resulting in a reduction of velocity and a corresponding decrease in sediment transport capacity. The percent of total incoming sediment that are transported out of a reservoir/lake depends primarily upon the fall velocity of particles and upon the rate at which the particles are transported through the reservoir.

2.2.2 Distribution of Sediment in Lakes/Reservoirs

The distribution of sediment in a reservoir is dependent upon several interrelated factors, including nature of sediment, inflow-outflow relations, shape of reservoir, and reservoir operation. Contrary to general belief, sediment deposition is not always concentrated in the lower increments of storage in the reservoir basin (Chow, 1964).

2.2.3 Sediment Characteristics

Knowledge of the sediment characteristics, primarily the grain size distribution and the volume weight relationship, is necessary to have better understanding of the lake sedimentation process. The grain-size distribution is important in:

- Assigning a trap efficiency value to the lake
- Predicting the horizontal and vertical distribution of sediment in the lake/reservoir

- Predicting the ultimate volume-weight relationship for determining the space occupied by sediment deposited in the reservoir.

The bulk characteristics of sediments, which are of particular concern in reservoir sedimentation problems, are the grain size distribution and the specific weight of deposited sediment. All size classes of sediment occupy reservoir space upon deposition and therefore are of concern. However, some classes, particularly clay and silt size particles, do not always achieve maximum consolidation immediately upon deposition and consequently may not reach their ultimate specific weight for many years to come. Also, the gradation of particles influences the distribution of sediment in reservoirs.

2.2.3.1 Specific Weight of Sediment

The term specific weight is used to denote the dry weight of sediment particles (solids) of a total, in-place volume of sediment mass. The specific weight of sediment must be predicted in order to estimate the storage, which will be displaced by sediment in a given period of time. The volume of voids, known as the porosity, varies, depending upon the size distribution of particles and their arrangement in respect to each other.

As the volume of solids is difficult to measure and the voids ratio difficult to predict in fine-grained sediments common practice, therefore, is to obtain field measurements and relate them to time and depth deposits. The specific weight of a sediment deposit can be readily obtained by an undisturbed sample of known volume, drying it under controlled conditions in the laboratory and determining its dry weight.

Lane and Koelzer as reported by Julian 1995 have presented the following general equation, based on time and the grain-size constituents of sediment, for estimating the unit weight of sediment. The relationships apply to the unit weight of the first year's deposit after T years.

$$W = W_1 + K * \log T \quad \text{----------Equation 2.1}$$

Where, W = Unit weight or density of sediment after T years of compaction
W_1= Initial unit weight considered at the end of 1 year
K = Constant

Table 2.1: Lists of the various values of W_1 and K for different types of materials and different conditions of reservoir operation (Chow, 1964)

Reservoir/Lake Operation	Sand		Silt		Clay	
	W_1	K	W_1	K	W_1	K
Reservoir always submerged or nearly submerged	93	0	65	5.7	30	16.0
Normally a moderate reservoir draw down	93	0	74	2.7	46	10.7
Normally considerable reservoir draw down	93	0	79	1.0	60	6.0
Reservoir normally empty	93	0	82	0.0	78	0.0

After Lane and Koelzer, Miller (Chow, 1964) further refined the data of Lane and Koelzer to determine average unit weight of deposits for a given period of time. The condensed equations were developed by him is given below.

Table 2.2: Equations for converting Lane's and Koelzer's Unit Weight W_1 to Average Weight for Different Periods of Time

Equations for different years
$W_{10} = W_1 + 0.675*K$
$W_{20} = W_1 + 0.938*K$
$W_{30} = W_1 + 1.093*K$
$W_{40} = W_1 + 1.210*K$
$W_{50} = W_1 + 1.298*K$
$W_{60} = W_1 + 1.372*K$
$W_{70} = W_1 + 1.438*K$
$W_{80} = W_1 + 1.493*K$
$W_{90} = W_1 + 1.542*K$
$W_{100} = W_1 + 1.588*K$

Table 2.3: Shows the relationship of Specific Weight to grain-size distribution and reservoir operation used by the U.S. Soil Conservation Service, for general design purpose Reservoirs (Chow, 1964)

Grain Size	Permanently Submerged (lb/ft^3)	Aerated (lb/ft^3)
Clay	40-60	60-80
Silt	55-75	75-85
Clay-silt mixtures (equal parts)	40-65	65-85
Sand-silt mixtures	75-95	95-110
Sand-silt-sand mixtures (equal Parts)	50-80	80-100
Sand	85-100	85-100
Gravel	85-125	85-125
Poorly sorted sand and gravel	95-130	95-130

According to Maidment (1992),

The total weight of sediment accumulation can be calculated by the following equation,

$$W_0 = p_c W_c + p_m W_m + p_s W_s \quad \text{……..Equation 2.2}$$

Where, W_0, W_c, W_m and W_s are the densities for total, clay, silt and sand respectively in kilograms per cubic meter and p_c, p_m and p_s are the percentages of the total sediment composition for clay, silt and sand respectively.

The average density of sediment accumulation after T_1 years of operation W_{T_1} is given by,

$$W_{T_1} = W_0 + 0.4343 K_0 [\frac{T_1}{T_1 - 1}(\ln T_1) - 1] \quad \text{…….Equation 2.3}$$

W_0 is the initial specific weight and K_0 is factors given in different modes of reservoir operation are given in Table 2.4.

Table 2.4: The Initial Specific Weight of Sediment Deposits and Constant K_0 based on the types of Reservoir Operation and Sediment Size

Mode of Reservoir Operation	Initial Density, Kg/m3	*K_0 (for metric units)*

	Wc	*Wc*	*Wm*	*Sand*	*Silt*	*Clay*
Sediment always submerged or nearly submerged	416	416	1120	0	91	256
Moderate to considerable reservoir draw down occurs often	561	561	1140	0	29	135
Reservoir normally empty	641	641	1150	0	0	0

2.3 METHODS TO ASSESS RESERVOIR SEDIMENTATION PROCESSES

The following methods can be used for assessing lake sedimentation processes and estimating sediment yield in a particular watershed.

2.3.1 Reservoir Sedimentation Surveys

The volume of sediment accumulated in a reservoir is computed as the difference between the present water capacity of the reservoir and a known water capacity at some prior date (Chow, 1964).

$$\text{Mean Annual Sediment Yield} = \frac{\text{Total Accumulated Sediment Volume}}{\text{Watershed Drainage Area} \times \text{Time Period}}$$

The total volume of sediment is converted to dry weight of sediment on the basis of the average specific weight of deposits (Chow, 1964).

$$\text{Dry Weight} = \text{Total Volume} \times \text{Average Specific Weight of Deposits}$$

The total weight of sediment accumulation in the reservoir plus that which is estimated to have passed through and out of the reservoir, based on the estimated trap efficiency provides the total estimated sediment yield for the period of record covered by the survey.

$$\text{Total Estimated Sediment Yield} = (\text{Volume of sediment accumulated} + \text{Amount of sediment passed through the reservoir})$$

2.3.2 Estimation of Sediment Fluxes through main rivers

Sediment yields can be determined by periodic sampling of the stream flow to measure sediment concentration for various water discharges. Average sediment concentration for various discharges is then related to expected frequencies of the various discharges to estimate long-term suspended sediment. Difficulty of measuring bed load is call for use of empirical formulas (Julien, 1995).

The time variability of sediment concentration measurements in natural channels depends on many factors such as the location of the measurement, the magnitude of the flood, the source of water and sediments and the seasonal watershed conditions prior to the flood. In general, the sediment concentration increases with discharge, although the sediment concentration at a given discharge may vary depending on the season, the source of sediment, and whether the discharge increasing or decreasing. The sediment concentration is given by the sediment flux at a given point multiplied by the point velocity. Since the flow velocity is maximum at the surface while the sediment concentration

is maximum near the bed, the sediment flux must be integrated over the entire cross sectional area to obtain the total sediment discharge passing through a given cross section.

Therefore, the underlying problem in load estimation involves evaluating an integral. The amount (or load) of a constituent (e.g. sediment or nutrients) transported through a river cross-section during a time interval $\{t_a, t_b\}$ is given by:

$$L = \int_{t_a}^{t_b} L(t).dt \quad \text{.....Equation 2.4}$$

$$L = \int_{t_a}^{t_b} K.Q(t).C(t)dt \quad \text{.....Equation 2.5}$$

Where,

L is the integrated load during $\{t_a, t_b\}$

L(t) is the instantaneous load at time t

K is a units conversion factor

Q(t) is stream flow at time t, (which can be accurately known)

C(t) is the average concentration of the constituent in the cross-section at time t

A Direct application of equation 2.4 is usually impossible because C(t), the continuous time trace of concentration, is known only at those times when concentration is measured.

The flux-averaged concentration C is the ratio between the total sediment discharge and the total water discharge. On a daily basis, the sediment load is the amount of sediment passing a stream cross-section and is given by,

$$Q_s = Q * C_s * k \quad \text{.....Equation 2.6}$$

Where,

Q_s = Sediment Discharge in metric tons/day

C_s = Concentration of suspended sediment in mg/l

Q = Discharge in m^3/sec

k = 0.0864, k incorporates a sediment specific gravity of 2.65

An alternative to estimating a continuous concentration curve is to evaluate the integral as given in the equation 2.4 direct loads can be estimated by observing the instantaneous loads: If load is measured at regular time interval, or at random, the same weight might be applied to each instantaneous load. However, more precise load estimates can usually be obtained by selectively sampling at those times when uncertainty about the instantaneous load is greatest.

2.3.3 Suspended Sediment Load Estimation

2.3.3.1 Suspended Sediment Rating Curves

Campbell and Bauder (1940,as in website: http://earth.agu.org) observed that the relation between the logarithm of sediment concentration and the logarithm of discharge was approximately linear. They suggested that this relation could be used as a rating curve. For periods when no sediment data had been collected, sediment concentrations could be estimated from water discharge.

Although the rating curve remains an empirical result without physical justification, it has come into widespread use. The rating curve is simple and by including additional regressor variables, can be easily modified to account for variability associated with non-linear flow dependence and time trends. One can stratify data (e.g. by season, discharge or other variable) or use multiple rating curves to describe more complicated concentration/discharge relations (Colby, 1955 as in website: http://earth.agu.org).
By making some assumptions about sediment transport functions, the rating curve can be converted into an intrinsically linear model [Draper and Smith, 1981 as in the same site.

$$\ln C(t) = \beta_0 + \beta_1 . \ln Q(t) + c \quad \text{.....Equation 2.7}$$

Where,

ln is the natural logarithm function

β_0 & β_1 are model coefficients

c is residual error

The regression residuals are commonly assumed independent and identically distributed normal random variables, with a mean of zero and variance is squared of the standard deviation. With coefficients β_0 and β_1 estimated by linear regression, a continuous trace of concentrations can be estimated from:

$$\overline{C_{rc}}(t) = \exp[\overline{\beta_0} + \overline{\beta_1} \ln Q(t)] \quad \text{.....Equation 2.8}$$

Where,

$\overline{\beta_0}$ and $\overline{\beta_1}$ are ordinary least squares regression coefficients.

The rating-curve's shortcomings, some of which are discussed below, are also well documented by many researches. Because this model provides a convenient statistical framework, much recent work has been devoted to correcting its deficiencies and expanding its applicability.

2.3.3.2 Retransformation Methods in Regression Models

The rating curve estimator of equation 2.8 is not statistically consistent [Lane, 1975; Delong, 1982; Thomas, 1985; Ferguson, 1986; Koch and Smillie, 1986; Cohn et al., 1989 as reported in the http/earth/agu.org]. Its results are biased, in general systematically underestimating loads. In studies with field data (Walling et al., 1981; Fenn et al., 1985 as in the http/earth/agu.org), this bias sometimes exceeded 50%. According to Thomas, (1985), Ferguson (1986) and Koch and Smillie (1986) the bias arises when model results computed using the logarithm of C are retransformed into real units. Three methods for correcting the bias are now commonly employed.
In this thesis following three methods of bias correction is applied for the data estimated from the sediment-rating curve according to the literature.

(a) The Quasi-Maximum Likelihood Estimator (QMLE),
(b) The Minimum Variance Unbiased Estimator (MVUE), and

(c) The Smearing Estimator (SM).

Two of these methods are recommended by Cohn and Gilroy (1991): the Minimum Variance Unbiased Estimator (MVUE) to use when the distribution of errors is assumed to be normal, and the Smearing Estimator (SM) for situations in which non-normal error distribution is identified. Although the focus here is on an appropriate bias correction factor, it is well worth emphasizing that miss-specification of the appropriate regression model in a particular situation can yield sizable errors and render any care taken in correcting for bias as a useless exercise.

(1) The Quasi-Maximum Likelihood Estimator (QMLE)

Having recognized the bias of the rating curve method, Ferguson (1986) recommends:

$$\hat{L}_{QMLE} = L_{RC} \exp(\frac{s^2}{2}) \quad \text{.....Equation 2.9}$$

Where:

$\hat{L}_{QMLE}$ = Estimated sediment discharge (load) using the quasi-maximum likelihood estimator (QMLE)

L_{RC} = Sediment load estimated from the rating curve

s^2 = Mean square error of the regression residuals

(2) The Smearing Estimator (Duan, 1983)

The Smearing estimator is a non-parametric method, which is based on the equation:

$$\hat{L}_S = \hat{L}_{RC} \frac{\sum_{i=1}^{n} \exp(e_i)}{n} \quad \text{.....Equation 2.10}$$

Where:

$\hat{L}_S$ = Estimated sediment discharge (load) using the smearing estimator

e_i = Residuals from least squares regression. They are the differences between the natural logarithm of measured and computed sediment discharge.

$\hat{L}_{RC}$ = Instantaneous Sediment discharge or load estimated

(3) The Minimum Variance Unbiased Estimator (MVUE) also called the Bradu-Mundlak Estimator

To apply this method, the bias correction is applied to each daily discharge (Q*) for the estimated period using the following expression:

$$\hat{L}_{MVUE} = L_{RC(t)} g_m \quad \text{.....Equation 2.11}$$

and,

$$g_m = [\frac{m+1}{2m}\{(1-V)s^2\}] \quad \text{.....Equation 2.12}$$

Where:

$\hat{L}_{MVUE}$ = Estimated sediment discharge (load) for the day using the minimum variance unbiased estimator

$L_{RC(t)}$ = Sediment load estimated from the transport (rating) curve for each day (t)

g_m = A function introduced by Finney (1951) and used by Bradu and Mundlak (1970).

m = degrees of freedom of the regression equation

V = an estimate of the variability at a given value of stream flow discharge and computed by the following equation

$$V = \frac{1}{N} + [\frac{(\ln(Q^*) - \overline{\ln(Q)})^2}{\sum_{i=1}^{N} \{(\ln(Q_i) - \overline{\ln(Q)})\}^2}] \quad \text{.....Equation 2.13}$$

$$V = \frac{1}{N} + [\frac{(\ln(Q^*) - QBAR)^2}{QVAR}] \quad \text{.....Equation 2.14}$$

Where:

Q* = daily mean stream flow for the day loads are being predicted

Q = instantaneous stream flow used in the regression

N = number of data points in the regression

2.3.4 Estimation of Bed load

Transport as bed-load as the mode of transport of sediments where the solid particles glide, roll or (briefly) jump, but stay very close to the bed, which they may leave only temporarily. The displacement of the particles is intermittent; the random concept of the turbulence plays an important role (Graf, 2001).

There exist a number of formulae, which can be used for the prediction of the bed-load transport. Many of these formulae are of empirical nature, but often have incorporated dimensionless numbers. This allows to make experiments in the laboratory, where the hydraulic conditions can be well controlled: subsequently it is possible to use such formulae for field conditions.

Theoretical Considerations will be that the bed of a channel is plane but mobile, composed of solid particles of uniform size and being non-cohesive. These particles displace themselves under the action of flow, which be uniform and steady. The sediment transport calculations made for the representative grain diameter, using three different total-load relations, namely: (1) Einstein, (2) Graf and Acaroglu and also (3) Ackers et White as described by the Graf (2001).

2.3.4.1 Einstein's Formula (1950)

The formula of Einstein (1950), which allows the calculation of the total load transported by the flow, is given by:

$$q_s = q_{sb} + q_{ss} \quad \text{.....Equation 2.15}$$

$$q_s = q_{sb}[1 + 2.303\log(30.2h/\Delta)\int_1 + \int_2] \quad \text{.....Equation 2.16}$$

Where,

q_s = Solid discharge as total load by volume
q_{sb} = Solid discharge, as bed load, by volume and by unit width
q_{ss} = Solid discharge as suspended load by volume and by unit width
h = Flow depth
Δ = Apparent roughness diameter (Figure 6.7a, Page 378, Graf, 2001)

The integrals, $\int_1$ and $\int_2$, which appear in the suspended-load formula, need to be determined to calculate the solid discharge q_{ss}, transported as suspended load Figure 6.12, Page 391, Graf, 2001). Assuming the grain size distribution is quasi uniform, the calculations are done using an equivalent grain diameter (d_{35}).

The intensity of transport is:

$$\Phi_* = \Phi = \frac{q_{sb}}{\sqrt{(s_s - 1) g d_{35}^3}} \quad \text{.....Equation 2.17}$$

Where;

S_f =Bed slope; s_s =Specific density of sediment particles

$q_{sb} = g_{sb} / \gamma_s$ is the volumic solid discharge for a unit width and g_{sb} the soild discharge by weight; both transported as bed load.

The intensity of shear (parameter of Einstein-Barbarossa, Figure 3.6, Page 86, Graf, 2001) is:

$$\psi_* = \psi' = (s_s - 1) \frac{d_{35}}{R_h' S_f} \quad \text{.....Equation 2.18}$$

Where, R_h' is the hydraulic radius of the bed due to the granulates with the functional relationship of:

$$\Phi_* = f(\psi_*) \quad \text{.....Equation 2.19}$$

Where,

Φ_* is the Intensity of transport. Detailed calculations were done on spreadsheet. Detailed explanations on the contents of the columns are given along with the calculations.

2.3.4.2 Formula of Graf et Acaroglu (1968)

The formula for Graf et Acaroglu (1968), which allows the calculation of the total load transported by the flow, is given by:

$$\Phi_A = f(\Psi_A) \quad \text{.....Equation 2.20}$$

with the parameter of transport:

$$\Phi_A = \frac{C_s U R_h}{\sqrt{(s_s - 1) g d_{50}^3}} \quad \text{.....Equation 2.21}$$

and the parameter of shear stress intensity,

$$\Psi_A = \frac{(s_s - 1)d_{50}}{S_e R_h}$$

Where, U = Average velocity; s_s =Specific density of sediment particles; R_h is the total hydraulic radius and $C_s = q_s/q$ is the average concentration by volume. The equivalent diameter is taken as d_{50}

2.3.4.3 Formula of Ackers et White (1973)

The formula of Ackers et White (1973), which allows the calculation of average concentration, C_s, by volume is given by:

$$C_s = G_{gr}\frac{d_{35}}{h_m}\left(\frac{U}{u_*}\right)^{n_w} \quad \text{.....Equation 2.22}$$

Where the equivalent diameter is taken as d = d_{35}

The sediment-transport parameter is calculated as:

$$G_{gr} = C_w\left(\frac{F_{gr}}{A_w} - 1\right)^{n_{W_w}} \quad \text{.....Equation 2.23}$$

With the mobility parameter defined as:

$$F_{gr} = \frac{u_*^{n_w}}{\sqrt{(s_s - 1)g d_{35}}}\left[\frac{U}{\sqrt{32}\log(10h_m/d_{35})}\right]^{(1-n_W)} \quad \text{.....Equation 2.24}$$

Where,

$$d_* = (g(s_s - 1)/v^2)^{1/3} d_{35} \qquad n_w = 1 - 0.56\log d_* \qquad m_w = 9.66/d_* + 1.34$$

$$A_w = \frac{0.23}{\sqrt{d_*}} + 0.14 \qquad C_w = 10^{(2.86\log d_* - (\log d_*)^2 - 3.53)}$$

Where; ρ_s =density of sediment particle; ν = Viscosity of water

U = Average velocity of the section; u_* =Total shear velocity; s_s= Specific Gravity of the sediment

2.4 GEOSTATISTICAL DATA ANALYSIS

It is difficult and expensive to collect field observations; one must make the best use of available data to estimate the needed parameters. In point estimation one uses measurements of a variable at certain points to estimate the value of the same variable at another point. The analysis of data typically starts by plotting the data and calculating statistics that they describe important characteristics of the sample.

2.4.1 PROCESSING AND ANALYSIS OF GEO STATISTICAL DATA SET

Geo-statistics studies spatial variability of regionalized variables: Variables that have an attribute value and a location in a two or three-dimensional space. However, process understanding is itself

incomplete and cannot produce a unique or precise answer. Statistical estimation methods complement process understanding and can bring one closer to an answer that is useful in making rational decisions. There main contribution is that they suggest how to weigh the data to compute best estimates and error bounds on these estimates. Statistics has been aptly described as a guide to the unknown; it is an approach for utilizing observations to make inferences about an unmeasured quantity. Tools to characterize the spatial variability are the spatial autocorrelation function and the variogram (Kitanidis, 1997).

The variogram is calculated from the variance of pairs of points at different separation. For several distance classes or lags, all point pairs are identified which matches that separation and the variance is calculated. Repeating this process for various distance classes yields a variogram. Similarly, the spatial autocorrelation can be calculated and plotted in an autocorrelogram. These functions can be used to measure spatial variability of point data. The experimental variogram is an important tool that provides information about the distribution of spatial variability with respect to scales.

2.4.1.1 Interpolation Techniques

(a) Kriging

Kriging is a method for optimising the estimation of a quantity, which is distributed in space or time and is measured at a network of points. Let $x_1, x_2, \ldots x_n$ be the locations of n measurement points and let $Z_1=Z(x_i)$ be the value measured at the point i. The problem of the point estimation lies in determining the value of the quantity Z_0 at any point X_0, which has not been measured. By continuously modifying the position of point X_0 it is thus possible to determine the entire field of the parameter Z. However, kriging is not limited to simple point estimation of the given variable Z but can also be used to obtain the estimation variance of the variable Z, ie. roughly, the confidence interval of the estimation.

Kriging involves applying the general methodology known as best linear unbiased estimation (BLUE) to intrinsic functions. Given n measurements of Z at locations with spatial coordinates $x_1, x_2, \ldots x_n$, estimate the value of Z at point x_0. An estimator is simply a procedure or formula that uses data to find a representative value, or estimate, of the unknown quantity.

$$\hat{Z}(x_0) = \sum_{i=1}^{n} \lambda_i Z(x_i) \quad \text{.....Equation 2.25}$$

Where,

Where $z(x_i)$ is the observed value of the variable at the sample point x_i, and $\lambda_1, \lambda_2 \ldots\ldots, \lambda_n$ is the weight attached to the value at sample point *i*. To ensure the estimate is unbiased, the weights are made to sum to 1.

$$\sum_{i=1}^{n} \lambda_i = 1 \quad \text{.....Equation 2.26}$$

And the difference between the estimate $\hat{Z}_0$ and the actual value $Z(x_0)$ is the estimation error.

$$\hat{Z}(x_0) - Z(x_0) = \sum_{i=1}^{n} \lambda_i z(x_i) - z(x_0) \quad \text{.....Equation 2.27}$$

The estimation variance is;

$$\text{var}[\hat{Z}(x_0)] = E[\{\hat{Z}(x_0) - Z(x_0)\}^2] = 2\sum_{i=1}^{n}\lambda_i\gamma(x_i, x_0) - \sum_{i=1}^{n}\sum_{i=1}^{n}\lambda_i\lambda_j(x_i, x_j) \quad \text{.....Equation 2.28}$$

Where $\gamma(x_i, x_j)$ is the semi variance of Z between the data points x_i and x_j and $\gamma(x_i, x_0)$ is the semi variance between the *i*th data point and the target point x_0. For each kriged estimate there is an associated kriging variance. Thus, the problem is to find the set of weights $(\lambda_1, \lambda_2 ....., \lambda_n)$ that minimize this variance, subject to the condition that they sum to one. This condition can be obtained by associating the Lagrange parameter with the minimization and by solving the set of equations using the matrix solutions.

For kriging, it is necessary to specify the variogram. When the variogram is specified we give the sill, Range and Nugget with the anisotropy information as the variogram is a three dimensional function with two independent variables (direction and separation distance h) and one dependant variable.

(b) Trend Surface Fitting

In trend surface fitting, the assumption is that the entire geographic field can be represented by a formula f(x,y) that for given location with coordinates (x,y) will give us the approximated value of the field in that location.

The key quest in trend surface fitting thus is to find out what is the formula that best describes the field. The field may be of the first order upto the sixth order. Various classes of formulae exist, with the simplest being the one that describes a flat, but tilted plane. Mathematical techniques of regression analysis will determine the best-fit plane with the measurements. In essence, a plane will be fitted through the measurements that make the smallest overall error with respect to the original measurements (ILWIS Manuel).

(c) Interpolation through Triangulation

This technique constructs a triangulation of the study area from the known measurement points. Preferably, the triangulation should be a delaunay triangulation. For each edge of a triangle, a geometric computation can be performed that indicates which isolines intersect it, and at what positions they do.

(d) Moving Average Method

In this method, assigns to pixels weighted averaged point values. The weight factors for the points are calculated by a user-specified weight function. Weights may for instance approximately equal the inverse distance to an output pixel. The weight function ensures that points close to an output pixel obtain larger weights than points, which are farther away. Furthermore, the weight functions are implemented in such a way that points which are farther away from an output pixel than a user-defined limiting distance to obtain weight zero (ILWIS Manuel).

(e) Inverse Distance Method

If one feels that measurements further away from the cell should have less impact than those nearby, a distance factor must be brought into averaging function. Functions that do this are called inverse

distance weighing functions. Let us assume that the distance from measurement point i to the cell centre is denoted by d_i. Commonly, the weight factor applied in inverse distance weighting is the distance squared, and then the averaging formula becomes,

$$\sum_{i=1}^{n} \frac{m_i}{d_i^2} \Big/ \sum_{i=1}^{n} \frac{1}{d_i^2} \quad \text{.....Equation 2.29}$$

In many cases in practice, one will have to experiment with parameter settings to obtain optimal results.

(f) Nearest Neighbour Method

This method is also called nearest point or Thiessen. It assigns to pixels the value of the nearest point according to Euclidean distance.

CHAPTER 3 - STUDY AREA, MATERIALS AND METHODS

3.1 LITERATURE REVIEW ON STUDY AREA & EXISTING DATA

3.1.1 Background Information about Study Area

The central Rift Valley of Kenya is an area of moderate altitude that resulted formation of the rift. The area forms a catchment for the drainage from two extensive forests which stand on both margins of the rift; the Nyandarua Mountains on the east rise to about 3960 m and Mau Escarpment on the west to above 3000 m. The catchment presently includes three lakes: Naivasha, Nakuru, and Elementeita.

The highest and purest of the Great Rift Valley lakes, Lake Naivasha located at longitude 0 45' S; latitude 36 20'E at an altitude of about 1890 m mean sea level. Lake Naivasha is a shallow fresh water lake, approximately 100 kms northwest from the capital city of Nairobi on the floor of the Rift. The lakeshores are lined with fertile and flourishing horticultural farms and thousands of yellow barked acacias. Naivasha, which is home to more than 340 species of birds, has a resident population of hippo and small herds of plains are found all around the shores.

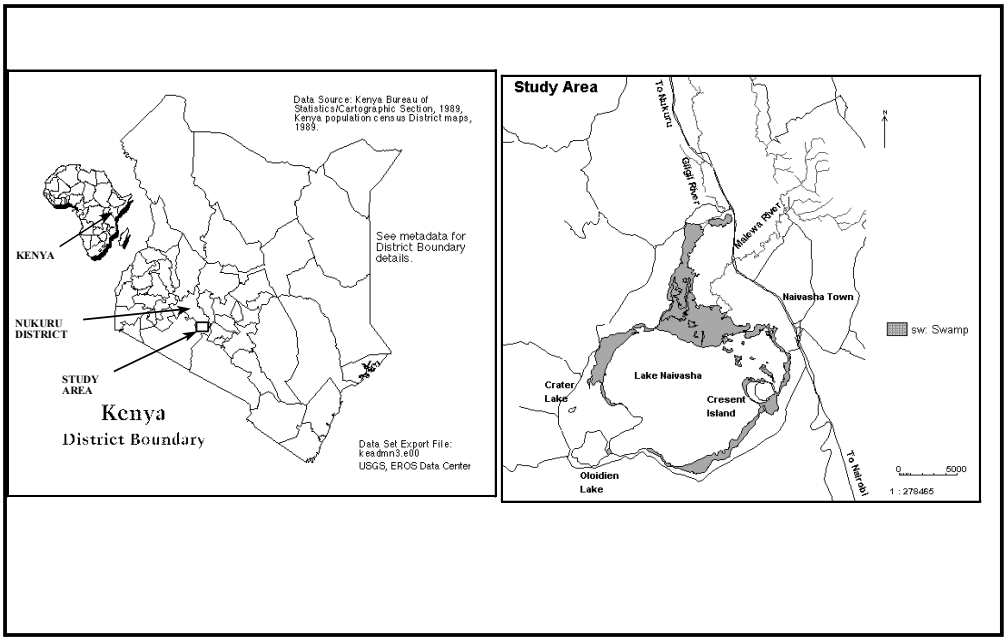

Figure 3.1: Location Map of Study Area (Source: Mmbui, 1999)

3.1.2 Lake Naivasha Basin

The Naivasha basin contains four topographically distinct water bodies viz. Lake Naivasha, Cresent Island basin of Lake Naivasha, Oloidien Lake and Sonachi (or Naivasha) Creater Lake. It has no outlet at present but is thought to have discharged during the middle Holocene through Njorowa Gorge to the south (Richardson et. al.,1972 as in Joseph, 1991).

Several factors combine to keep the lake's water fresh. A large fraction of the water supplied to the lake comes from dilute rivers and rain. The Naivasha catchment covers an area approximately 3300 km^2 and is drained by three major rivers. These are, the river Malewa, the river Giligil and the river Karathi. All rivers feed the lake from north, where the Malewa River forms the main inlet. About 90% of the surface water input to the lake comes from the Malewa River. The other streams (Gilgil and Karati) are either dry or flow intermittently during low rainfall periods. According to past records maximum discharge normally occurs in September-October (Ase et al., 1986).

The Naivasha area holds many different wetland plants, mammals, birds and amphibians. Over 60,000 people live close to the lake. Most lands around the lake are privately owned. Three major threats exist to the lake and its biodiversity are the abstraction of freshwater for drinking water and for agricultural production, the human activities on the shores and the untreated water flowing back into the lake (LNRA, 1999).

3.1.3 Hydrology and Meteriology

Analysis of rainfall in the Naivasha catchment is very important, because rainfall is the major factor to be taken into account in order to find the causes of the variations in lake level and to forecast its future behaviour (Per Syren, 1986). Ase et al., (1986), studied the evaporation during the period of 1965-1982 and reported the evaporation amounts to 1492 mm (with the pan factor of 0.80), i.e. more than twice the annual precipitation in Naivasha D.C. which pointed out very decisive influence of evaporation upon the water budget of Lake Naivasha. Also their studies indicated strongly that there is important groundwater flow to and also from the lake.

Ase et al., (1986) studied the Water Budget of Lake Naivasha and its Drainage Area and concluded that return periods of annual precipitation at Naivasha D.C., an annual rainfall of 1083 mm was estimated to occur once in 100 years while the actual maximum rainfall is 942 mm, which was received in 1961. The values computed by Brind and Robertson (1958) as reported by Ase et al., (1986), of return periods at Naivasha D.C estimate an annual rainfall once in 100 years to 1156 mm and the recorded maximum rainfall at this study was 1036 mm.

Sikes (1936, p78) as reported by Ase et al., mentioned the possibility of a subsurface inflow to the lake, but he stated that such seepage water would be immediately subject to evapor-transpiration, and that it may be discarded as a contribution to inflow. But Ase et al., (1986) reported that the average annual high water level in the lake occurs half a year after the period of the long rains, and about two months after the high water discharge, implies a subsurface inflow to the lake.

Sikes (1936,P82) and Edmondson (1977), as in Ase (1986), also studied about lake levels and made comments on that the lake was dry around the middle of the 19th Century and Teleki and Von Honnel (1892, P793) presented a small-scale map and over the area indicating that the Cresent Lake clearly isolated from the main lake shore. The Railway Survey of 1898 recorded that the lake levels on September 14th and November 19th. According to Ase(1986), the continuous records were commenced at the end of 1908 and he published a curve for the water level variations of Lake Naivasha by using the available water level records.

Vincent, Davies and Beresford (1979) made a statistical study of the water level variations of lake Naivasha as in Ase (1986), found an indication of an 11-year cycle. But more statistically significant was a variation with a period of about 7 years. According to the Ase (1986) studies, the lake levels normally drops during the beginning of the year, until the long rain start in April. Further he mentioned that the water level normally continues to rise even during June, July and August and the maximum occurs in September.

Litterick et al.,(1979) mentioned in their report that the daily recording of the main lake level was started in 1909 and showed repeated fluctuations with an 8 m decline between 1931 and 1952 followed by a 5 m increase during the next 10 years. Mmbui (1998) has done a long-term water balance studies on lake Naivasha and modelled on monthly time steps for the period of 1932-1997. In his thesis, he mentioned that the ground water plays a crucial role in the water budget of the lake and an exchange of water between the lake and ground water. He revealed that the average ground water outflow from the lake averages 4.6 $x10^6$ m^3 per month and since mid 1980s abstractions from the lake have increased progressively to a current average value of 57 mcm/month. The model predicts that without these abstractions the current lake level would be at least 2 meters higher.

3.1.4 Lake Water Quality and Sedimentation

Harper et al., (1993), examined the present and future risks posed by eutrophication to Lake Naivasha, by measuring the nutrient content of lake and inflow waters, iron and phosphorus concentrations of sediment pore water and lake chlorophyll a concentrations. In their paper titled "Eutrophication prognosis for Lake Naivasha, Kenya" document that the capacity of the lake to cope with probable accelerated nutrient inputs and highlight the management strategies necessary to maintain the integrity of the ecosystem.

Further, they reported the changing limnology of the freshwater Lake Naivasha is based upon the consequences of alien introductions and the effects of water level fluctuations combined with intensive lakeside agricultural development. During period of their study, when lake level falls (upto 1987) and the buffering effect of papyrus is lost by clearance, dissolved salts and algal biomass buildup in the lake water as a consequence of direct river inflow and evaporative concentration.

Gaudet et al., (1981), studied about the major ion chemistry in a tropical African lake basin and mentioned that the amount of water lost by seepage from Lake Naivasha, calculated as the residual in the water budget, was 5%(1973), 11%(1974) and 20% (1975) of the total water loss. Also they found from the direct measurements of seepage in near shore shallows that water entered the lake via ground-water seepage in the northern portion and left the lake in the southern portion.

The lakebeds are mainly composed of reworked volcanic material or subaqueously deposited pyroclastics and organic matter produced locally (Gaudet et al., 1981).. The structures of the area comprise faulting on the flanks and in the floor of the Rift valley and slight folding in the Njorowas Gorge. Slight non-conformities are present in the lake beds and can most clearly be seen along the Malewa river drainage (Gaudet et al.,1981).

3.1.5 Bathymetric Surveys of Lake Naivasha

One of the most important tools for the study of a lake is of course, a bathymetric survey. A depth survey could serve as a basis for the water balance studies as well as the lake limnological studies and assess the lake sedimentation process.

Lake Naivasha has a very flat bottom and towards the lakeshore depth decreases while it spreads over a large surface area (about 150 km^2). The deepest part of the main lake is close to the Hippo Point on the southwestern section of the lake. A profile of the lake shows that the main lake is flat while the two deepest sections displays a crater like morphology.

According to the literature, Lake Naivasha depth surveys had been done on 1927(PWD), 1957, 1983(Ase team), 1991(Hickley) and 1998 (WRAP). Survey methods as well as the accuracies are not well defined except for few surveys done in recently.

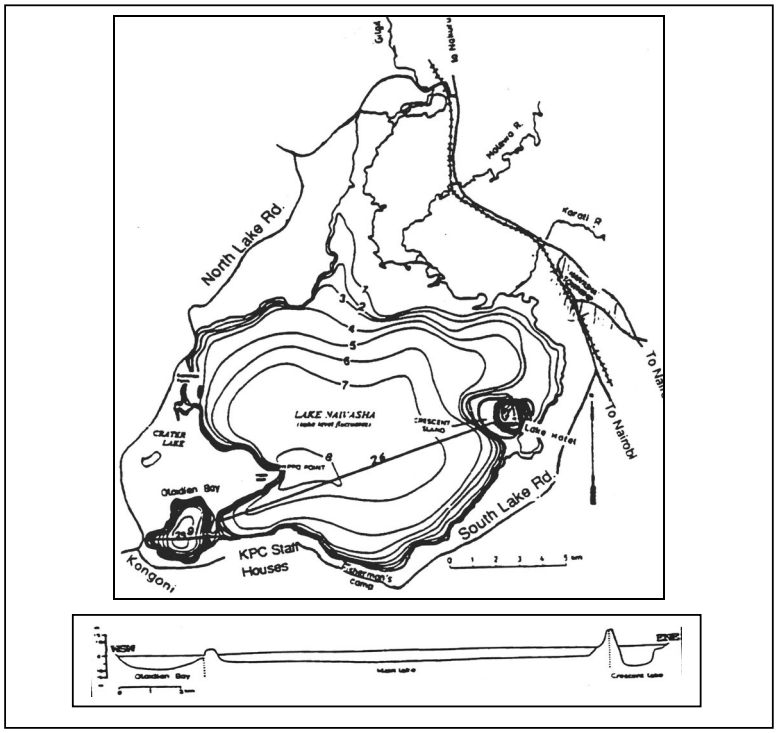

Figure 3. 2: Bathymetric map of Lake Naivasha based on October 1983 levels, modified from Ase et. al, 1986 (Source: Harper et al (1990)

3.2 MATERIALS AND METHODS

Data gathering and review, establishing bathymetric depth survey, hydrologic, and sediment input information, and assess the sedimentation process using the GIS and RS techniques will be the key components of this task. Fieldwork consisted of geo-referenced sonar bathymetric depth, turbidity and suspended sediment surveys of the lake, sediment core sampling, flow and suspended sediment analysis of river inflows. Under the section of Materials and Methods, on-site lake sampling methods and river sampling methods will be discussed.

3.2.1 ON-SITE LAKE SAMPLING

3.2.1.1 Lake Geo-referenced Sonar Bathymetric Survey

The lake Naivasha bathymetric survey was carried out over a 7-day period ranging from 25-31 September 2001. The idea was to measure the depth readings at defined positions in the lake along the certain cross sections reference to the lake level. The following methodology was adapted for the lake sonar bathymetric survey.

Planning was done using the 1:50,000 topographical maps and remote sensing digital images. They were used to define the cross sections across the lake at certain intervals in order to get the best routes to be followed by the boat. This means picking on a section along an Easting or Northing and moving along it. According to the map it shows that it is more convenient to move North to South since it was shorter to cross the lake.

From TM-2000 image, a segment map was prepared by digitizing the segments to follow the boat track, using the GIS-ILWIS software. Then a point map was created having 500 m spacing between the points. All point co-ordinates were uploaded to the GPS and this was used to guide the navigator along the defined section (Easting or Northing). While the boat was running along the defined cross section, another GPS was used to locate the points. The latter was very convenient since the boat could not follow exactly the previously defined cross sections. Lake depths were measured using the Sonar-bathymetry instrument (Fish Finder 100) and on each observation, co-ordinates and depths were recorded.

Figure 3.3: Methodology for Planning and Execution of Bathymetric Survey

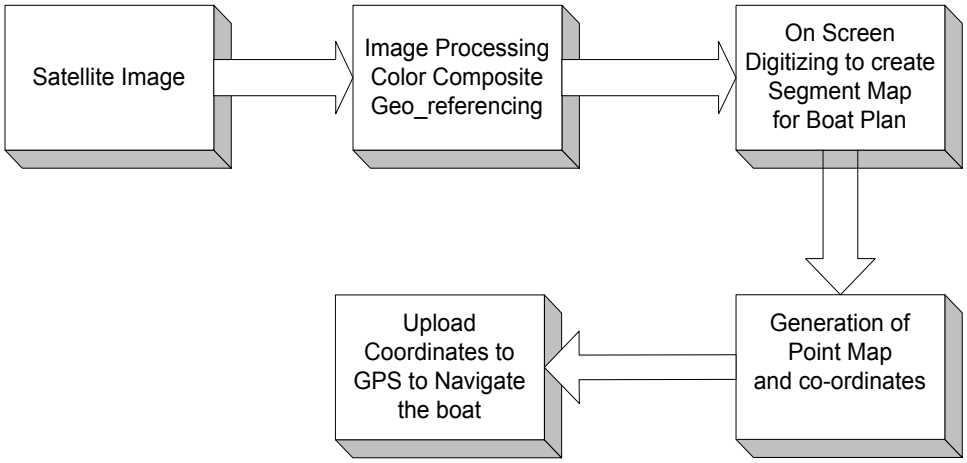

Figure 3.4: Methodology for Preparation of Bathymetric Map

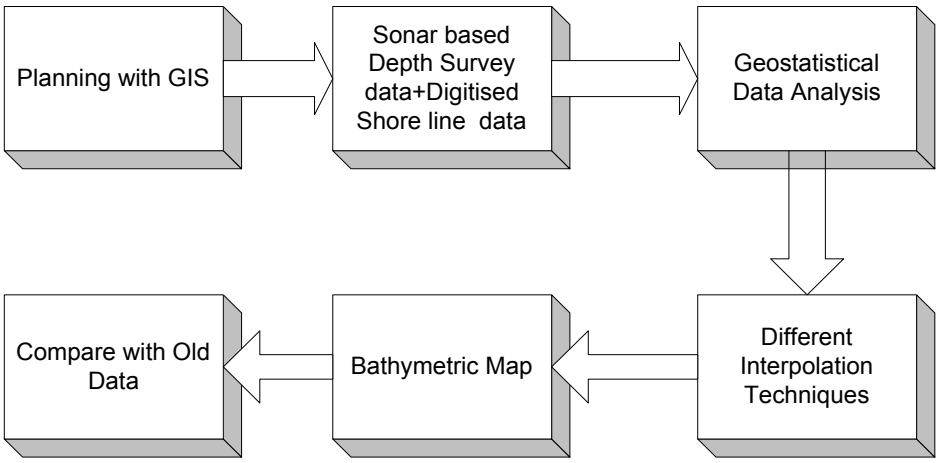

Sonar Bathymetry Instrument – Fishfinder 100

The Sonar instrument used for the lake bathymetry survey was the Fishfinder 100. This instrument is able to display a variety of useful information about the under water environment: water depth, water temperature, and speed over water, fish, bottom shape and type. Furthermore it can provide a warning for shallow or deep-water conditions.

The unit operates by transmitting sound waves towards the bottom of the lake in a cone shaped pattern. It acts as the eyes and ears in the under water environment. The larger the cone angle the larger the coverage area at a given depth, but at a decrease bottom resolution. A narrow cone angle transducer provides a smaller viewing area with improved bottom resolution and a smaller dead zone.

When a transmitted sound wave strikes an underwater object such as the bottom, a piece of structure, or a fish, it is reflected back to the transducer. The latter instrument collects the reflected sound waves and sends the data to the unit to be processed and displayed on the chart. The area covered by the transmitted sound waves is determined by the cone angle of the transducer and the water depth.

Calibration of the instrument is necessary with local field conditions to ensure that instrument will provide accurate readings. Since sound wave travel through fresh and salt water at different rates, it is necessary to calibrate the instrument with water type and few manual depths readings obtained in the lake. As the transducer is fixed to the boat hull, correction should be made for the water depth to the transducer location.

3.2.1.2 Turbidity and Suspended Sediment Parameters

In the lake, other than the suspended sediment and turbidity, secchi depth and lake sediment core samples were collected for further analysis of sediment input characteristics to the lake. Grab samples were collected from the lake as well as from rivers for suspended sediment analysis in ITC laboratory.

3.2.1.2.1 Turbidity

Turbidity is an expression of the optical property that causes light to be scattered and absorbed rather than transmitted with no change in direction or flux level through the sample. Turbidity in water is caused due to suspended and colloidal matters such as clay; silt finely divided organic and inorganic matter, and plankton and other microscopic organisms.

Turbidity measurements were carried out in the lake using the model 2100P Portable Turbidity meter. This instrument operates on the nephelometric principle of turbidity measurement. The optical system which includes a tungsten-filament lamp, a 90 detector to monitor scattered light and a transmitted light detectors. This ration technique corrects for interferences from color and/or light absorbing materials (such as activated carbon) and compensates for fluctuations in lamp intensity, providing long-term calibration stability. The optical design also minimizes stray light, increasing measurement accuracy. The turbidity is calibrated with formazin primary standard and needs calibration once every three months according to the manual. Measurement can be made manually with the signal average mode “on” or “off” or in automatic range selection mode.

The Nephelometric principle is based on a comparison of the intensity of light scattered by the sample under defined conditions with the intensity of light scattered by a standard reference suspension under the same conditions. The higher the intensity of scattered light, the higher the turbidity. Formazin polymer is used as the primary standard reference suspension.

An accurate turbidity measurement depends on the good measurement technique applied by the analyst, such as using clean sample cells in good condition. Proper measurement techniques are important in minimizing the effects of instrument variation, stray light and air bubbles (degassing). Samples should be measured immediately to prevent temperature changes and settling. Better results could be obtained by avoiding sample dilutions when possible. When the sample is diluted the particles suspended in the original sample may dissolve, otherwise change characteristics when the sample temperature changes or, resulting in a non-representative sample measurement.

3.2.1.2.2 Suspended Sediment Measurements

Grab samples were collected in the lake to measure suspended sediment concentration in the lake-selected points. Samples were then analysed in ITC laboratory.

Solids refer to matter suspended or dissolved in water or wastewater. *Total solids* the material residue left in the vessel after evaporation of the sample, which is then dried in an oven at defined temperature. *Total suspended solids*, the portion of total solids retained by a standard sized filter**,** and *total dissolved a solid* that passes through the filter. *Suspended solids* are the portions retained on the standard filter.

During experiments, the following methodology was adopted to measure the total suspended sediments in the samples due to practical constraints.50 ml volume of sample is transferred into the standard glass tube and centrifugal force is applied using a centrifugal pump for 10 minutes under the revolution of 4000 rpm. This allows suspended particles to settle down in the water column. The supernatant was removed carefully and the sample is dried to a constant weight at 103 to 105^0C. The increase in weight of the glass tube represents the total suspended solids in the sample.

3.2.1.2 Sediment Core Sampling

Sediment core samples were collected from five locations in the lake to obtain representative samples. They were used to calculate the specific weight of lake sediment and to perform the particle size analysis of the deposits. The gravity corer was fitted with cylindrical transparent plastic liners with a 4 cm inside diameter and 1-meter length, which used to collect and store the undisturbed sediment core sample.

For the determination of specific weight, undisturbed sample volume was measured in the site and the sample was dried under controlled condition (105^0 C) in order to determine the dry weight.

Using the standard procedures described in the International Soil Reference and Information Center, Food and Agriculture Organization of the United Nations, 5th Edition by the L.P Van Reeuwijk in 1995, particle size analysis and organic content of the sediment core samples were analyzed.

3.2.2 SAMPLING OF RIVERS

In order to evaluate the sediment input parameters to the lake through river inflows, turbidity and suspended sediment, measurements were carried out in each river reach together with detailed cross section surveys.

3.2.2.1 Suspended Sediment and Turbidity Sampling in Rivers

All samples were collected as grab samples in each river reach while the turbidity was measured onsite. The same principles and methodology were applied to analyse the river samples for suspended sediment in ITC Laboratory.

3.2.2.2 Detailed Cross Section Surveys in Rivers

Detailed cross section surveys were carried out in river Malewa and Gilgil during the period ranging from 17-21 September 2001. In Malewa, 16 detailed cross sections were measured four different river reaches, while in Gilgil 11 detailed cross sections were carried out in 3 river reaches.
The surveys were performed using Engineering Levelling Instrument, Engineering Staff and 50-meter tape. Standard surveying techniques were followed to measure elevation in each river reach. GPS was calibrated with the fixed benchmark at Naivasha Railway Station in order to measure the approximate elevations in the field. Using the topo maps +/-3 m accuracy was found. Standard height of collimation surveying technique was used to calculate the measured levels to absolute levels using temporary benchmarks for each river reach.

For estimation of parameters for HEC RAS modelling such as Manning's roughness coefficient and boundary conditions, field photos and details of the sites (river banks and bed details) were recorded for each river reach. During the cross section survey, river discharge gauging was done in each location using the current metering and the salt dilution techniques. Due to the high discharge in river Malewa at the time of investigation, measurements have done with the help of a portable boat.

3.2.3 Methodology for Assessing Lake Sedimentation Processes

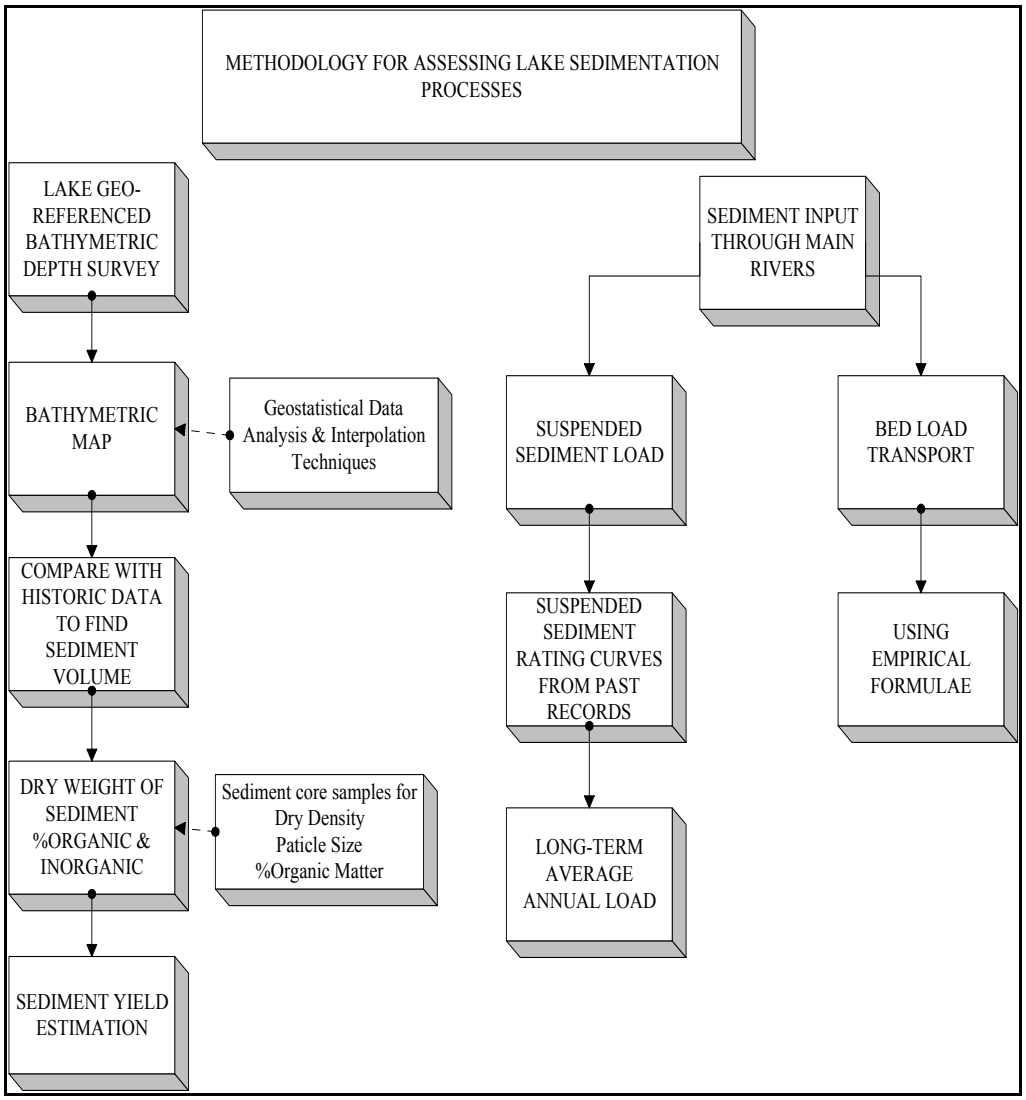

CHAPTER 4 - FIELD DATA COLLECTION AND ANALYSIS

In this chapter, Onsite Lake and River Sampling locations, data collection, analysis and results will be discussed.

4.1 ON-SITE LAKE SAMPLING

4.1.1 Lake Bathymetric Survey - 2001

As described in Chapter 2.0 under Materials and Methods, lake bathymetric survey was done using the sonar bathymetric instrument (Fishfinder 100) and the observation was made on each location co-ordinates and the depth variable.

During the survey, measurements were taken only below the water level at that time due to practical limitations. Accessibility to some sampling locations was limited due to danger in wild animals. Especially measurements of lakeshore and marshy areas were restricted due to inaccessibility from the boat. As there are no data points close to the shoreline, the 2000 TM image lake boundary was digitised and obtained another set of points around the lake boundary with the lake level of May 2000 (1886.67 masl). Therefore the study of lake bathymetry was limited below the lake level of 1886.67 masl. Due to practical difficulties following deviations were made from planning during the bathymetric survey.

- Instead of having 500 m. spacing between cross sections, in some areas 1000 m. between cross sections were accepted due to time constraints as well as the observed depth variations were very limited.
- Only depth measurements were recorded where the boat could reached that is the water depth was more than 0.80 m.
- Lakeshore line points obtained from Landsat 2000 image, used with the measured data in order to make the bathymetric map.

Figure 4.1: Lake Bathymetric Survey Observed Points in 2001 overlaid in TM image

The data was processed using the GIS_ILWIS software in order to make lake bathymetric map by using different interpolation techniques to compare with historic data.

4.1.1.1 Processing and Analysis of Geo-statistical Data Set

Geo-statistical data analysis is important to make the best use of observed data and to estimate the depth parameters in other locations. Following steps were adopted for depth data processing.

- Recorded GPS co-ordinate points were transferred to Excel software and the depth data was entered manually. Depth data set was processed in order to adjust the correction required for the transducer position in the boat with reference to the water level.
- Lake depths were converted to absolute heights using the available water level recorders with reference to the mean sea level. Lake level during the survey was 1886.38 masl.
- Surface maps were made with defined survey routes in ILWIS software and combined measured points with digitised shoreline points from TM2000 image.

Summary statistics were calculated for measured data set and combined data set (with TM image data) as shown in Table 4.1 & 4.2 and Figure 4.2 & 4.3 (locations of points) respectively.

Table 4.1 and Figure 4.2 -Summary Statistics for 2001 depth data and Observed points

Parameter	*Bed Level (masl)*
No. of observations	*1477*
Minimum Value	*1872.23*
First Quartile	*1882.08*
Median	*1883.48*
Third Quartile	*1884.93*
Maximum Value	*1885.49*
Mean	*1882.97*
Standard Deviation	*2.57*
Skewness	*1.79*

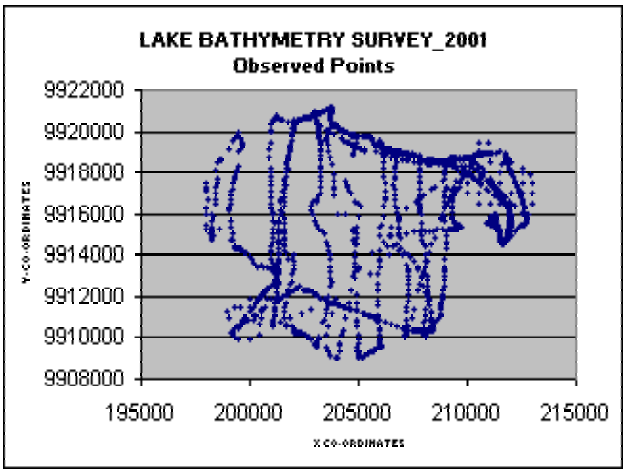

According to the statistics, mean lake depth is about 3.41 m. (1886.38-1882.97 m) at the time of survey. Highest depth recorded in the Crescent lake is about 14.15m.(1886.38-1872.23m)

In measured data set, mean and median give different results indicating that the distribution is asymmetric and the skew ness is positive, which indicates, data set contain many values slightly smaller than the mean and a few values much larger than the mean. This is due to the flat bottom shape of the lake, many values below the mean. Also due to very high depth in the crescent lake compared to other areas mean value compelled to shift towards the higher side.

Table 4.2 and Figure 4.3 - Summary Statistics for combined data and combined points

Parameter	*Bed Level (masl)*
No. of observations	*1619*
Minimum Value	*1872.23*
First Quartile	*1882.18*
Median	*1883.88*
Third Quartile	*1885.16*
Maximum Value	*1886.67*
Mean	*1883.30*
Standard Deviation	*2.66*
Skewness	*-1.59*

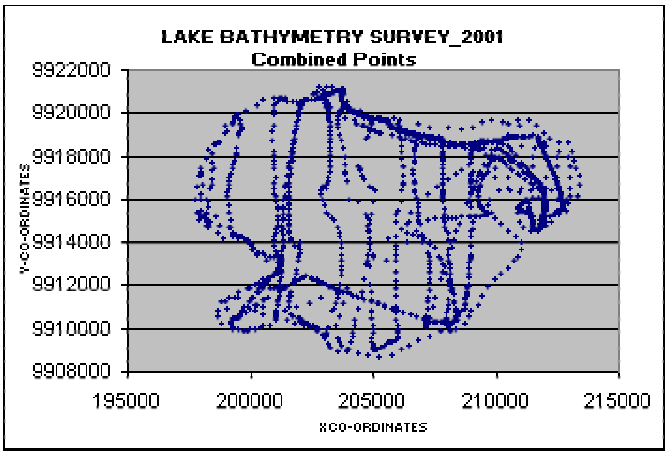

But, in combined data set having skewness negative indicate that there are many values slightly larger than the mean compared to few values smaller than the mean. In the combined data set, having many digitised lakeshore points (zero depth) gives high mean value.

4.1.1.2 Use of Different Interpolation Techniques

A point interpolation performs an interpolation on randomly distributed point values and returns regularly distributed point values. Different maps were made using different interpolation techniques as described in the Chapter (2.0), Background Theory. ILWIS and Surfer software was used to make the lake bathymetric maps. Interpolation techniques i.e. Nearest Neighbour, Moving average, inverse distance power, Natural Neighbour Method and ordinary kriging were used to generate different lake bathymetric maps. Resulting maps are shown in Appendices 4.1 to 4.3.

As shown in figures 4.2 & 4.3, the observed data points are densely populated (number of points 1619), use of different interpolation techniques do not show significant differences in final output maps. But techniques like nearest neighbour, natural neighbour and moving average methods showed poor results where there is less data points and they do not interpolate beyond the depth data range. Ordinary kriging with spherical model showed an acceptable results and kriging can extrapolate grid values beyond the data set's depth range. Also another advantage using kriging interpolation technique is that it produces error maps. For further analysis ordinary kriging map has been selected. But, even in kriging map, some anomalies recorded where there were no data points especially southeastern side of the lake.

For the interpolation of depth data using kriging, Spherical Model with Sill 7.25 m, Nugget 0.70 m and Range 500 m was selected. Figure 4.4 shows the selected semi variogram model to produce the lake bathymetric map. Interpolated Kriged map as shown in Figure 4.5 was verified with 2000 data set (60 data points), which is almost similar to the 2001 data points.

Boundary level of the 2001 lake bathymetric map is 1886.67 m.a.s.l.

Figure 4.4: Omni directional Semi Variogram for Depth

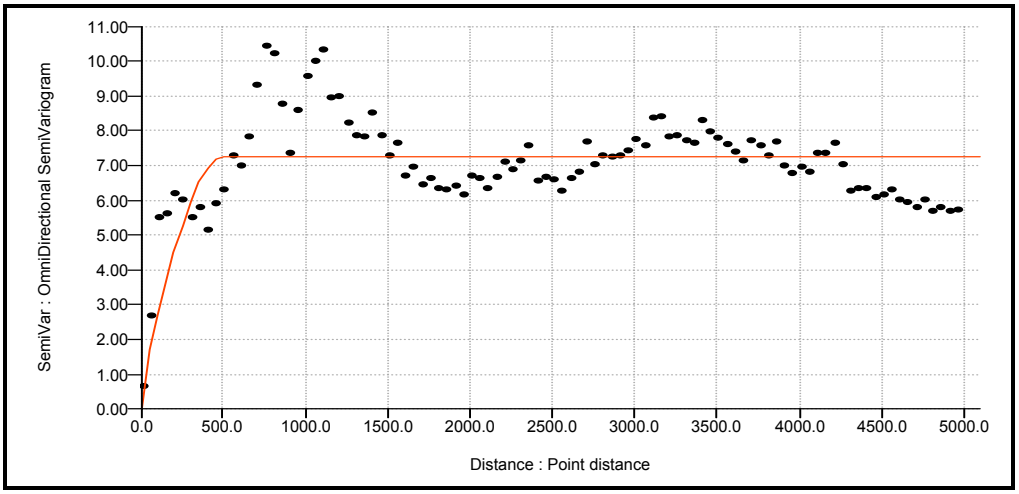

Figure 4.5: Bathymetric Map of Lake Naivasha (2001) and Kriging Error Map

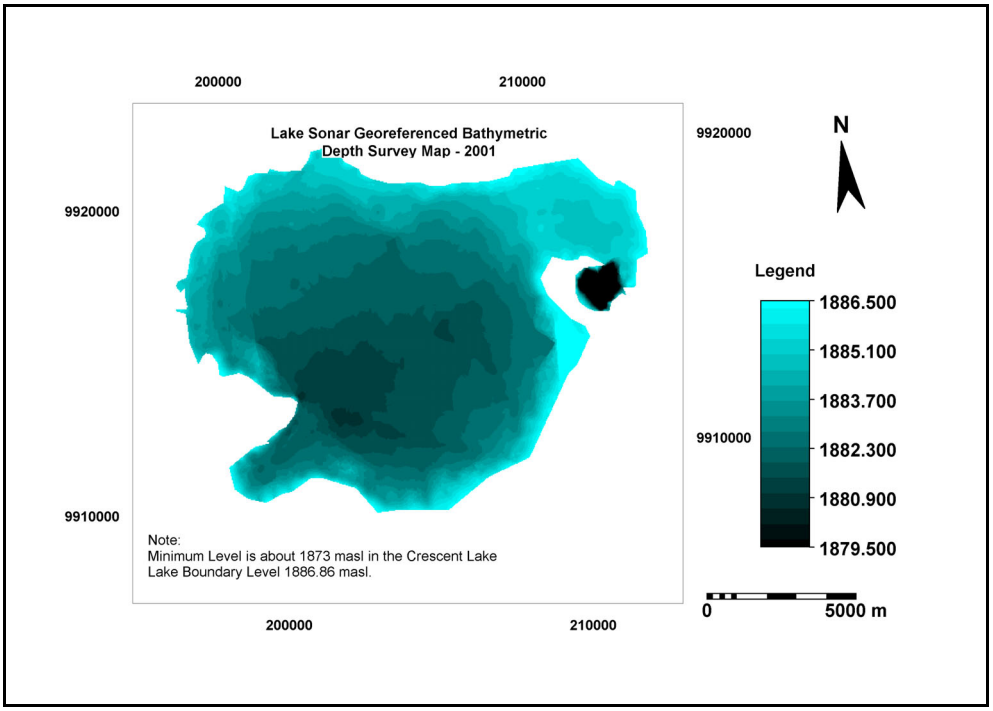

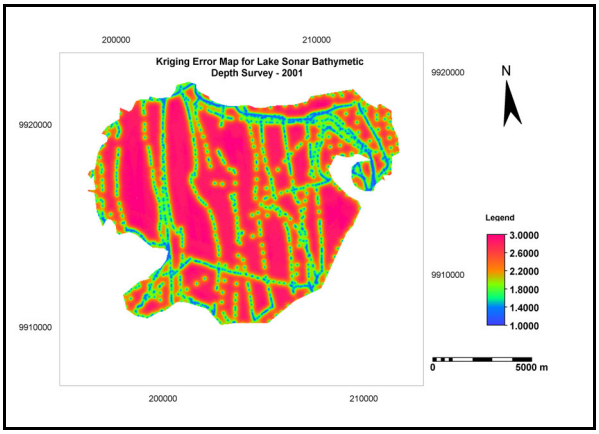

4.1.1.3 Limitations of Bathymetric Survey

- Tolerance limits of the GPS –Sometimes in the lake, GPS coordinates get affected due to bad signals. Also the accuracies of two GPSs used were about +/-20 meters. Therefore precision of the point locations could be affected within that range.
- Due to highly turbulent water waves especially in the afternoon, sonar bathymetric instrument displayed low précised depth data. This happened according to the boat movement due to high waves lead highly sensitive transducer to display less accurate data. But during the survey, care had been taken to avoid such measurements. Also most of the time, lake survey was done in the morning session, especially when the lake was under transient conditions.
- Measurements were not taken in areas inaccessible especially where hippo families.
- In very shallow water, less than 0.80 meters transducer doesn't work and provides shallow water alarming signal. Other than that once the sonar bathymetric instrument well calibrated to the local water, it gave good and accurate results. This was verified with the frequent manual measurements.

4.1.2 Old Bathymetric Surveys

According to the literature, number of depth surveys has been carried out in lake Naivasha. Details of the surveys and the status are given in Table 4.3.

Table 4.3 – Details of Old Bathymetric Surveys

Year of Survey	By whom	Equipment used	Data Availability	Remarks
1927	Public Works Department	Spot levelling	Yes	Approximate analogue contour map.
1957-Feb-July	Hydraulic Engineer, Secretary of Kenya Colony	Spot levelling	Yes	Contour maps in 7 nos/A3 sheets in Casini System Scale 1:20,000
1983	Ase Team	An Echo Sounder	No	Article available with comparison of 1927 survey
1990	Harper	An Echo Sounder	No	Article available
1991	Hickley	Unknown	No	Improved Ase data
1998	WRAP Project	Echo Sounder (NASA)	Yes	Detail data available
2000	MClean (ITC)	Spot levelling	Yes	Only 60 points in the lake

Out of these lake Naivasha bathymetric surveys, detailed survey data are available only in 1957, 1998 and 2000 surveys. Therefore in order to make comparison with 2001 survey, these available historic records were considered.

4.1.2.1 Bathymetric Survey –1927

Approximate 1927 survey data is available in the ordinary contour map prepared by the Water Resources Authority of Kenya. Even though detailed data in 1983 survey is not available, detailed comparison made between 1927 and 1983 bathymetric surveys has been published in the literature. Ase et al., (1986), in his studies on Lake Naivasha, reported that the Lake Naivasha's depth map was made as early as 1927 (Thompson and Dodson 1963). According to him, the quality of the survey was obviously not very good, especially as the echo sounding technique was not practiced at that time. In 1983, Sernbo of the Ase team carried out the depth survey of Lake Naivasha with the aid of echo sounding technique and compared the results with earlier depth survey done in 1927.

According to their findings, the 1927 map indicates a very flat bottom with major decrease in depth only close to the shores. Deepest parts of the lake that topographically differ greatly from the dominating pattern are namely Crescent Lake and Oloidien Bay. According to this map, Crescent Lake has a maximum depth of 17 m, which was the deepest spot in the lake, and Oloidien Bay has a maximum depth of 9 m. The deepest registered spot in the main lake was 9 m, registered just outside Hippo point. The mean depth was 4.7 m. The volume of the lake was calculated to 9.0 $x10^8$ m^3 at a lake level of 1889 masl.

4.1.2.2 Bathymetric Survey –1957

The Hydraulic Engineer, Secretary of the Kenya Colony, carried out Lake Naivasha bathymetric survey in 1957. Lake level during the survey of 5th July 1957 was 1886.95 masl (6191.1 feet).

1957 contour survey data was available in seven (A3 size) analogue maps in Cassini co-ordinate system. All maps were digitized in ILWIS using the same coordinate system and transformed the coordinate system from Cassini to UTM system using ILWIS software. Methodology used for the transformation of coordinates from Cassini system to UTM system is given in Appendix 4.4**.** This transformation was verified with two benchmark surveys carried out recently with reference to the Cassini system.

After coordinate transformation, digitised 1957 contour map was overlaid with the TM2000 image to verify the data reliability. It shows that the contour data is reliable in order to compare with 2001 data. In 1957 map, due to papyrus belt, along the shoreline (especially north of the lake) contour lines has not shown in the original map. But this area has been indicated as the papyrus swamp in 1957 original map.

Figure 4.6 shows the digitised 1957 data overlaid on the TM 2000 image in ILWIS software.

Figure 4. 6: Contour Map based on 1957 survey overlaid on TM 2000 Image

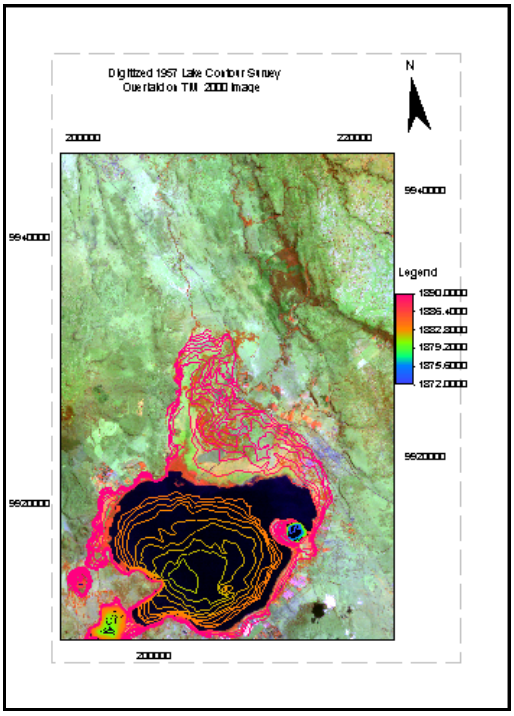

4.1.2.3 Bathymetric Survey -1998

Under the Water Resources Assessment Project in Kenya (WRAP Project) in 1998, a bathymetric survey was done on Lake Naivasha. During this survey cross sections across the lake at a spacing of 500 meters and the depths at defined positions along the grid at 500 meters intervals were recorded. Figure 4.7 shows the locations of grid points and the interpolated map of 1998 survey.

Figure 4.7: Bathymetric Survey of 1998

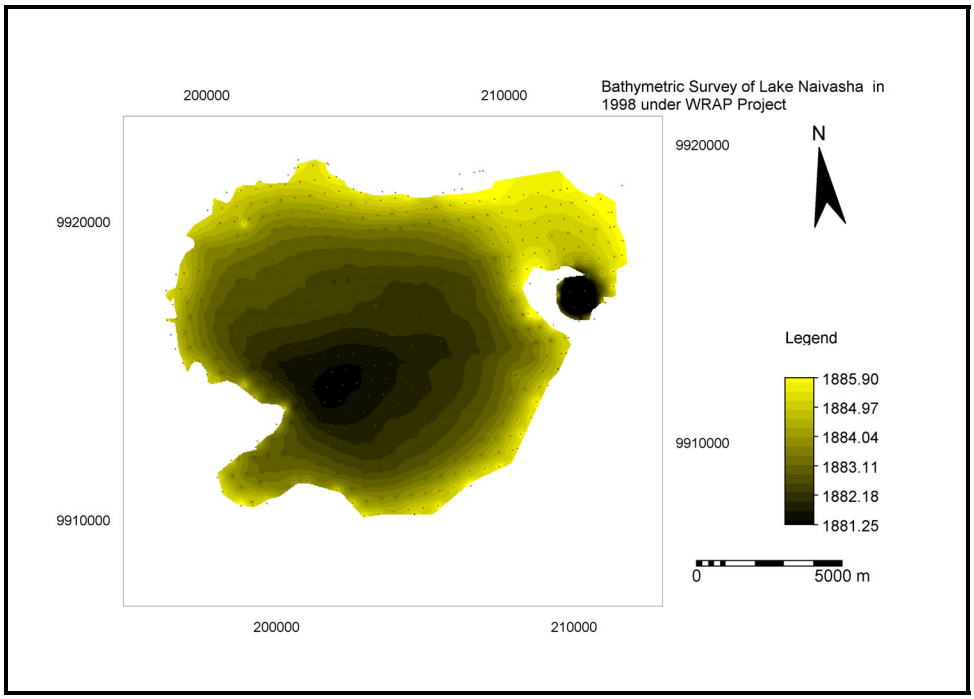

During this survey, lake depths were read using NASA Echo Sounder instrument where the water was more than 1.5 meters deep and a 5-meter surveyors staff was used where the depth was less than 1.5 meters. Survey was done from a motorboat, which followed the defined sections with the guide of a German GPS receiver as indicated in the survey report of Remconsult(1998).

According to their report, the Navigator was guided along a defined section (Easting or Northing) +/-8 meters since the PDOP (Position of Dilution of Precision) for the German GPS was 4 meters and the motorboat was stopped every 500 meters (+/- 10 meters) because the boat could not remain standstill due to water currents. The readings were then taken from the boat. Following limiting factors hindered the precision of observations during the depth surveys in 1998(Remconsult, 1998).

- The PDOP of the German GPS that was used is about 4 meters, and water waves disturbed when the readings were being taken.
- The accuracy of NASA Echo sounder, which was used, is 0.1 meters. When the Surveyor's staff was used, it was found to sink into the silt by about 0.1 to 0.2 meters while the Echo sounder read the depth from top of the silt.
- No readings were taken on Marshy area where the boat could not go through floating or growing vegetation. The bottom morphology of the lake depicted by the cross sections was limited to the points where the spot heights were read and do not correspond with the current extent of the perimeter boundaries.

4.1.2.4 Bathymetric Survey –2000

In 2000, Patrick MClean, one of the ITC M.Sc student collected 60 depth data points in the lake during his research using an ordinary measuring techniques. The sampling scheme was designed according to an optimal spatial sampling scheme using Spatial Stimulated Annealing (MClean, 2001). First 30 points obtained based on the mean shortest distance criterion (MMSD) and subsequently the additional 30 observations were selected using the Maximum Kriging Variance criterion in conjunction with a variogram inferred from a previous study of Donia (1998). This data set as shown in Figure 4.8 also selected to compare with 2001 data set.

Figure 4.8: Lake Survey Points in 2000

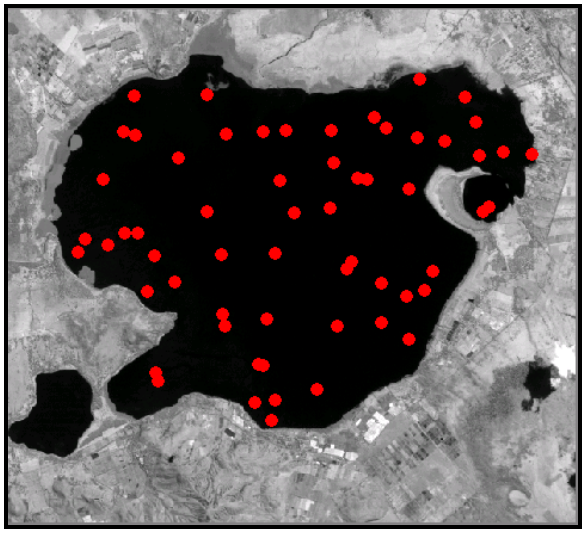

4.1.3 Comparison with Historical Data

4.1.3.1 Comparison Between 1927 and 1983 (From Literature)

According to Ase, et al. (1986), in 1927 survey flat bottom topography of the lake contrasts with the hilly topography of the surroundings and the difference is that the lake basin has filled up with large amounts of sediments, resulting in even bottom topography. Further, the depth map, clearly shows a more shallow area in the northern part of the lake has been interpreted as a delta built up by sediment loads deposited by the main inflows, from the rivers Malewa, Gilgil and Karati, which all enter the lake in this area.

Further, he compared the depth map in 1983 with the depth map of 1927, even though it was not clear that what kind of material and the degree of accuracy of the map in 1927. Comparing two maps following remarks had been made.

- The deepest spots in the main lake and in Crescent Lake are the same in both 1927 map and the 1983 map, and the figures for depth in these places are also correspond. It is also possible in both of the maps an indistinct slope from the northeastern part of the lake towards the southwest.
- On the other hand, there are many major differences as on the 1927 map, Oloidien Bay was drawn completely different as compared to the 1983 map. Thompson and Dodson (1963) note that as reported by Ase, et al.,(1986), probably sufficient readings were not taken in the south-western part of the lake.
- The map from 1927 doesn't show the presence of a delta as clearly as the map from 1983 survey. Between 1927 and 1983 changes in the bottom topography might have occurred and possible that delta has been built up and enlarged during this period. Further he mentioned that the comparison was not so fruitful as it was hard to believe that Oloidien Bay has become more than seven meters deeper in 55 years.

4.1.3.2 Comparison of 2001 Survey with 2000, 1998 and 1957 Surveys

In order to compare 2001 bathymetric map with old bathymetric surveys, all the data sets were transferred to mean sea levels using standard elevations and imported to ILWIS software. All point data were overlaid with the TM 2000 image and verified the spatial data reliability. 1957 bathymetric map was created using contour interpolation in ILWIS. All bathymetric maps lake outer boundary was limited to 1886.67-masl to compare with the 2001 survey.

It is observed that the 2000 survey data (60 points) were not enough to well represent the entire lake bottom variations especially in the Crescent Island compared to other surveys due to less number of points. Therefore, 2000 data set were not used for mapping, but compared with points itself with the 2001 bathymetric map. It was found that they same as 2001 except minor changes (+/-0.1) may be due to the different measuring techniques used in 2000 & 2001.

Moving average interpolation technique was used to create the 1998 lake bathymetric map, as the 1998 survey data set was dense and in a regular grid. From the experience of the lake survey, it was difficult to follow the defined cross section by a boat due to large surface area as well as due to drift. But, 1998 survey points shows that they followed exact grid survey, and mentioned that the accuracy of the used GPS lied within 4 meters during their survey. Even though, comparison was made with 2001 survey data and created a difference of bathymetric maps from 1998 to 2001. It shows that almost around the

lake central area do not have many differences between 1998 and 2001 surveys. But, in lakeshore areas shown higher elevation in 2001 survey in many locations may be due to sedimentation or another reason. As there was no significant difference between 1998 and 2001, 1957 survey data was selected as the best data set to compare with 2001 bathymetric survey.

A difference map was made from 1957 and 2001 maps in order to have the visual interpretation of changes in lakebed levels from 1957 to 2001. This is shown in Figure 4.9. It shows highest sedimentation has taken place around the southeastern part of the lake. But, in this area due to lack of data points some anomalies recorded during point interpolation of 2001 map. High grounds recorded in the northern area in 1957 survey, which gives negative values in the difference map. According to the difference map in figure 4.9, it shows most lake bed changes has taken place around the lakeshore line as well as north to south direction where rivers enter the lake and due to redistribution of sediment in the lake. Five cross sections across different profiles as shown in Figure 4.10 were made using the developed maps in 1957, 1998, and 2001 in order to interpret the differences. Figures 4.11 to 4.20 shows these cross sections and the changes of lakebed topography along each profile.

Figure 4.9: Changes of Lake Bed Topography from 1957 to 2001

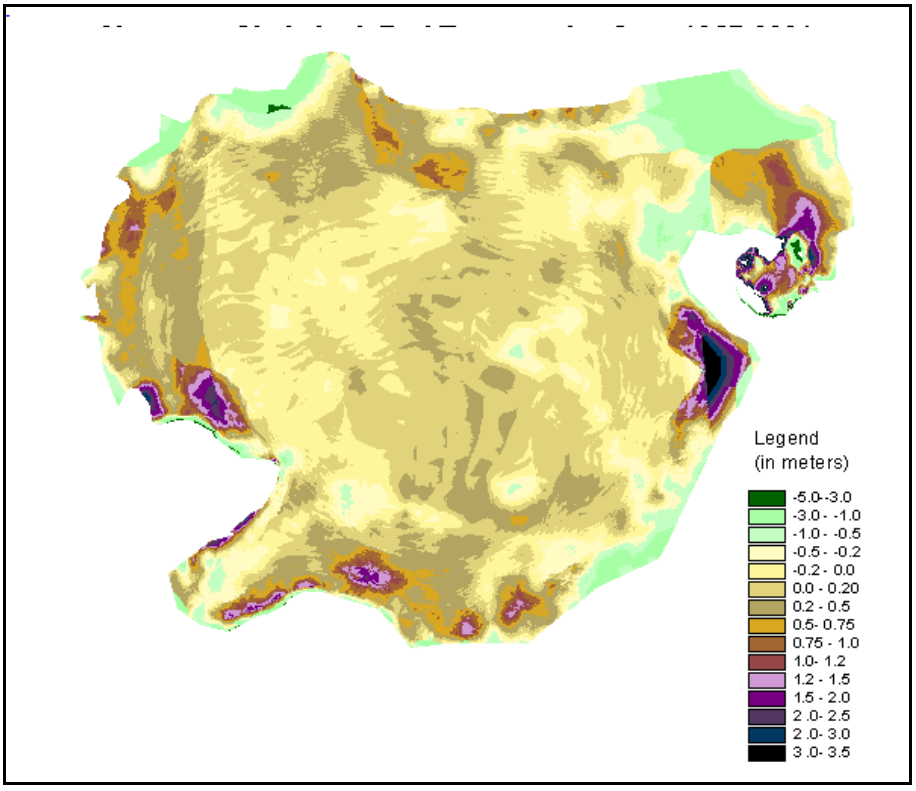

It is also important to monitor changes in northern delta levels and perimeter position variations especially in river intakes to the lake. But in our study this is one of limitations in the field due to constraints of accessibility to the area as well as due to time constraint.

Cross Sections Across Different Profiles

Figure 4.10: Cross Section Profiles in the Lake

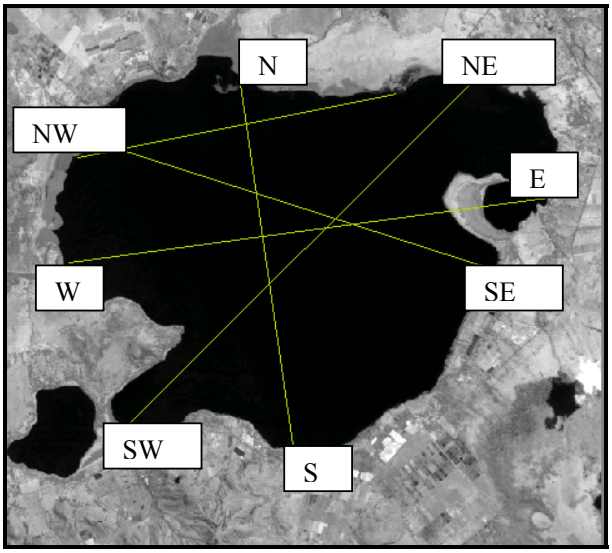

Figure 4.11: Cross Sections along the Profile North to South (N-S)
Lake Naivasha

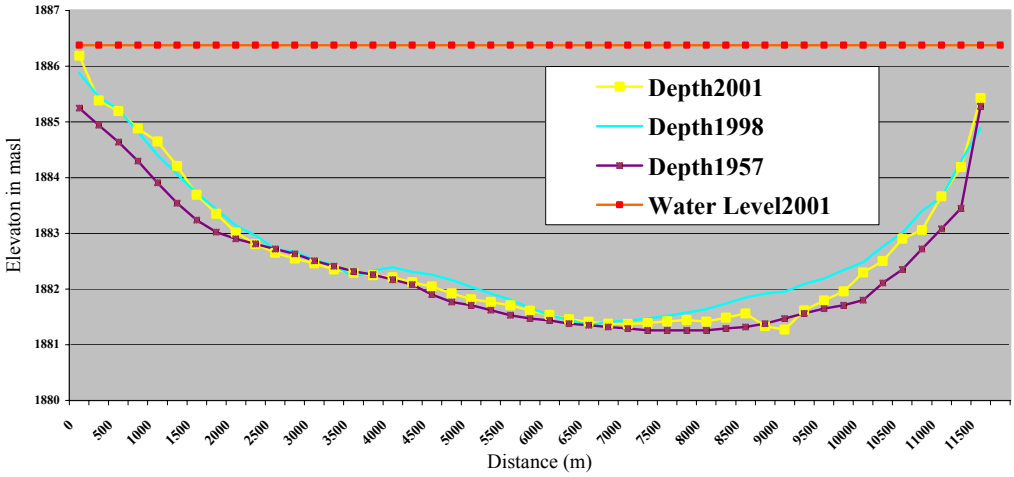

Figure 4.12: Change of Lake Bed from 1957 -2001
Along the Profile North to South (N_S)

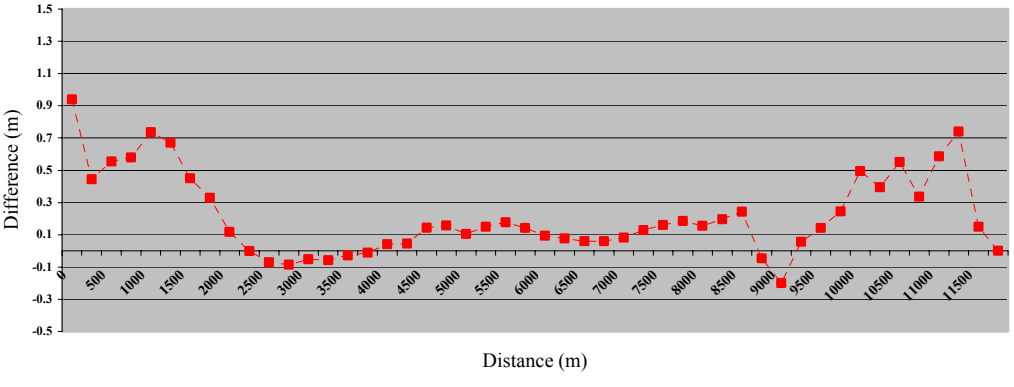

Figure 4.13: Cross Sections along the Profile West to East (W-E)
Lake Naivasha

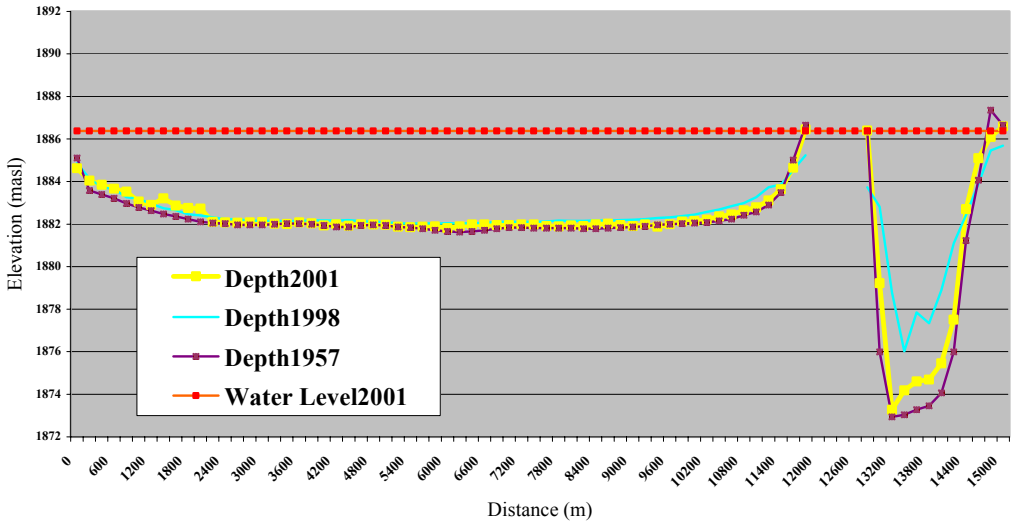

Figure 4.14: Change of Lake Bed from 1957-2001
Along the Profile West to East (W-E)

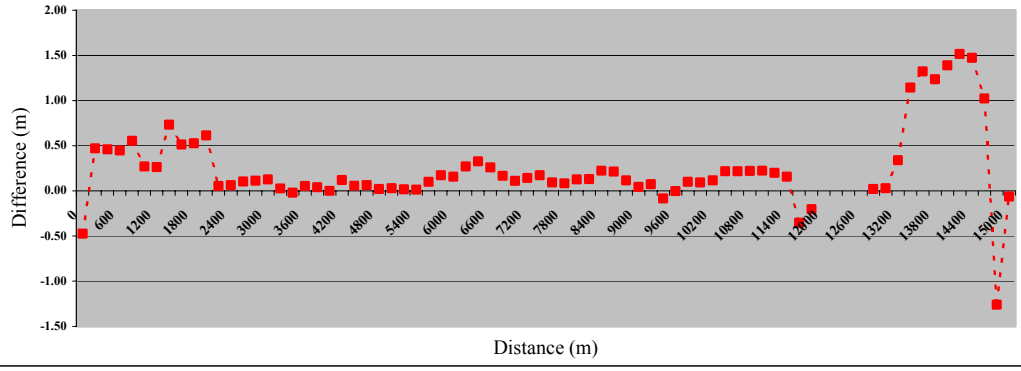

Figure 4.15: Cross Sections along the Profile NW TO SE
Lake Naivasha

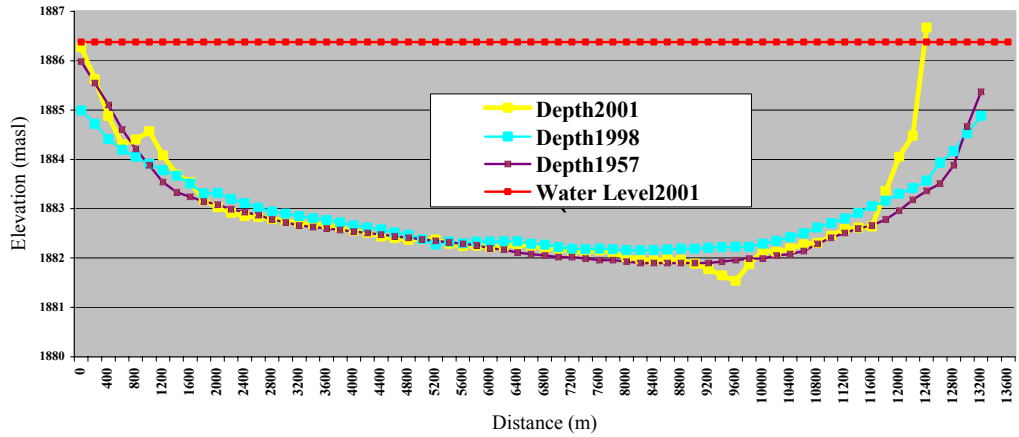

Figure 4.16: Change of Lake Bed from 1957-2001
Profile NW-SE

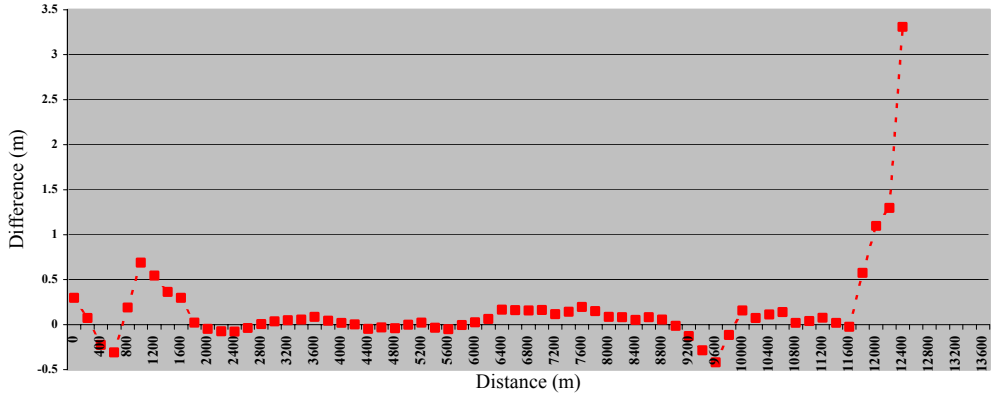

Figure 4.17: Cross Sections Along Profile SW TO NE
Lake Naivahsa

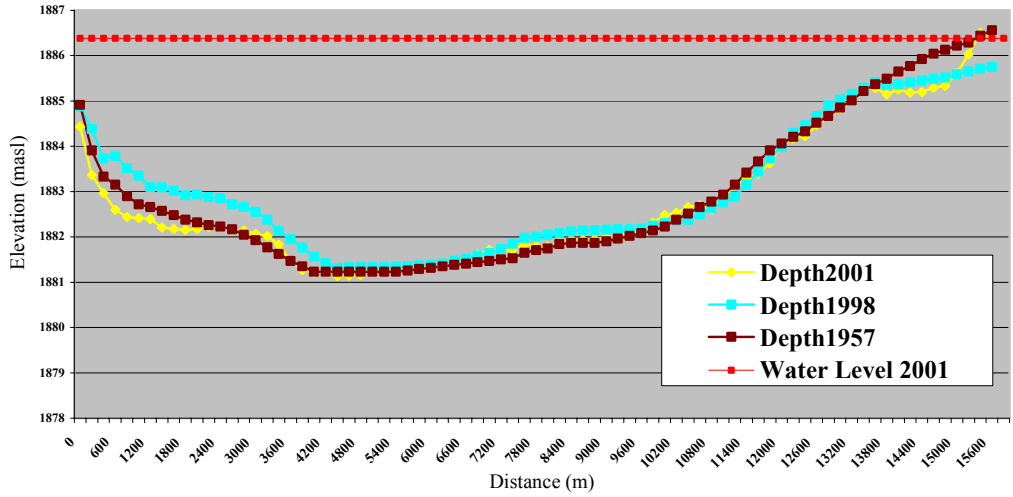

Figure 4.18: Lake Bed Changes from 1957 to 2001
Along the Profile SW to NE

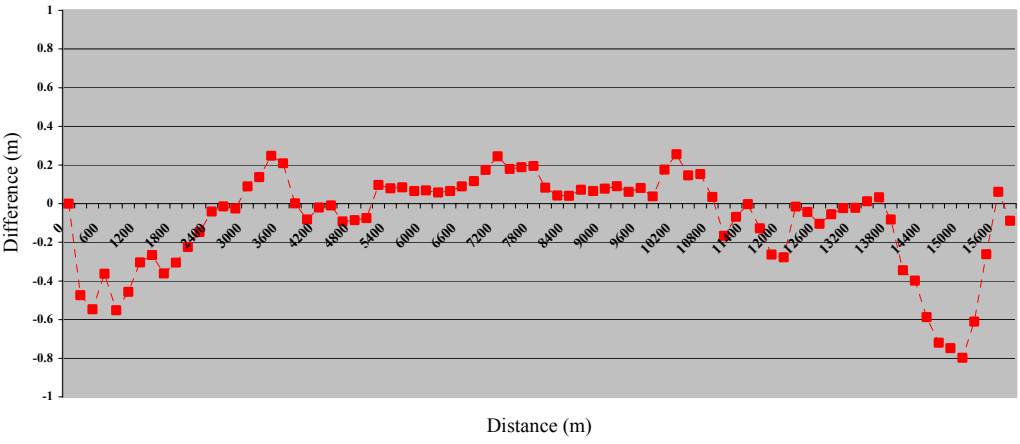

Figure 4.19: Cross Sections Across the Profile of River Intakes

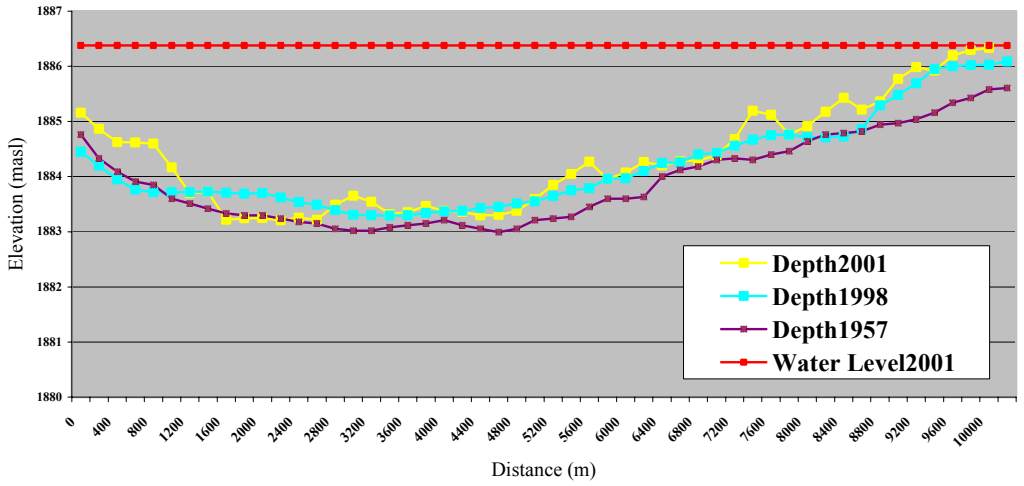

Figure 4.20: Lake Bed Changes from 1957 to 2001 Across the Profile of River Intake

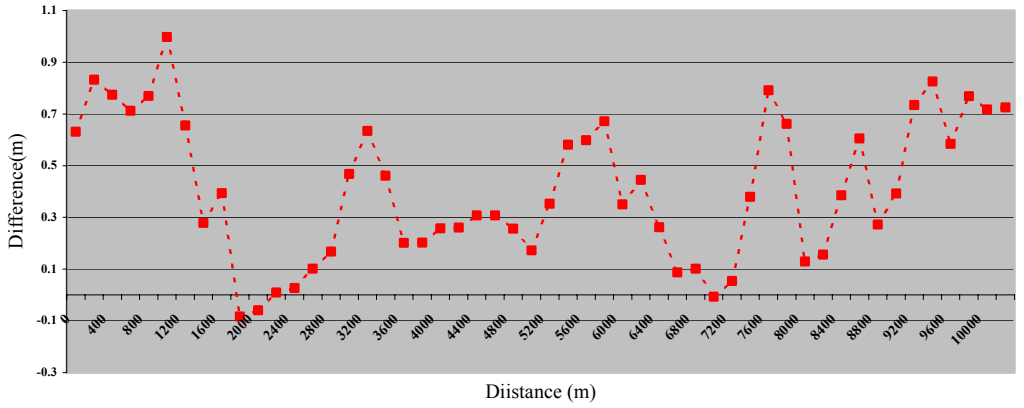

From Figures 4.11 to 4.14, it is important to notice that 1957 and 2001 survey bed profile follows almost the same profile especially in the Crescent Lake. Even though different techniques were used in 1957 and 2001 surveys, coordinates fit each other indicating the considerable accuracy of 2001 data points. In 2001 survey, as the lake outer boundary was limited to 1886.67 masl, Cresent Island top levels are not indicated.

According to Figures 4.11 and 4.12, cross section along the profile from north to south, it shows that there was sediment deposition from 1957 to 2001. It indicates that the lake central area less deposition compared to the lakeshore. Maximum deposition of 0.9 m was recorded in the north side of the lake. Along the profile from west to east only shore area indicated sediment deposition while in the other side Cresent Lake has maximum deposition is about 1.5 meters during 1957 to date. Also this shows the lakebed topography changes due to sediment deposition in the direction from west to east. Around shoreline, higher deposition takes place may be due to increase of human intervention from 1957 to 2001 or may be due to sediment redistribution.

Cross-sections along the profile southwest to northeast show that the lakeshores in 2001 survey are below than the 1957 survey. During the period of 1957 survey, this area was under the papyrus belt, which highlighted in 1957 original analogue maps. Therefore, 1957 survey contours could not extended. This may lead to interpolation problems within the area or another reason could be the loss of papyrus belt in the area during 1957 to 2001. Another possible reason could be the activities of hippo families in the lake. But in central lake area, it clearly indicates that the sediment deposition of about 0.2 m and also eroded areas. Lake cross-section profile along the direction of northwest to southeast shows the higher sediment deposition only in the southwest corner of the lake. This area recorded the maximum depth of deposition about 3.50m. As indicated by earlier surveys, deepest point is in the Cresent Lake and the recorded deepest bed level was 1872.23 masl.

In lake Naivasha, redistribution of suspended sediment takes place along the north to south direction as the rivers enter to the lake in Northern part. The forces acting upon a sediment particle brought to a lake by stream flow include a horizontal component due to the force of water acting upon the particle in the direction of flow and a vertical component due to force of gravity. Explanation of having maximum deposition in the south east area is the shape of the lake and particles remains in suspension and is transported through wind into the lake south east area so as long as turbulence exists, creating an upward force equal to, or exceeding, that of the force of gravity.

For a particular water body, the locations of the outlets in respect to distribution of sediment concentration within the lake determine the extent of sediment venting which will occur (Chow, 1964). But in the case of Lake Naivasha, as there is no surface outlet, case is different from other water bodies. The distribution of sediment in the lake is dependent upon several interrelated factors, including nature of sediment, wind direction, inflow-outflow relations, shape of lake etc., When a flow enters the lake the increased cross section area and wetted perimeter result in a decrease in velocity and turbulence of the original stream flow, forced to settle down the coarse grained particles eventually, specially in the u/s of the lake (Northern delta). Therefore mainly suspended sediment deposition could be expected within the main lake area.

4.1.4 Analysis of Sediment Core Samples in the Lake

Five undisturbed lake sediment core samples were collected and analyzed for dry density of deposits and particle size analysis in the ITC Laboratory as described in the Materials and Methods. Dry weight of sediment deposition used to convert lake sediment volume to dry weight while particle size analysis used to estimate the sediment Trap Efficiency of the lake. These calculations are presented in Chapter 5.0.

4.1.4.1 Specific Weight of Core Samples

Out of the five samples one sample (Gilgil Intake to the lake coordinates at 203734, 9918910) was analyzed as four separate samples to represent four layers as top sediment, middle, bottom 20cm-40 cm and bottom. This was done to check the variation of dry density according to the depth of deposition. Other four samples were analyzed separately as a whole. Details of the sample analyzed for separate four sub samples are given in table 4.4 and Figure 4.21. Results of all samples along with sampling locations are shown in Table 4.5 and Figure 4.22.

It shows that the dry weight is increasing when the depth of sediment core is increasing. This is due to the increase of pressure of water column as well as increase of sediment weight. Average Specific weight of the deposition is about 0.3238 g/cm^3 .

Table 4.4 and Figure 4.21: Variation of Specific Weight over the Depth Profile

Sample Depth	Specific Weight (g/cm^3)
Bottom	0.32
Bottom 10-20 cm	0.28
Middle	0.21
Top	0.13

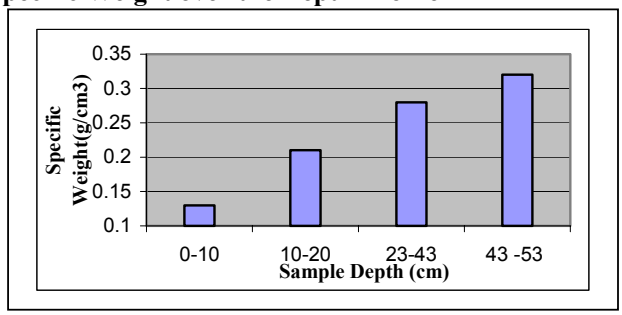

Table 4.5 and Figure 4.22: Specific Weights and Locations for Sediment Core Sampling

Sample Location	Coordinates	Specific Weight (g/cm^3)
Sewage to the lake (S-1)	(211725, 9918910)	0.474
River Intakes (S-2)	(203734, 9918910)	0.24(avg.)
SE side of the lake (S-3)	(199761, 9910977)	0.153
SW part of the lake (S-4)	(208399, 9910381)	0.255
Gilgil Intake (M-1)	(203697, 9921152)	0.497

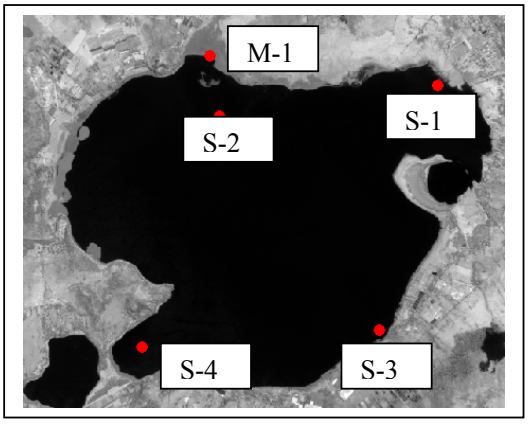

4.1.4.2 Particle Size Analysis

Particle size analysis was carried out for the same samples in order to find the % sand, silt, clay and organic matter content using the standard procedures (Van Reeuwijk, 1995). Results are shown in the Table 4.6 below.

Table 4.6: Particle Size Analysis and Organic Matter Content

Sample	ID	%Sand	%Silt	%Clay	% Carbon Content	% Organic matter
1	M-1	1.31	25.31	73.38	2.84	5.67
2	S-1	6.75	57.77	35.49	7.02	14.04
3	S-2	0.87	39.03	60.10	10.53	21.06
4	S-3	13.43	41.36	45.21	8.60	17.19
5	S-4	11.07	51.23	37.70	11.50	23.00

Form the results of particle size analysis; it shows that the highest clay contents recorded in the river intakes to the lake. In overall basis, lake sediment contains higher percentage of clay and silt while % sand is very low. In southern part of the lake, core samples have high silt content as well as in the location of sewerage inlet to the lake. Also high percentage of organic matter content reported in the southern part of the lake.

4.1.5 Lake Suspended Sediment and Turbidity

Lake turbidity and suspended sediment parameters were measured as described in Chapter (3), Materials and Methods. In-situ measurements of lake turbidity were carried out in 104, well-distributed locations in the lake as grab samples in order to observe the lake turbidity variation.

4.1.5.1 Lake Turbidity Sampling

Summary statistics for turbidity is given in table 4.7. Lake Turbidity map was created using the ordinary kriging interpolation techniques. For the ordinary kriging, Spherical Model with Nugget 40, Sill 185 and Range 3000 was selected as shown in Figure 4.23. Resultant Lake turbidity map and kriging error maps are shown in the Figure 4.24.

Table 4.7 and Figure 4.23: Summary Statistics and Semi variogram for Turbidity

Parameter	*Turbidity*
No. of observations	*104*
Minimum Value	*3.2*
First Quartile	*12*
Median	*14.5*
Third Quartile	*21.3*
Maximum Value	*72.7*
Mean	*19.8*
Standard Deviation	*14.2*
Skewness	*1.8*

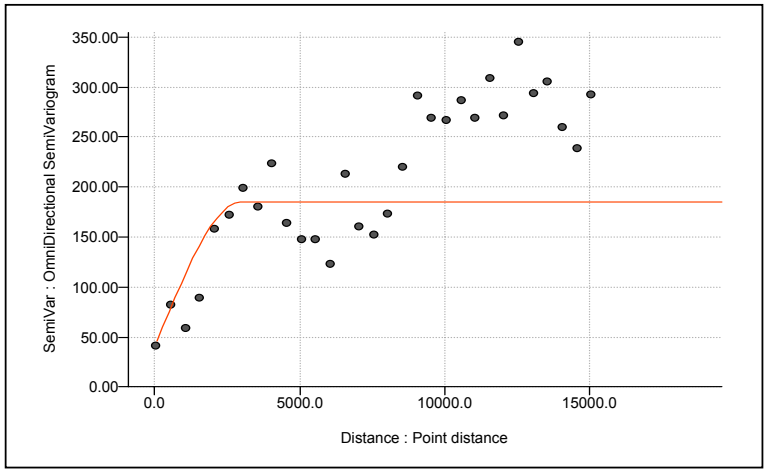

Figure 4.24: Lake Turbidity Map and Error Map using Ordinary Kriging

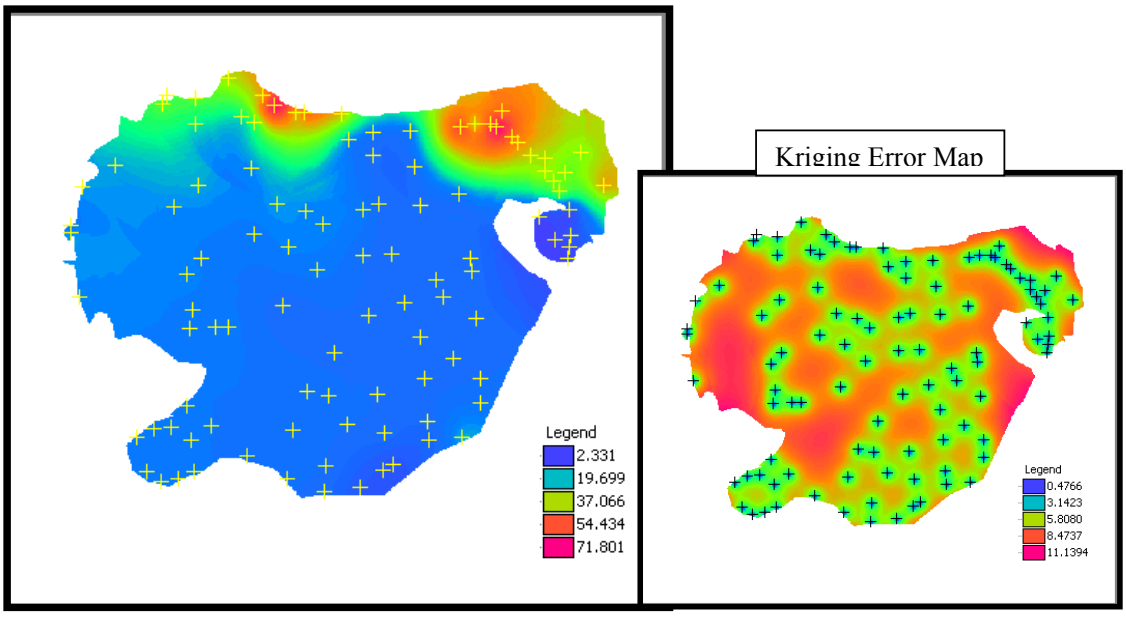

High turbidity values recorded in the northern parts of the lake, where rivers enter the lake. Also, another red spot of high turbidity recorded in the northeast part of the lake where Naivasha town sewerage enters to the lake.

4.1.5.2 Lake Suspended Sediment Sampling

Suspended sediment samples were collected in 14 locations especially around the lakeshore locations to observe the shoreline effect. Samples are analysed in the ITC laboratory as described in Chapter (3), Materials and Methods. Figure 4.25 shows the sampling locations while Table 4.8 gives the results of the analysis.

Figure 4.25 and Table 4.8: Locations of Suspended Sediment Sampling

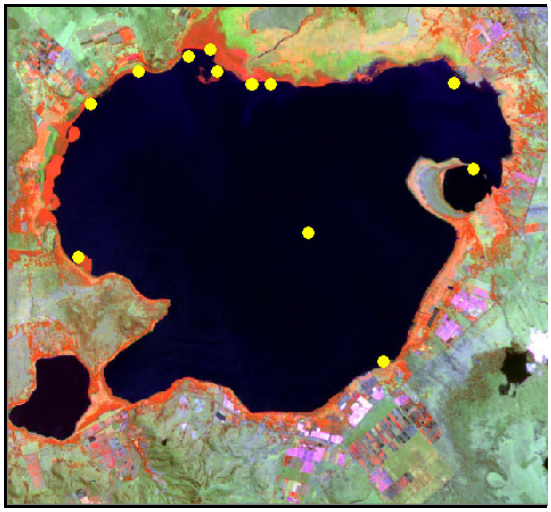

Date	Location	SS (mg/l)
26/09/01	Lake Naivasha	62.0
26/09/01	Lake Naivasha	58.0
26/09/01	Lake Naivasha	82.0
27/09/01	Lake Naivasha	68.0
27/09/01	Lake Naivasha	72.0
28/09/01	Shore North near Malewa	82.0
28/09/01	Malewa inflow	82.0
29/09/01	Crescent Island	40.0
29/09/01	Channel farm discharges	56.0
30/09/01	Sewage Inlet	116.0
30/09/01	Malewa I	184.0
30/09/01	Malewa II	140.0
30/09/01	Gilgil Inflow	74.0

From the data it shows river intakes to the lake and sewerage intake has high-suspended sediment concentration of about 140-180 mg/l while other part of the lake around 70-80 mg/l. Lowest value recorded in the Cresent Lake.

4.1.5.3 Correlation Between Turbidity and Suspended Sediment

Correlation between turbidity and suspended sediment concentration is important to estimate the suspended sediment concentration through turbidity measurements. In order to develop a correlation between suspended sediment and Turbidity in the lake, seven sample sets were selected in the same location and same sampling data. Figure 4.26 shows the variation of turbidity and suspended sediment concentration in the lake.

Figure 4.26: Turbidity and Suspended Sediment in Lake Naivasha

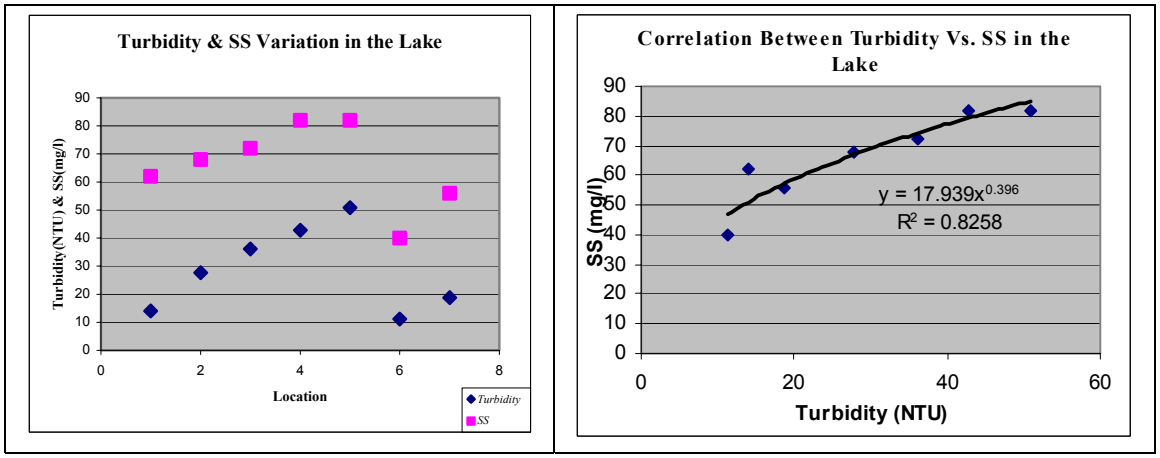

According to the graph of lake turbidity vs. suspended sediment, it shows better correlation between suspended sediment and turbidity. This relationship can be used to develop lake suspended sediment map.

4.2 RIVER SAMPLING

4.2.1 Detailed Cross Section Survey on Rivers Malewa and Gilgil

Detailed Cross Section Survey was carried out using Engineering Levelling instrument in selected river reaches along Malewa and Gilgil rivers to develop discharge-rating curves as described in Chapter (3), Materials and Methods.

Sites selection criteria for the cross section survey was as follows. Primary factor was the accessibility to the river sections through private lands. Also wild animals make access to the area difficult and selection of less danger sites was the one of prime concern. Apart from that, a fairly uniform, straight reach was selected for each river locations. As it is necessary to link information on each river reach to a common datum, for altitude measurements GPS was calibrated at the Naivasha Railway Station benchmark and used to get the approximated instrument height in each location. Accuracy of the GPS altitude measurements was check with top sheets and it was within the range of +/-1 – 3 m.

Surveying techniques used in this cross section surveys are the standard engineering levelling practices. Cross section data was processed and transferred to the approximate mean sea levels using the standard height of Collimation method. Photographs were taken for each river reach cross sections during the time of survey. Observation was made on riverbeds and bank characteristics in order to estimate the roughness coefficient along with the photos. Location map indicating each river reach is given in Figure 4.27.

Figure 4.27: Location Map and Details of Cross Sections

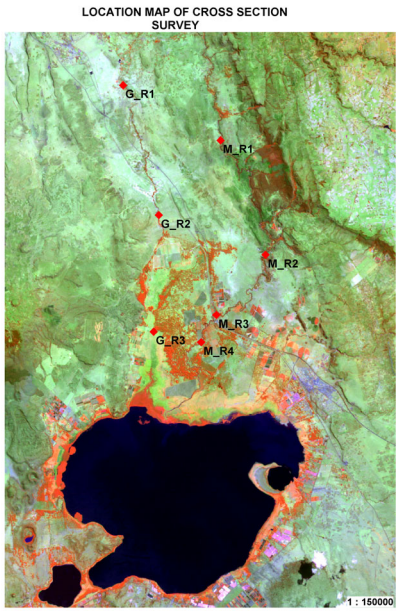

Table 4.9: Details of River Reaches

Location ID	Coordinates	No. of Sections
Malewa		
M_R1	**(0210964, 9937492)**	**05**
M_R2	**(0212775, 9929758)**	**05**
M_R3	**(0209112, 9926354)**	**01**
M_R4	**(0207893, 9924762)**	**04**
Gilgil		
G-R1	**(0205309, 9941910)**	**04**
G_R2	**(0206379, 9933272)**	**05**
G-R3	**(0204987, 9925862)**	**02**

4.2.2 Analysis with HEC RAS Software

HEC-RAS 2.2, (River Analysis System, Version 2.2 developed by the U.S. Army Corps of Engineers) software is an integrated package of hydraulic analysis programs, in which the system is capable of performing steady flow water surface profile calculations. Out of the various simulation models available in the software, in this thesis concentrates only on the development of rating curves for each river reach. These parameters were used to estimate the bed load transport calculations for each river.

Theory based on the software is the open channel flow formulas (HEC RAS User Manuel). The Manning's Equation, one of the well-known Equations, was used as the basis for computing the reach properties and the roughness coefficients. As input Parameters cross sections, estimated Manning's n values and contraction and expansion coefficient for each river reach was used. Processed cross sectional data were used for the geometric boundary of the rivers in Malewa and Gilgil.

Manning's n values

Familiarity with the geometry, appearance and roughness characteristics of known channels will improve the ability to select roughness coefficients for other channels. Manning's roughness was estimated for each river reach according to the reference made by (Harry H. Barnes, 1849) and using the HEC_RAS Manuel along with the river cross sectional properties and the photographs for each river reach in Malewa and Gilgil.

Table 4.10: Estimation of Manning's Roughness Coefficient

River Station	Description	Estimated n		
		Left	Bed	Right
River Malewa				
Reach (1)	D/S of the main gauging station			
D/S of 2GB1	Clean, straight, full stage, no rift or deep pools, but more stones in bank. Bed and sides composed of large angular exposed rock boulders.	0.053	0.06	0.07
Reach (2) Diary Training School	Riverbed composed of sand and gravel. Banks are lined with trees and small underbrush. Left bank covered with high-density vegetation while right bank less density trees and eroded faces.	0.037	0.034	0.036
Reach (3) Close to lake Italian premises.	Steep banks with overhanging trees and bushes. Bed with gravel and cobbles. Straight reach.	0.040	0.039	0.040
River Gilgil				
Reach 1 -After confluence of little Gilgil	Riverbed composed of sand, silt and clay. Banks are covered with grass.	0.027	0.025	0.026
Reach 2 Gauging Station	Bed consists of sand and clay. Banks are generally smooth and covered with grass. Specially left bank dense growth while right bank is less dense.	0.027	0.02	0.025

4.2.2.1 Results of HEC-RAS Analysis

Results of river reach analysis using HEC-RAS for Malewa, Reach (1) is shown below. Detailed calculation tables are given in the Appendix 4.5.

Figure 4.28: Malewa – Reach (1) – Downstream of the Gauging Station 2GB1

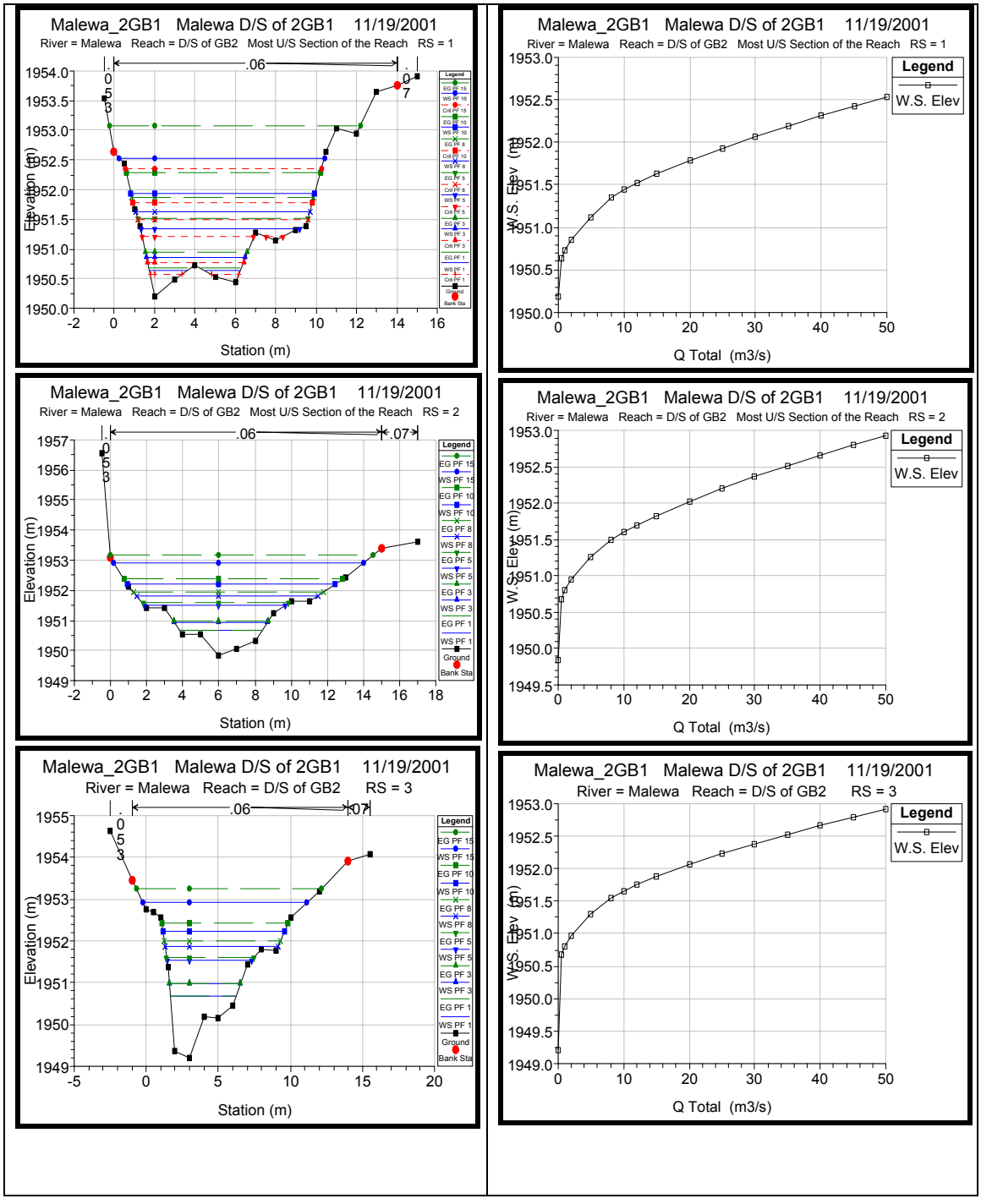

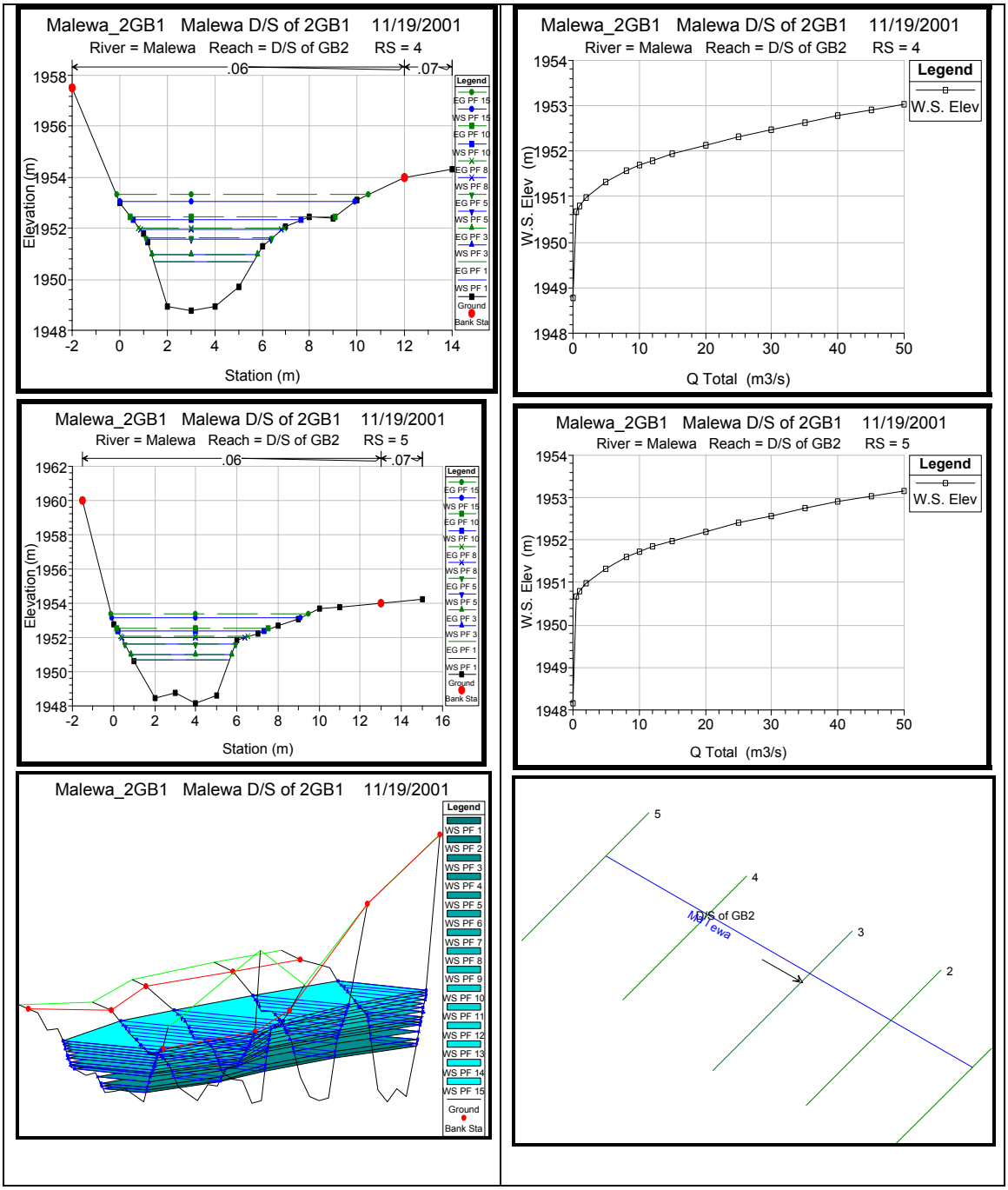

Malewa – Reach (2) – Diary Training School

In Malewa River at Diary Training Institute has been selected as the River Reach (2). Simulated model results are shown below. Detailed cross section tables and calculation tables are provided in the Appendix 4.6.

Figure 4.29: Malewa Reach (02) Results

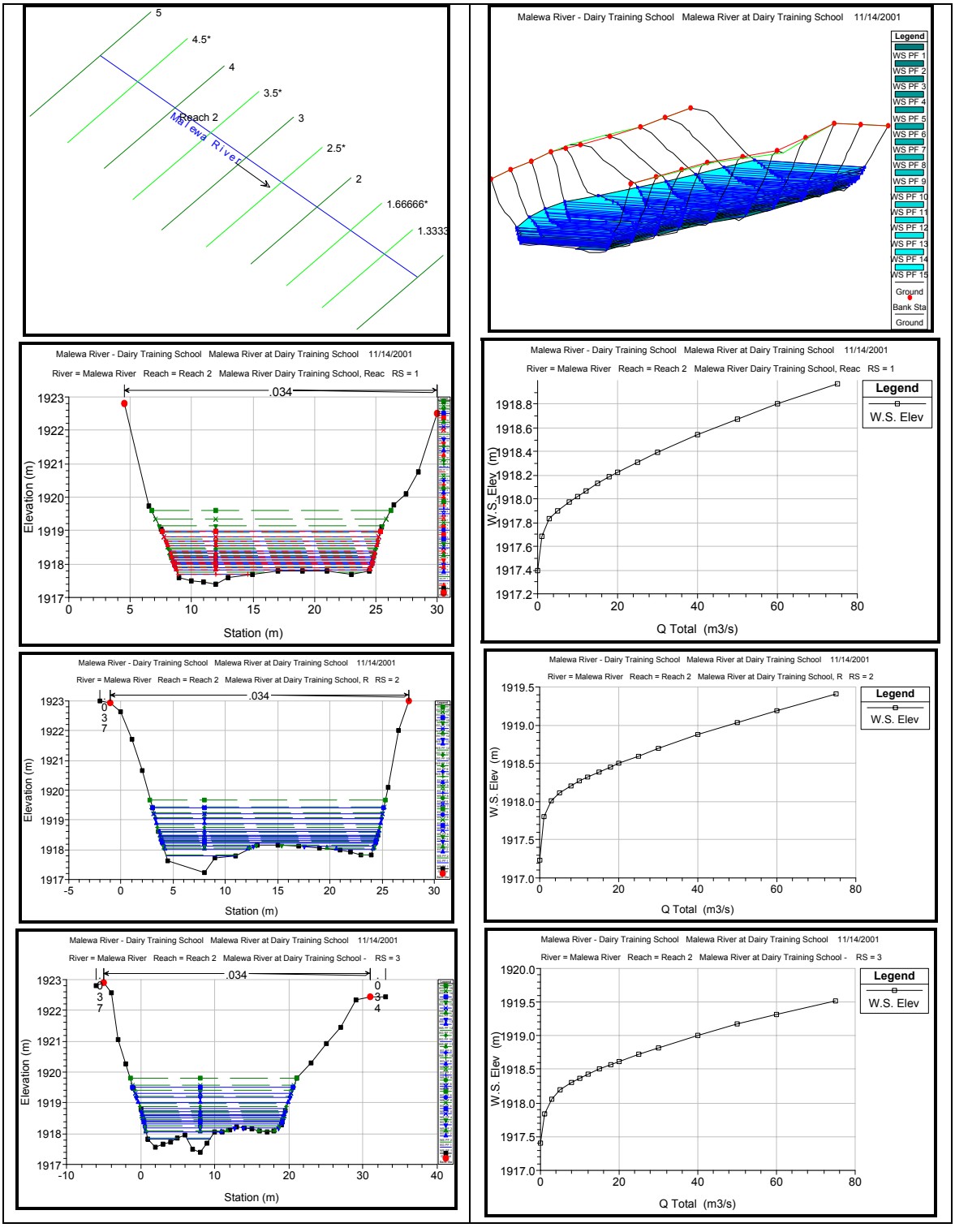

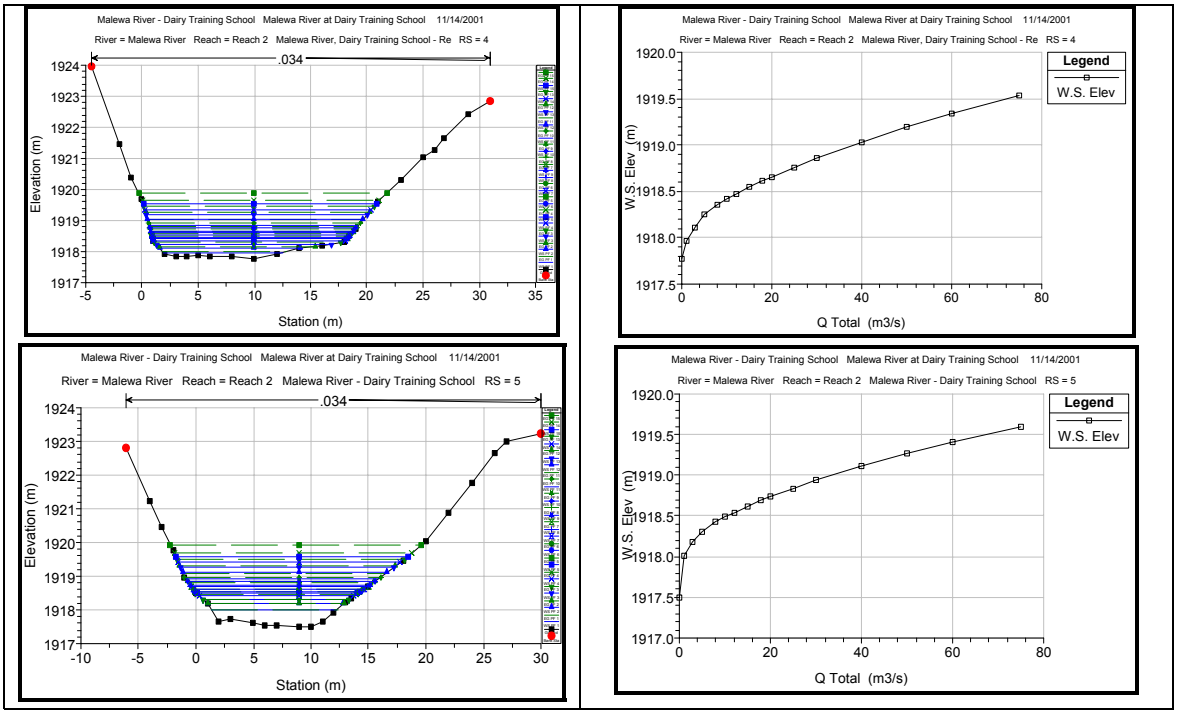

Figure 4.30: Malewa River – Reach (4) - Close to the Lake at Italian Premises

Detailed calculation tables are shown in the Appendix 4.7.

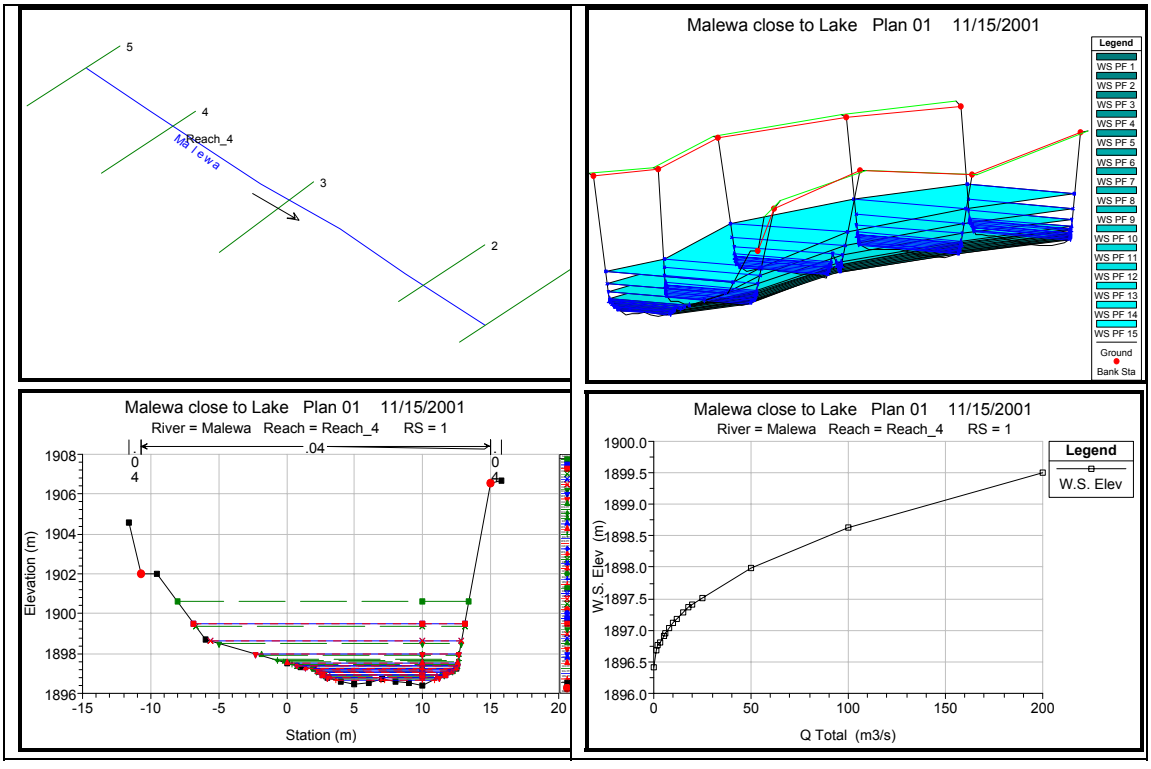

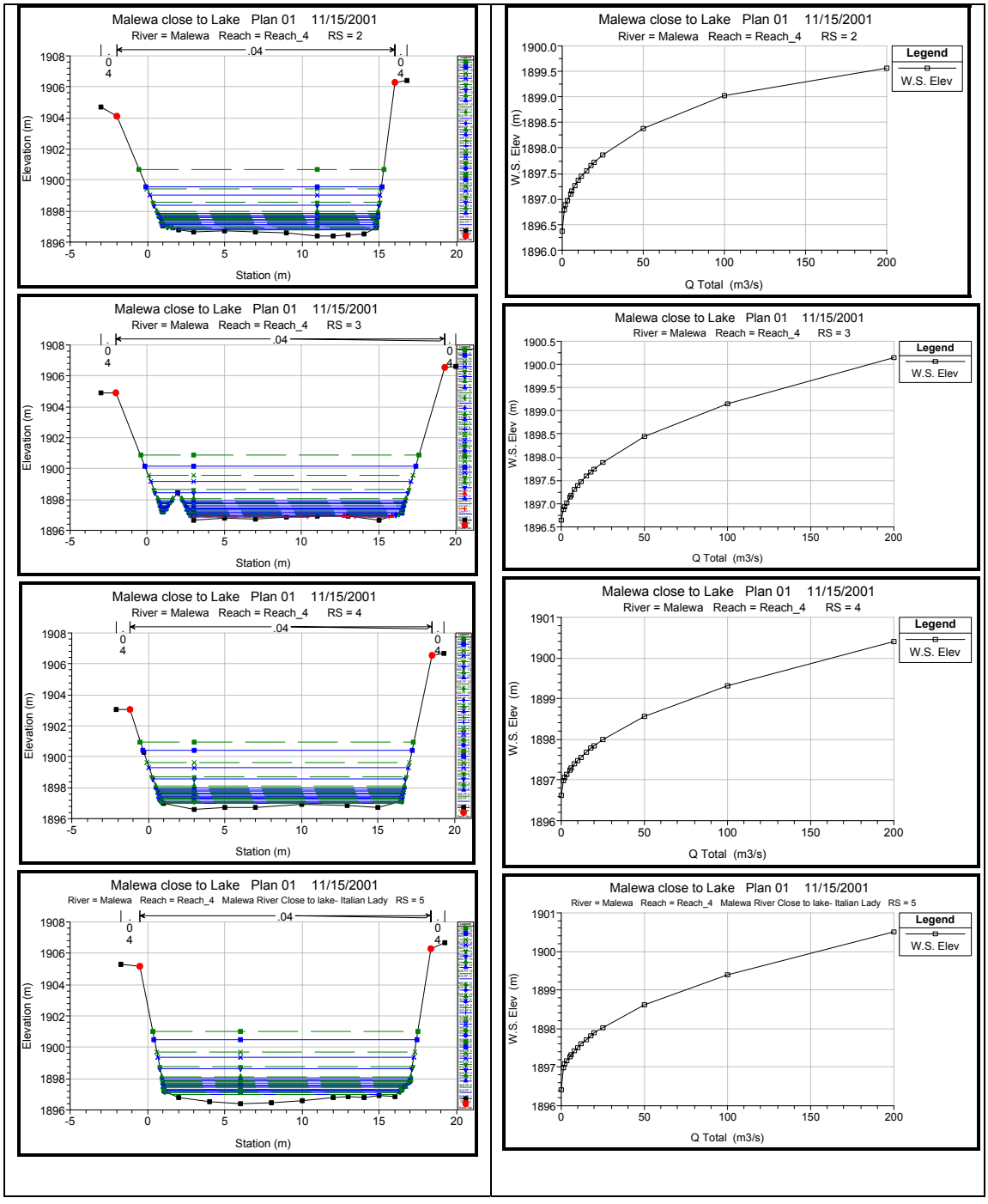

Gilgil River

In Gilgil River, two river reaches were modelled while third reach only measured two cross sections close to the lake.

Reach (1) location was just below the confluence of little Gilgil and Reach (2) was at the Gauging Station 2GA1. Results obtained from HEC RAS modelling are given below while the Appendices 4.8 and 4.9 provides the detailed calculations.

Figure 4.31: Gilgil Reach (1)

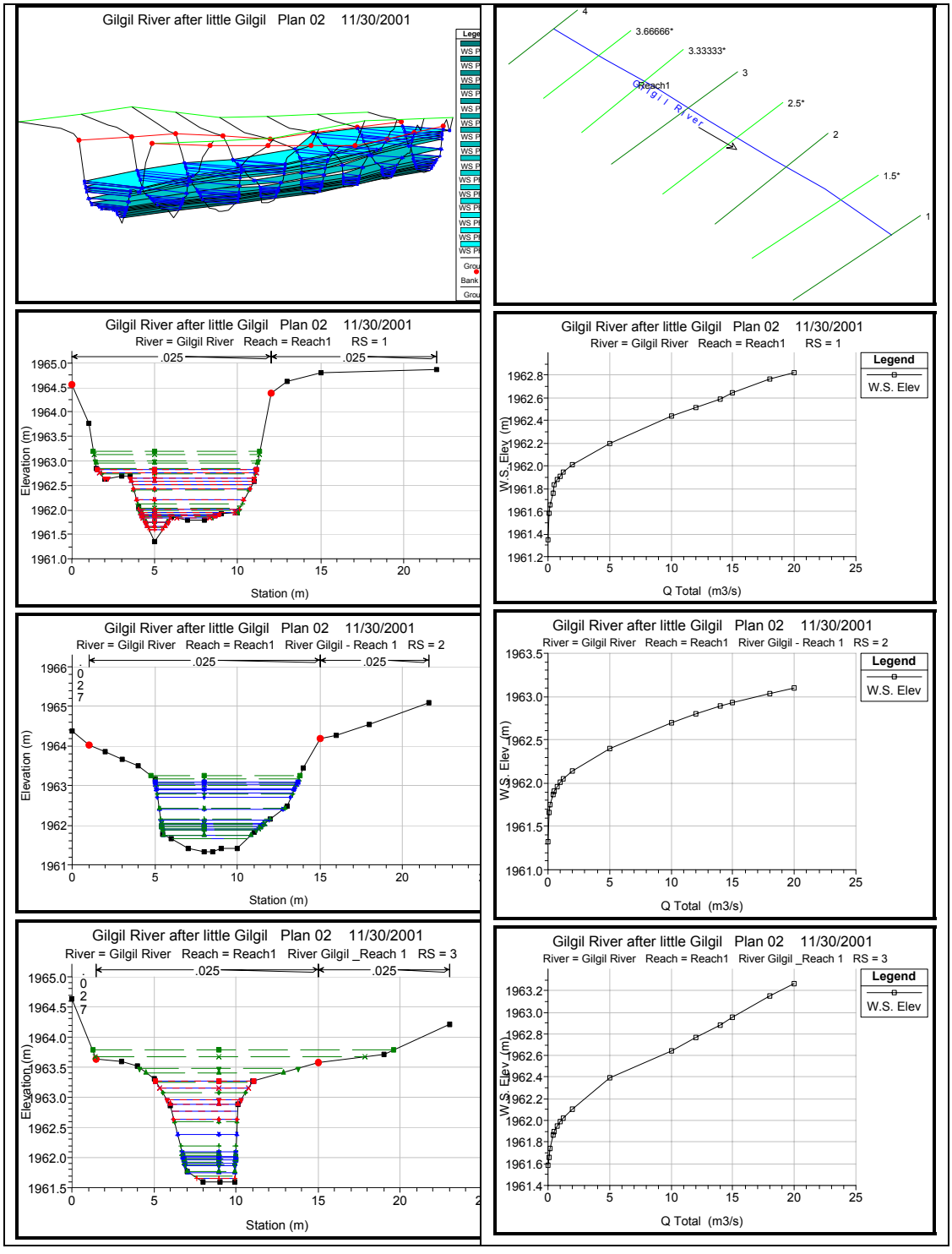

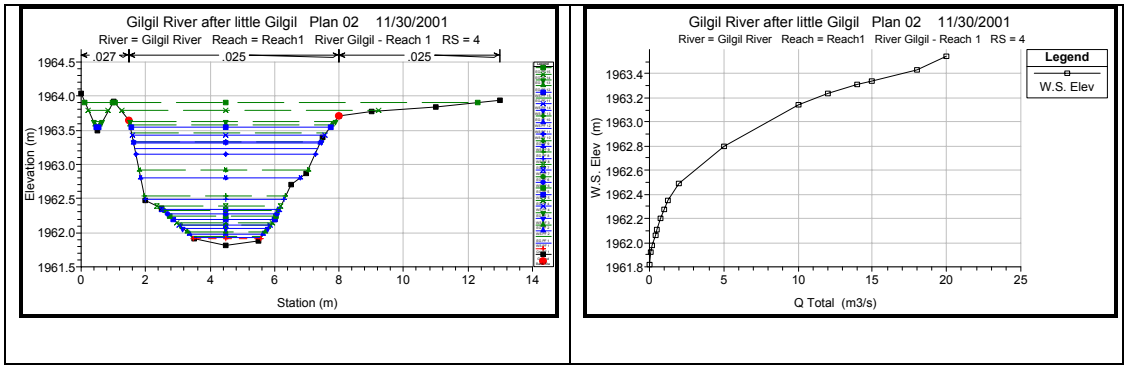

Figure 4.32: Gilgil Reach (02) at Gauging Station 2GA1

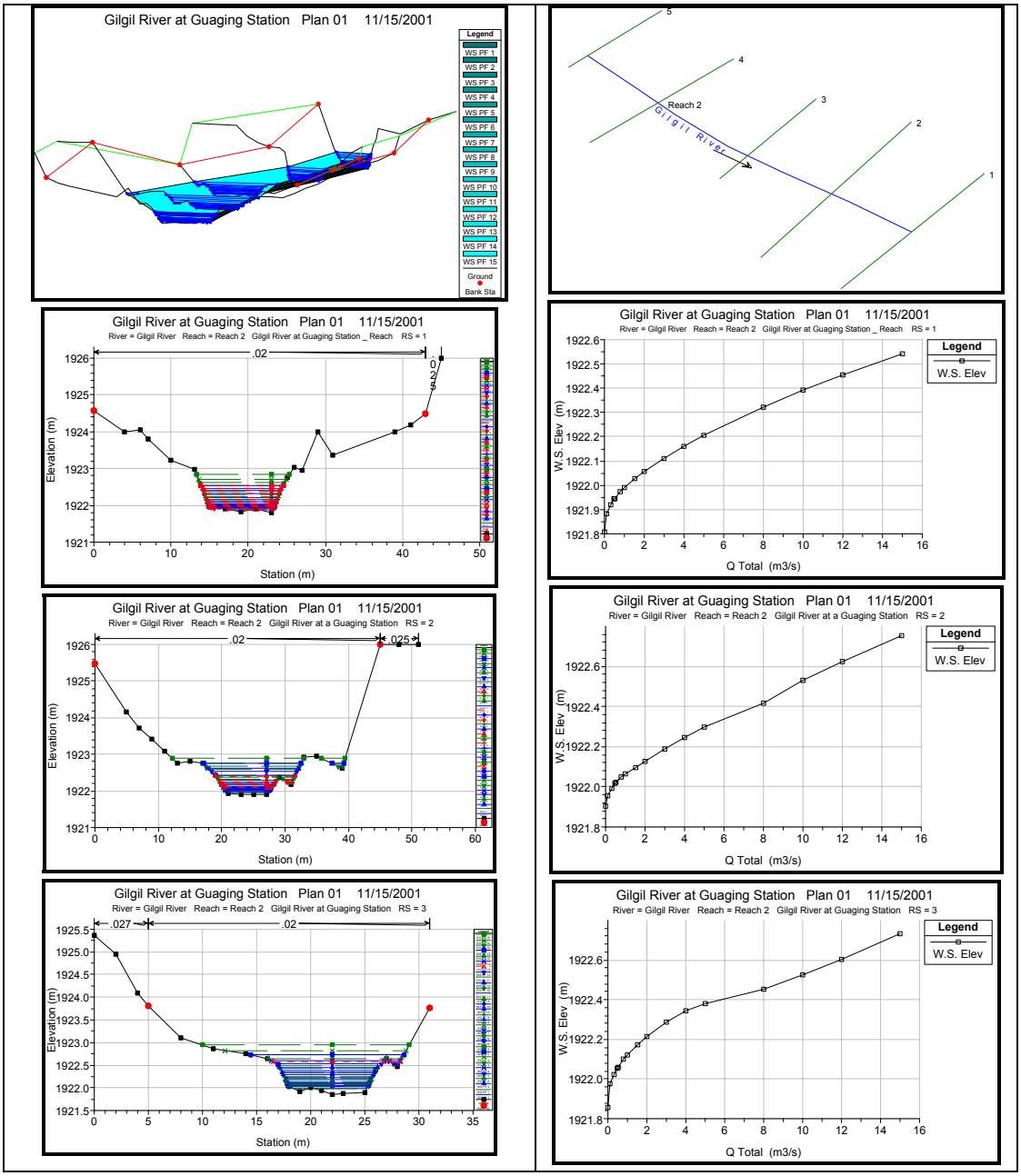

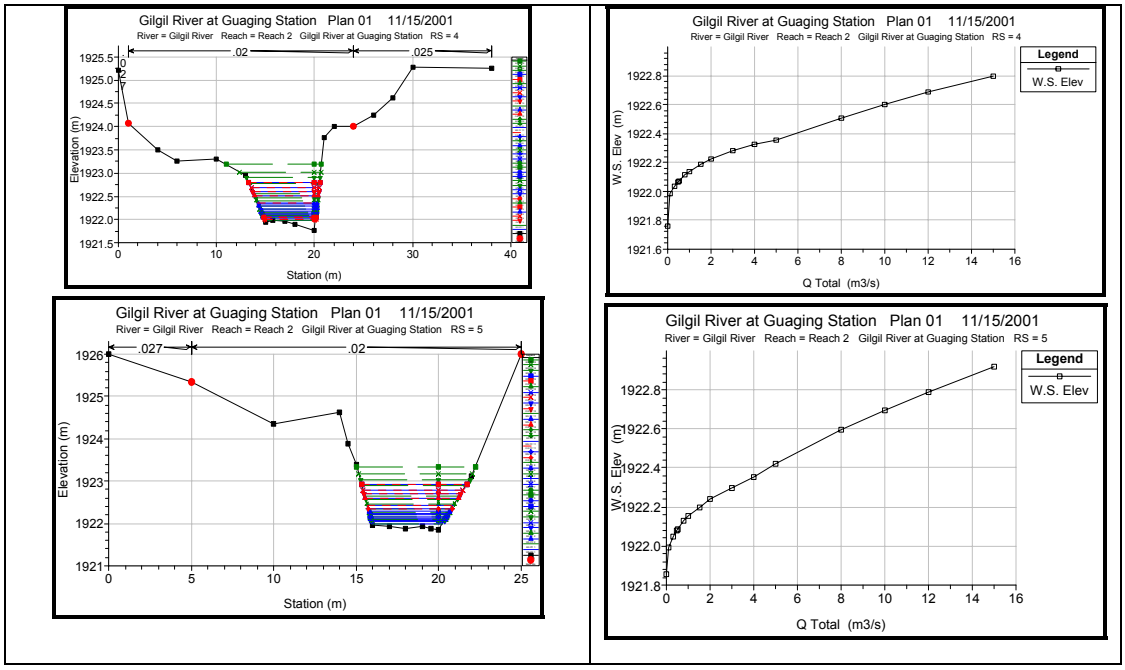

Validation of HEC_RAS Results

The results of HEC_RAS were checked with the measured discharge and average water surface elevation within the reach. This allowed validating the estimated parameters such as Manning's roughness. Results are as follows.

Table 4.11: Comparison between Measured parameters and HEC_RAS Results

Reach	Measured parameters		Results
	Avg. water level Elevation (masl)	Flow (m^3/sec)	Avg. water level Elevation (masl)
Malewa			
Reach (1)	1951.44	5.50	1951.316
Reach (2)	1918.35	8.10	1918.258
Reach (4)	1897.15	3.0	1897.048
Gilgil			
Reach (1)	1962.15	0.724	1961.99
Reach (2)	1922.15	0.555	1922.04

The differences in the measured and modelled water surface elevation for the measured discharge could be expected due to various reasons. Measurement errors of the discharge and elevations as well as may be due to the estimated modelled parameters. But it is important to notice that average values obtained for the reach don't shows significant difference.

4.2.3 Turbidity and Suspended Sediment Sampling in Malewa

During field visits, grab samples were collected at following locations to estimate the turbidity and suspended sediment concentration in Malewa and Gilgil Rivers. This was done during the period between 14th to 21st September 2001, which prevails base flow condition in the rivers. Another set of samples was collected immediately after heavy rains to the Malewa catchment, during the period 01st

to 3rd October 2001. It was observed immediately after the rain Malewa had high flow with high turbid water compared to the normal base flow conditions. Sampling locations are shown in the Figure 4.27.

Figure 4. 33: Suspended Sediment and Turbidity Variation during base flow and after rain

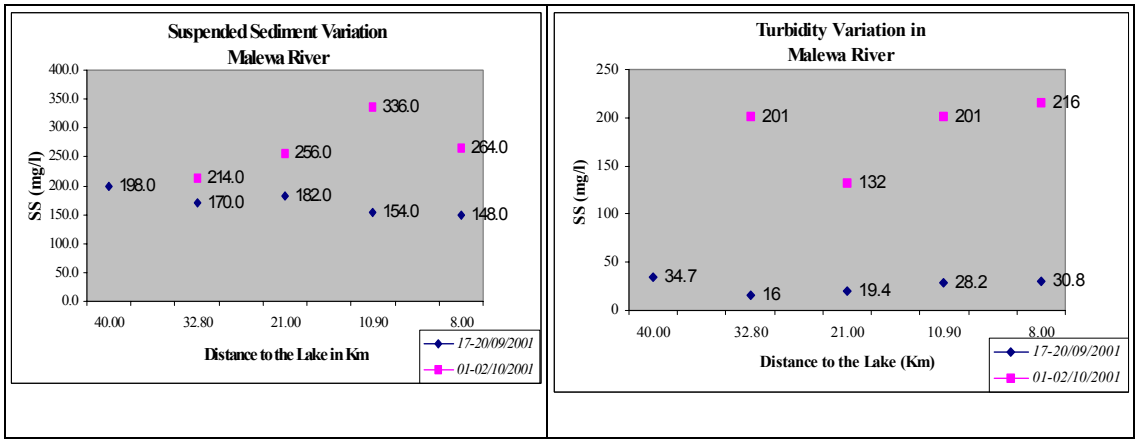

Figure 4.34: Correlation Between turbidity and SS

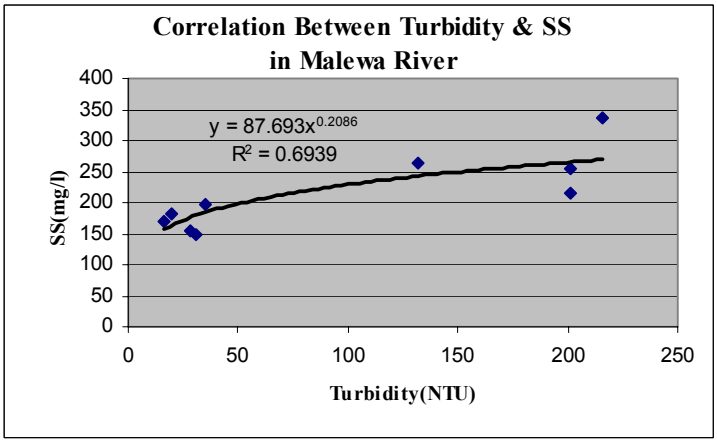

Graphs show the variation starting from the gauging station towards the lake. During the period of base flow condition; suspended sediment in Malewa River shows low values and reducing trend towards the lake. It shows clearly from the turbidity measurements, immediately after the rain turbidity has increased in river Malewa dramatically compared to the base flow conditions. This was due to the high discharge and high velocity tends to maintain the suspended sediment particles in motion. On 1st October,2001 immediately after the rain, three measurements in different locations indicated that higher turbidity values around 200 NTU. On 2nd October, just after one day, in Malewa at Dairy Training Institute, shows less value of 132 NTU compared to 1st October measurements.

4.2.4 Turbidity and Suspended Sediment Sampling in Gilgil

Turbidity and suspended sediment measurements were carried out using the turbidity meter and grab sampling respectively in the Gilgil River. G-R1, G-R2 and G-R3 indicates the locations as shown in the Figure 4.27.

Figure 4.35: Turbidity and SS variation in different dates

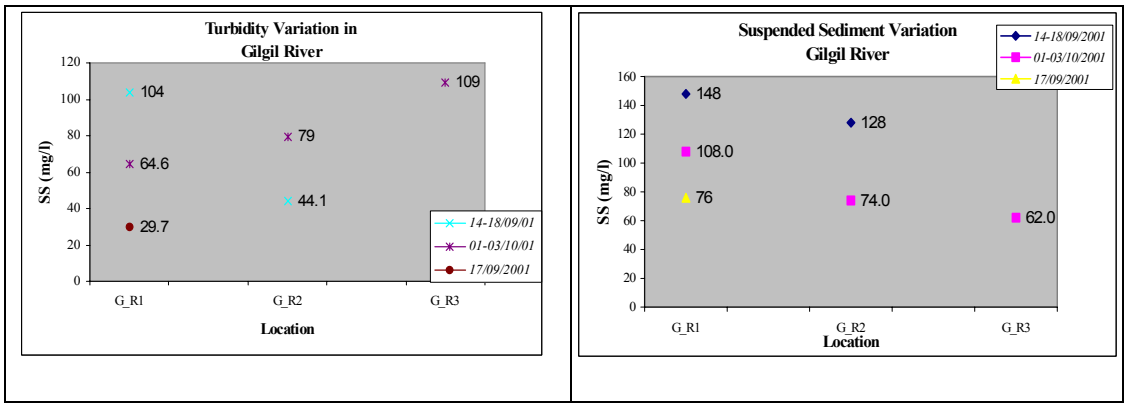

During field observations, Gilgil shows apparently high turbid condition compared to Malewa, even during base flow condition due to high human interaction especially in the sampling point G_R1 (After the confluence of little Gilgil). From the measured data it shows the turbidity variations in the same location in different dates.

In the gauging station 2GA1(G-R2), low turbidity values were recorded compared to other locations in the same day. Around the gauging station, less human activities and quiescent flow conditions enhanced particles to settle and this gives low turbidity. Also it was observed that close to the lake higher values recorded compared to the gauging station during the same day. As Gilgil River has many diversion points through private farms only little percentage of Gilgil discharge finally reaches to the lake. This could be observed in the sampling location G_R3 (Close to the lake). Even though with few samples, it can be observed that the suspended sediment concentration reduces towards the lake.

Correlation of turbidity with the concentration of suspended matter is sometimes difficult because the size, shape and refractive index of the particles affect the light scattering properties of the suspension. When present in significant concentrations, particles consisting of light absorbing materials cause a negative interference. In low concentrations these particles tend to have a positive influence because they contribute to turbidity. The presence of dissolved; color-causing substances that absorbed light may cause a negative interference**.**

In the case of Malewa, it shows better correlation between turbidity and suspended sediment concentration. As the river turbidity measurements were not carried out site in-situ, measurement errors or presence of light absorbing substances may contribute to an error component. Gilgil River measurements show a bad correlation due to few outlier measurements. This is also possible due to measurement error or applying post measurement techniques, which contribute wrong results.

CHAPTER 5.0 – ANALYSIS OF RIVER SEDIMENT FLUXES AND LAKE SEDIMENTATION

5.1 EXPLANATORY ANALYSIS OF MALEWA RIVER SEDIMENT FLUX

Malewa and Gilgil are perennial rivers. Inflows from Malewa and Gilgil rivers for 29 years period from 1936 to 1964 were calculated by Englend and Robertson(1969) as in Phase I Report of LNRA, to produce a change in volume of the lake equivalent to 269 mcm of which 89.9% was attributed to the Malewa. This shows remarkable contribution of Malewa flows to the lake.

5.1.1 River Malewa –Time Series of Discharge

For Malewa river, **Ase et al.,(1986),** constructed a discharge rating curve from the available hydrological data collected by the Ministry of Water Development in Nairobi for gauging station 2GB1, during the periods 1931- 1949 and 1951-1959.
Using the above rating curve (during the period 1932-1980),

Average annual flow = 153 x 10^6 m^3 (= water column of 100 mm over the drainage area)
Recorded annual maxi. flow = 328 x 10^6 m^3 in 1964 (= 211 mm over the drainage area)
Recorded annual min. flow = 53 x 10^6 m^3 in 1939 (= 34 mm over the drainage area)

Mmbui(1990), Podder(1989) and Tessema(2001) studied the water balance models for lake Naivasha and they made calculations including filling of data gaps for the Malewa river. The time series of discharge data as shown in Figure 5.1 was used to calculate the annual sediment load to the lake.

Figure 5.1: Monthly Discharge at 2GB1, Malewa

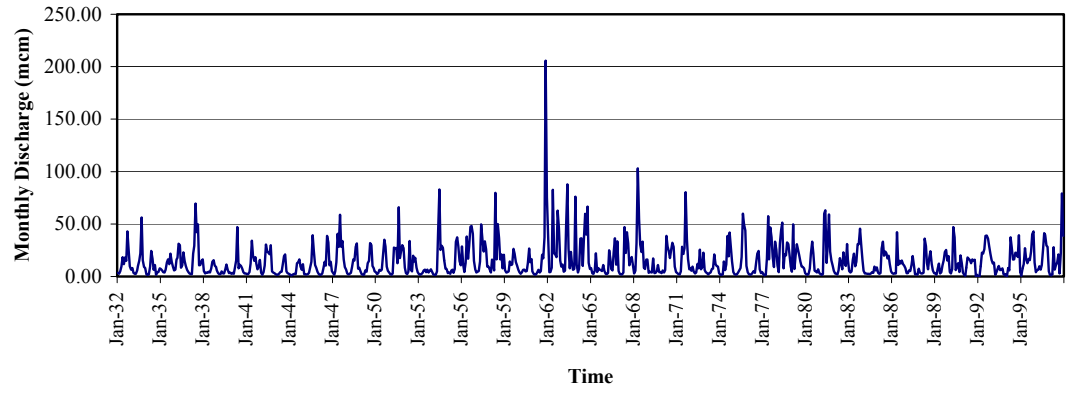

5.1.2 Available Suspended Sediment Data

Sediment measurement of Malewa river at Gauging Station 2GB1 had been recorded during early 1950's. Unfortunately no evidence was found on continuous sediment concentration records in Malewa. Available past records are given in Appendix 5.1.

A suspended sediment-rating Curve for Malewa at gauging station 2GB1, has been included in the Report published by the Viak for the Ministry of Agriculture for Naivasha Water Supply Project in 1974. It seems that during that period sediment measurements had been carried out and used for suspended load calculations. The Sediment Rating Curve for Malewa included in the Viak Report is given in Appendix 5.2.

5.1.3 Suspended Sediment Load Estimation

5.1.3.1 Direct Estimation using Measured Sediment Data

As reported in Chapter 4.0, Field Data Collection and Analysis, Turbidity and suspended sediment measurements were carried out during fieldwork in different locations along the Malewa river. This was done at base flow conditions and just after rainstorm.

Daily-suspended sediment discharge can be computed with a relatively high degree of accuracy if the discharge and sediment concentration don't change rapidly. Total suspended sediment discharge in tons/day is the product of the flux averaged total sediment concentration, the daily mean water discharge and a conversion factor. The daily-suspended sediment load calculation is done using the following equation as described in Chapter 2.0.

$$\mathbf{Qs\ (metric\ tons/day) = 0.0864C_{mg/l} * Q_{m3/s}}$$

Daily sediment load has calculated from the instantaneous measurements assuming, discharge and sediment concentration were not changing rapidly. These calculations were done for the two data sets separately i.e., during river base flow and just after rainstorm.

Figure 5.2: Measured Daily Suspended Sediment Load – Malewa

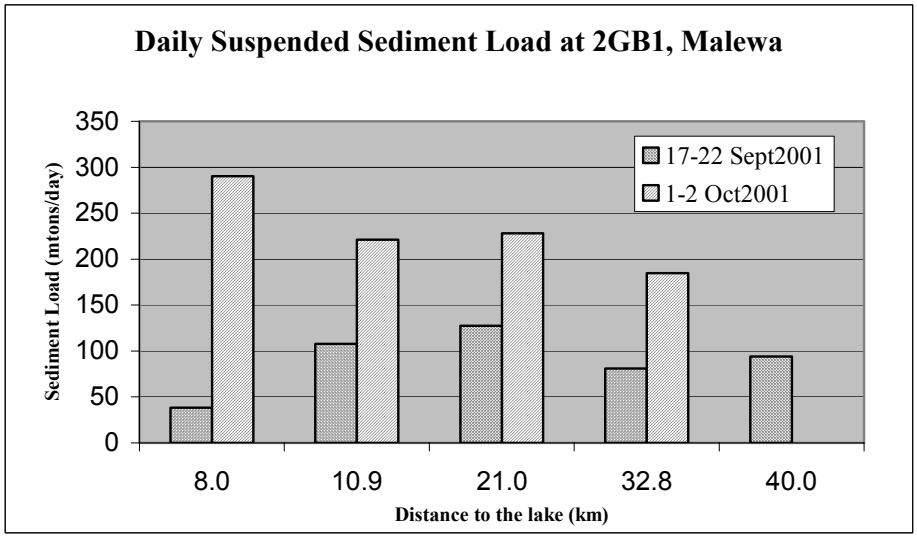

5.1.3.2 Suspended Sediment Rating Curve

Past records of suspended sediment data in Malewa River at gauging station 2GB1, recorded by the Ministry of Water Resources were used to estimate the suspended sediment-rating curve. Original data was in parts per million units, which is equal to the milligram per litre. Relevant river discharge was picked from the time series and daily-suspended sediment load was calculated in metric tons/day. Suspended sediment rating curve for Malewa has given by the graph of discharge vs. suspended sediment load in natural log scale as shown in figure 5.3. Power model was used to get the best fit for Regression Model.

The developed suspended sediment-rating curve is verified with the Malewa suspended sediment-rating curve included in the Viak Report (1974) as in Appendix 5.2. It shows that the records are identical in both rating curves and reliable to predict the suspended sediment load through Malewa using the daily time series of discharge. Measured suspended sediment loads in Malewa River; during 2001 fieldwork is plotted on the same rating curve. 2001 data lies on the upper side of the developed regression line, which indicates the changes in suspended sediment concentration in Malewa during the time passage.

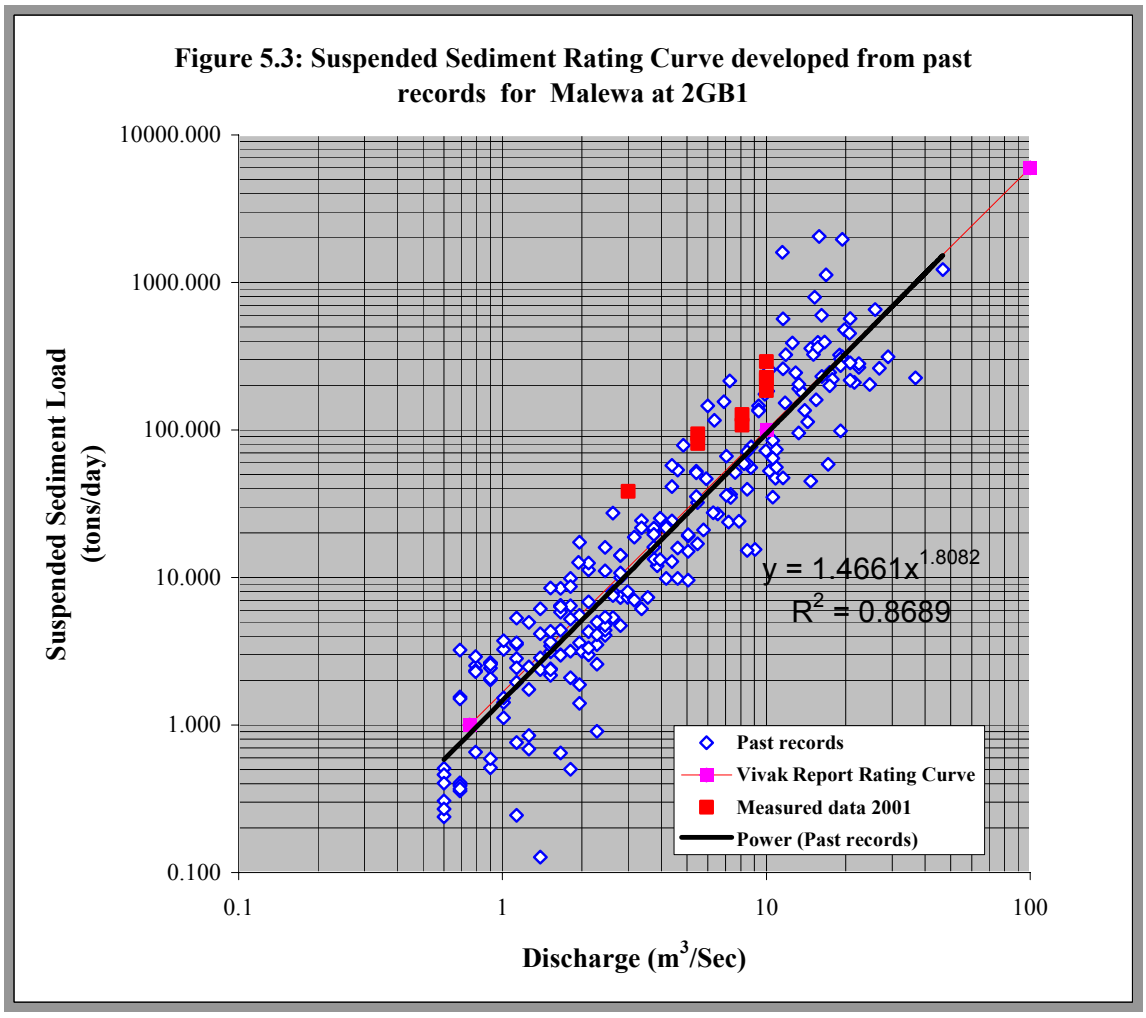

Figure 5.3: Suspended Sediment Rating Curve developed from past records for Malewa at 2GB1

The power equation obtained for the suspended sediment-rating curve is:

$$Y = 1.4661 * X^{1.8082} \quad \text{.....Eq (5.1)}$$

Where,

Y = Daily sediment load in tons/day

X = Daily discharge in m^3/sec

Note: All suspended sediment calculations are in metric tons.

Table 5.1: Summary Output of Regression Statistics

Observations	234				
ANOVA					
	df	*SS*	*MS*	*F*	Significance F
Regression	1	916.845	916.845	1537.982	2.4053E-104
Residual	232	138.303	0.596		
Total	233	1055.148			

Figure 5.4: Frequency Distribution of Regression Residuals

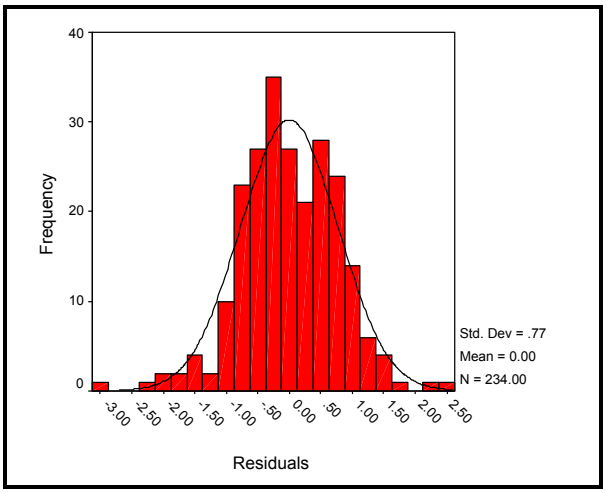

The Summary Output of Regression Analysis shows a good correlation of discharge and suspended sediment data. The significance of F statistics (MS in Regression/MS in Residual) is very close to zero, and this implies observed values and fitted line has no significant difference.

Following procedure was adopted, to estimate the suspended sediment loads to the lake through Malewa at gauging station 2GB1 using the daily discharge time series.

- Daily Sediment load estimation was done using the derived equation from suspended sediment rating curve and the available daily discharge data.
- Sum of daily-suspended sediment loads for a particular period provides the suspended sediment load within that period to the lake.

Accordingly, estimated annual suspended sediment load to the lake is shown in Figure 5.5, with the annual discharge from 1932 to 1990.

Figure 5.5: Estimated Annual Suspended Sediment Load through Malewa at 2GB1, with Annual Discharge

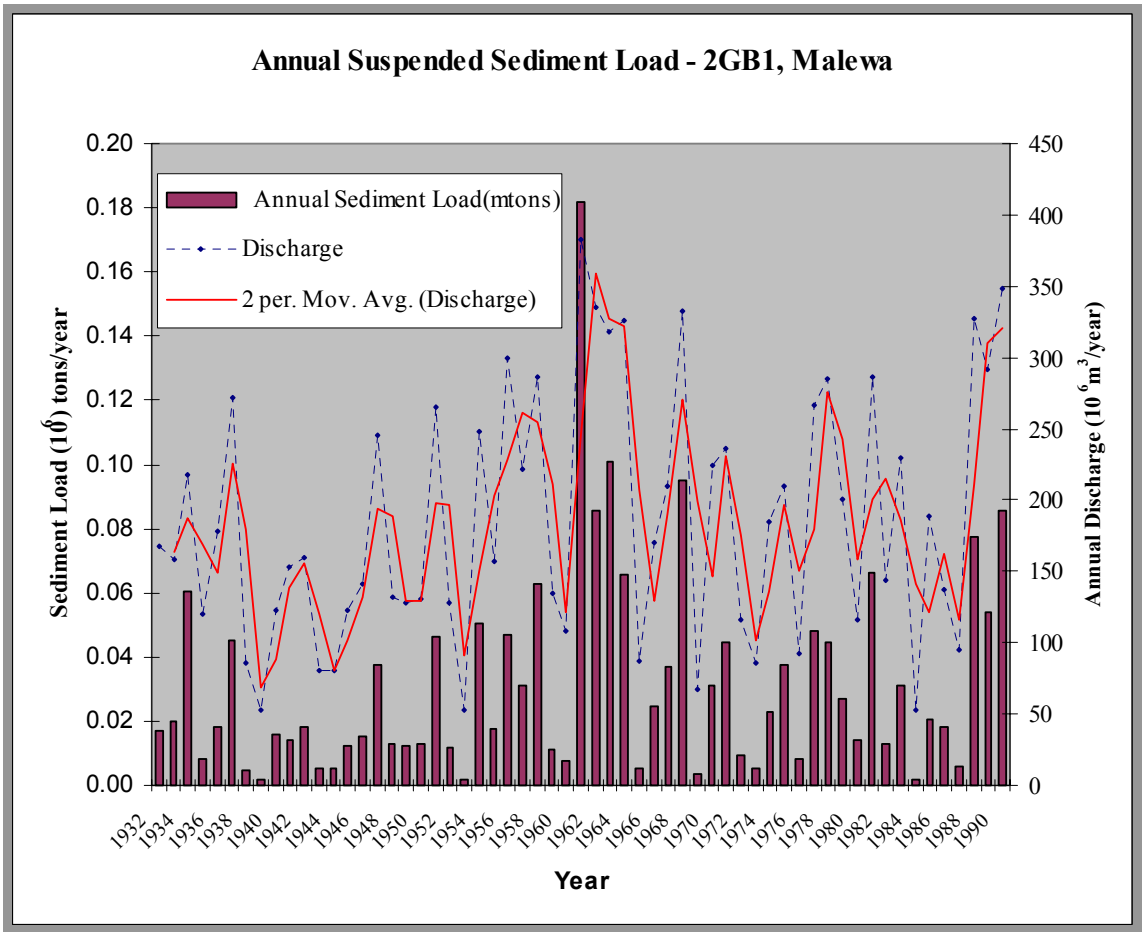

According to the sediment load calculations, from 1932 to 1990,

Total suspended sediment yield, from 1932-1990 = 1.89×10^6 tons for 59 years

Estimated Long-term annual average suspended sediment load through Malewa at 2GB1,

= 1.892×10^6 / 59

= **$\underline{32 \times 10^3}$ tons/year**

For the period from 1957 to 1990,

Total suspended sediment yield from 1957 to 1990 = 1.380×10^6 tons for 33 years

Estimated Long-term Annual average suspended sediment load through Malewa at 2GB1

= 1380662 / 33

= **$\underline{40.6 \times 10^3}$ tons/year**

According to the calculations, it shows that the higher annual average suspended sediment load recorded during the period 1957-1990 compared to 1932-1990. This is due to the variation of Malewa annual discharge during 1932-1990. After 1957, there was very wet years during the period 1961-1964. From the graph, it clearly shows that the same cycle repeating around 1990's even though we have daily data up to 1990. According to literature, recorded highest discharge was in 1964. Due to this highest discharge range, higher long-term annual suspended sediment load was recorded during the period from 1957-1990 through Malewa.

5.1.3.2.1 Bias Correction for Regression Modelled Data

Suspended Sediment Rating curves obtained by least squares regression on logarithmic transformed data may underestimate long-term sediment transport rates by 10-50% (Asselman, 2000). The most commonly used sediment-rating curve is a power function (Walling 1974, 1978 as in Asselman, 2000). This power equation covers both the effect of increased stream power at higher discharge and the extent to which new sources of sediment become available in weather conditions that cause high discharge.

According to Asselman, despite its general use several problems are recognised that regard the accuracy of the fitted curve as well as the physical meaning of its regression coefficients. Inaccuracies in predicted instantaneous suspended sediment concentrations are related to the statistical method used to fit the sediment-rating curve and to the scatter about the regression line.

Therefore, estimated data from regression model has to be corrected statistically. In order to correct estimated values, bias correction was applied for the estimated suspended sediment loads from the regression power model. Three bias correction methods as described in Chapter (2) were used in this thesis for correction of the estimated data and compare the results in each method.

(1) The Quasi-Maximum Likelihood Estimator (QMLE)

According to the equation 2.9 in Chapter (2), Background Theory,

$$\hat{L}_{QMLE} = L_{RC} \exp(\frac{s^2}{2})$$

s^2 = mean square error of the regression residuals = 0.596135

$\hat{L}_{QMLE} = L_{RC} \exp(\frac{s^2}{2})$ = Suspended Sediment Load from the Rating Curve x {exp (0.596135/2)}

$\hat{L}_{QMLE} = L_{RC} \exp(\frac{s^2}{2}) = = L_{RC} * (1.34725)$

(2) The Smearing Estimator (Duan, 1983)

The Smearing estimator is a nonparametric method, which is based on the equation 2.10, in chapter (2):

$\sum_{i=1}^{n} \exp(e_i) = 315.04$ and n = 234; $\quad \frac{\sum_{i=1}^{n} \exp(e_i)}{n} = 1.35$

(3) The Minimum Variance Unbiased Estimator (MVUE) also called the Bradu-Mundlak Estimator

In this method, the bias correction is applied to each daily discharge (Q*) for the required period using the equations 2.11 to 2.14 in Chapter (2). To apply the minimum variance unbiased estimator (MVUE) to estimate the corrected sediment load, the Fortran computer program developed by Cohn and others in 1989 was used. This program as given in Appendix (5.3), evaluates the expression *gm and V* (Chapter 2.0) along with the corrected suspended sediment load for the given period.

Input Parameters for the Fortran Program:

- An input file called MVUE.IN containing a single column of stream flow discharges (should be in first column) for which the predicted daily sediment discharge needs to be corrected for bias.
- The output for the program is a file, MVUE.OUT, which contains the bias corrected daily sediment discharges and the total sediment discharge for the period.

According to the developed Regression Model, following parameters provided as input data variables.

XN (Number of data pairs)	= 234.000
QBAR (Mean of ln Q)	= 1.335
QVAR [Sum of ((LN Q - LN Q MEAN)**2)]	= 280.418
XM (No of degrees of freedom)	= 232.000
S2 (Mean square error)	= 5.961E-01
A (Intercept of Qs-Q relation)	= 1.446
B (Slope of Qs-Q relation)	= 1.808

A sample output obtained from the Fortran Program is given in the Appendix 5.4, while summary of results are included in Table 5.2.

The results obtained from three different bias correction methods along with the sediment load obtained from the Sediment Rating Curve are given in Table 5.2. Detailed calculations on annual basis are given in Appendix (5.5). Using the estimated annual average value for the period 1957-1990, the total suspended sediment load for the period from 1957-2001 was estimated.

Table 5.2: Comparison of Results from three Bias Correction Methods

Description	Suspended sediment Load (tons)	Suspended sediment load after bias correction (tons)		
	Using Rating Curve	QMLE	SE	MVUE
Total 1932-1990	1.89×10^6	2.55×10^6	2.54×10^6	2.53×10^6
Annual average	32.0×10^3	43.2×10^3	43.2×10^3	42.8×10^3
Total 1957-1990	1.38×10^6	1.86×10^6	1.85×10^6	1.84×10^6
Annual average	41.8×10^3	56.3×10^3	56.3×10^3	55.9×10^3
Total 1957 - 2001	1.84×10^6	2.48×10^6	2.47×10^6	2.46×10^6

The results of three bias correction methods are almost similar, but little high value given by the Quasi Maximum Likelihood Estimator while lowest corrected values obtained from the MVUE method. After the correction from MUVE method, estimated sediment load has increased about 33.62%.

Although used extensively, Quasi-Maximum Likelihood Estimator is generally not recommended because the results are not unbiased estimates and the method often over-corrects for the downward bias of the rating curve. This QMLE method may be suitable if the predicted discharges are within the interval of a fairly large calibration data set and the sample mean square error (s^2) is a satisfactory estimator for the population mean square error (Cohn and Gilroy, 1991).

Cohn and Gilroy, 1991, suggest methods Smearing Estimator and the Minimum Variance Unbiased Estimator for use. The Smearing Estimator is a nonparametric method that only requires the

assumption that the residuals are independent and identically distributed but they can follow any distribution. When residuals are normally distributed it performs nearly as well as Method (3)-MVUE. Even though, three methods of bias corrections applied for the estimated data for comparison, it is essential to select the appropriate bias correction method according to the selected regression model. For the Regression Model of Malewa, 234 numbers of observations is used and the sediment load is estimated from 1932 to 1990. Therefore, QMLE method is not a suitable method for this model, as it doesn't represent the whole discharge range.

According to the Frequency Distribution Plot of regression residuals (Figure 5.4), it shows that the regression residuals are normally distributed. Therefore, as mentioned in the literature MVUE is the best method to correct statistically the estimated suspended sediment load discharge through Malewa at 2GB1 station. According to results, in Malewa at 2GB1 station, long-term average annual suspended sediment concentration was 0.23 Kg/m^3 and 0.26 kg/m^3 from 1932-1990 and 1957-1990 respectively. From the measured values of suspended sediment during 2001 fieldwork based on nine measurements, average concentration was about 0.21 kg/m^3 along the Malewa river.

5.1.4 Sediment Rating Curves for Bed Load Transport

As explained in Chapter (2), Background Theory, sediment transport calculations were made to develop sediment rating curves for total load transport at Malewa river using three different total-load relations, namely: (1) Einstein, (2) Graf and Acaroglu and (3) Ackers et White as described by Graf(2001).

Stage-Discharge relationships developed in Chapter (4) in HEC_RAS software for station (5) at Dairy Training School location in Malewa were used for these calculations together with the measured parameters in the field.

- Hydraulic radius for different water depth profiles, riverbed slope, average velocity of the section and stage-discharge relationship for the location.

- During fieldwork 2001, Measured temperature = 17 ^{0}C
  Physical properties of water (Maidment, 1992)
  Density of water = 998.80 kg/m^3
  Kinematic viscosity of water = 1.082 x 10^{-6} m^2/sec
  Specific Gravity of sediment = 2.65

- On every line, calculations start by assuming an initial set of values of hydraulic radius due to grain roughness ($R_h^{'}$). The values for $R_h^{'}$ are selected such that the calculations cover the entire range of desired water discharges in the river (Graf, 2001).

- In this case, as stage-discharge relationship and average velocity of the section are available, an iterative procedure was adopted to estimate an approximate value for d_{50} for the particular section. From field observations assuming fine to medium sand (200-400 micrometer) and to satisfy the following equation for average velocity of the entire section for different flow profiles, approximate grain size of d_{50} = 0.30 mm was selected to tally with the measured average velocity of the section.

- Then backward calculations were made to find unknown parameters by incorporating observed parameters. By using the estimated values of intensity of shear parameter and the relationship with grain size distribution, d_{35} was estimated as 0.25 mm for the particular section. Assuming grain size distribution is quasi uniform and by assuming granulometric distribution to be logarithmic, d_{65} was estimated as 0.36 mm.

According to the trial and error procedures, following values were estimated as the representative values for the bed granulometry.

d_{35} = 0.25 mm and settling velocity v_{ss} =0.032 m/sec (Julian, 1995)
d_{50} = 0.30 mm; d_{65} = 0.36 mm

But, all these parameters could vary along the watercourse as well as temporal variations can take place due to armouring of the riverbed. Furthermore, they will depend on the way the bed samples are taken and are analysed (Graf, 2001). Calculations made assuming that the following theoretical considerations exist; the bed of a channel is plane but mobile composed of solid particles of uniform size and being non-cohesive.

The spreadsheet is used to make the calculations. The detailed calculations and explanations on the contents of the columns are given in Tables 5.3 & 5.10. Results obtained from three different formulae are given in Figures 5.6 and 5.7

During calculations, measured river parameters and estimated Q-H relationship is incorporated along with the hydraulic radius and average velocity. Einstein's method, uses d_{35} and d_{65} as the representative bed granulometry(Graf,2001). In the method of Garf et Acaroglu (1968), d_{50} diameter used as the representative of bed granulometry. The formula of Ackers et White (1973), uses d_{35} as the representative diameter for the calculations (Graf, 2001).

Table 5.3: Computations of Bed Load Transport Parameters using Stage-Water Discharge Curve (Method of Einstein-Barbarossa (1952), in Garf, 2001)

Computation Sheet for determining Bed Load Transport Parameters using Stage-*Water*-Discharge Curve Using the method of *Einstein-Barbarossa (1952)*									
b =	20 m		T =	17 ^{0}C			ρ_s =	2650 kg/m^3	
m =	1		ρ =	998.8 kg/m^3			d_{35} =	*0.00025* m	
S_f =	0.0005		v =	1.08E-06 m^2/s			$k_s = d_{50}$ =	*0.00030* m	
							Ss =	*2.65* m	
1	2	3	4	5	6	7	8	9	10
Q	h	R_h	u_*	R_h'	R_h''	u_*''	U	U/u_*''	ψ'
m^3/s	m	m	m/s	(m)			m/s		
3	0.52	0.506	0.158	0.02	0.486	0.05	0.49	10.034	9.00
5	0.6	0.591	0.170	0.05	0.541	0.05	0.66	12.810	4.90
8.1	0.68	0.704	0.186	0.10	0.604	0.05	0.88	16.170	3.00
10	0.72	0.739	0.190	0.15	0.589	0.05	0.99	18.419	2.40
12	0.76	0.788	0.197	0.20	0.588	0.05	1.10	20.491	2.00
15	0.81	0.831	0.202	0.25	0.581	0.05	1.25	23.424	1.60
18	0.85	0.859	0.205	0.30	0.559	0.05	1.37	26.159	1.40
20	0.88	0.924	0.213	0.35	0.574	0.05	1.45	27.326	1.30
25	0.95	0.982	0.219	0.45	0.532	0.05	1.62	31.727	1.25
30	1.01	1.189	0.241	0.60	0.589	0.05	1.76	32.749	1.20
50	1.23	1.562	0.277	0.90	0.662	0.06	2.19	40.120	1.00
100	1.63	1.562	0.277	1.00	0.562	0.05	2.84	54.072	0.80
150	1.97	1.879	0.304	1.50	0.379	0.04	3.21	74.404	0.65

Table 5.4: Explanations of Expressions used for Calculations (Graf, 2001)

Column	Symbol	Explanation	Expression
1	R_h'	Hydraulic Radius due to grain roughness	(Assumed initial value)
2	u_*'	Friction velocity due to grain roughness	$\sqrt{gR_h'S_f}$
3	U	Average velocity in the cross section	$u_*'\sqrt{8/f'}$ $(\sqrt{8/f'} = 5.6\log(R_h'/k_s) + 6.25)$
4	ψ'	Parameter of Einstein-Barbarossa	$\frac{(s_s - 1)d_{35}}{R_h'S_f}$
5	U/u_*''	Ratio of velocities corresponding to ψ'	Figure 3.6, page 86(Graf, 2001)
6	u_*''	Friction velocity due to bed forms	$U/(U/u_*'')$
7	R_h''	Hydraulic Radius due to bed forms	$(u_*'')^2/(gS_f)$
8	R_h	Total Hydraulic Radius	$R_h' + R_h''$
9	u_*	Total friction velocity	$\sqrt{gR_hS_f}$
10	h	Flow depth	
11	Q	Water discharge	*Uh (b+mh)*

Figure 5.5: Computation of Stage-Solid Discharge Curve using Einstein (1950) Formula for Malewa at Diary Training School

Computation Sheet for determining the stage-*Solid*-discharge curve for Malewa at DTS
Using the method of *Einstein (1950)*

b =	20	m		ρ =	998.8	kg/m^3	$k_s = d_{65}$ =	0.00036	m		d_{35} =	0.00025	m	ρ_s =	2650	kg/m^3					
S_f =	0.0005			v =	1.08E-06	m^2/s	Ss =	2.65	m		$V_{ss}(d_{35})$ =	0.032	m/s	k =	0.4							
1	2	3	4	5	6	7	8	9	10	11	12	13	14	15	16	17	18	19	20	21
h	R_h'	u_*'	∂	k_s/∂	x	Δ	P_e	ψ'	Φ	q_{sb}	Q_{sb}	A_E	z	I_1	I_2	q_{ss}	Q_{ss}	Q_s	G_s	G_s
(m)	m/s	m/s	m		m/s	m				m^3/s/m	m^3/s					m^3/s/m	m^3/s	m^3/s	kg/s	N/s
0.52	0.02	0.010	1.26E-03	0.287	0.98	3.53E-04	10.71	9.00	0.15	2.39E-06	4.77E-05	9.62E-04	8.077	5.00E-02	-1.95E-01	8.12E-07	1.62E-05	6.39E-05	0	2
0.6	0.05	0.016	7.95E-04	0.453	1.32	4.73E-04	10.55	4.90	0.72	1.15E-05	2.29E-04	8.33E-04	5.108	5.00E-02	-4.00E-01	1.46E-06	2.92E-05	2.58E-04	1	7
0.68	0.10	0.022	5.62E-04	0.641	1.52	5.48E-04	10.53	3.00	1.90	3.02E-05	6.04E-04	7.35E-04	3.612	9.00E-02	-6.50E-01	9.00E-06	1.80E-04	7.84E-04	2	20
0.72	0.15	0.027	4.59E-04	0.785	1.59	5.72E-04	10.55	2.40	2.51	3.99E-05	7.98E-04	6.94E-04	2.949	1.20E-01	-8.70E-01	1.58E-05	3.16E-04	1.11E-03	3	29
0.76	0.20	0.031	3.97E-04	0.906	1.60	5.76E-04	10.59	2.00	3.40	5.41E-05	1.08E-03	6.58E-04	2.554	1.70E-01	-2.00E-01	8.66E-05	1.73E-03	2.81E-03	7	73
0.81	0.25	0.035	3.55E-04	1.013	1.60	5.76E-04	10.66	1.60	4.32	6.87E-05	1.37E-03	6.17E-04	2.285	1.90E-01	-6.07E-01	9.74E-05	1.95E-03	3.32E-03	9	86
0.85	0.30	0.038	3.24E-04	1.110	1.60	5.76E-04	10.71	1.40	5.19	8.25E-05	1.65E-03	5.88E-04	2.085	2.02E-01	-1.34E+00	6.79E-05	1.36E-03	3.01E-03	8	78
0.88	0.35	0.041	3.00E-04	1.199	1.59	5.72E-04	10.75	1.30	5.63	8.95E-05	1.79E-03	5.68E-04	1.931	2.02E-01	-1.34E+00	7.43E-05	1.49E-03	3.28E-03	9	85
0.95	0.45	0.047	2.65E-04	1.359	1.58	5.67E-04	10.83	1.25	5.84	9.29E-05	1.86E-03	5.26E-04	1.703	2.00E-01	-1.34E+00	7.68E-05	1.54E-03	3.39E-03	9	88
1.01	0.60	0.054	2.29E-04	1.570	1.51	5.43E-04	10.94	1.20	6.06	9.64E-05	1.93E-03	4.95E-04	1.475	4.43E-01	-2.62E+00	2.14E-04	4.29E-03	6.22E-03	16	162
1.23	0.90	0.066	1.87E-04	1.922	1.39	5.00E-04	11.22	1.00	7.50	1.19E-04	2.39E-03	4.07E-04	1.204	7.00E-01	-3.00E+00	5.79E-04	1.16E-02	1.40E-02	37	363
1.63	1.00	0.070	1.78E-04	2.026	1.37	4.93E-04	11.51	0.80	9.53	1.52E-04	3.03E-03	3.07E-04	1.142	1.70E+00	-5.73E+00	2.10E-03	4.20E-02	4.50E-02	119	1170
1.97	1.50	0.086	1.45E-04	2.482	0.05	1.91E-05	14.96	0.65	11.90	1.89E-04	3.78E-03	2.54E-04	0.933	2.14E+00	-8.90E+00	4.37E-03	8.75E-02	9.12E-02	242	2372
BED LOAD												SUSPENDED LOAD						TOTAL LOAD		

Table 5.6: Explanations of expressions in the Method of Einstein (1950)

Column	Symbol	Explanation	Expression
1	h	Flow depth	
2	$R_h^{'}$	Hydraulic Radius due to grain roughness	(Assumed initial value)
3	$u_*^{'}$	Friction velocity due to grain roughness	$\sqrt{gR_h^{'}S_f}$
4	δ	Thickness of viscous sub layer	$\delta = 11.5\nu / u_*^{'}$
5	k_s/δ	Relative roughness	$k_s/\delta = d_{65}/\delta$
6	χ	Correction term for logarithmic velocity distribution	Figure 6.7a, Pg 378 (Graf, 2001)
7	Δ	Apparent roughness diameter	$\Delta = d_{65}/\chi$
8	p_e	Transport parameter	$P_e = 2.303\log(30.2h/\Delta$
9	$\psi^{'}$	Intensity of shear	$\frac{(s_s-1)d_{35}}{R_h^{'}S_f}$
10	Φ	Intensity of transport	$\Phi = \frac{q_{sb}}{\sqrt{(s_s-1)gd_{35}^3}}$
11	q_{sb}	Solid discharge, as bed load, by volume and by unit width	$q_{sb} = \Phi\sqrt{(s_s-1)gd_{35}^3}$
12	Q_{sb}	Solid discharge, as bed load, by volume	$Q_{sb} = q_{sb}b$
13	A_E	Dimensionless height	$A_E = \frac{Z_{sb}}{h} = \frac{2d_{35}}{h}$
14	ξ	Rouse exponent	$\xi = \frac{V_{ss}}{ku_*^{'}}$; V_{ss} settling velocity
15	$\int_1$	Einstein first integral	Figure 6.12, Page 391, Graf, 2001)
16	$\int_2$	Einstein second integral	Figure 6.12, Page 391, Graf, 2001)
17	q_{ss}	Solid discharge, as suspended load, by volume and by unit width	$q_{ss} = q_{sb}(P_e\int_1 + \int_2)$
18	Q_{ss}	Solid discharge, as suspended load, by volume	$Q_{ss} = q_{ss}b$
19	Q_s	Solid discharge, as total load, by volume	$Q_{ss} = Q_{sb} + Q_{ss}$
20	G_s	Solid discharge, as total load, by mass	$G_s = Q_s\rho_s$
21	G_s	Solid discharge, as total load, by weight	$G_s = Q_s\rho_s g$

Table 5.7: Computation Sheet for Stage-Solid Discharge Curve from Graf et Acaroglu(1968)

Malewa: Diary Training School			Computation Sheet for determining the stage-***Solid*** -dischage curve, Using the method of ***Graf et Acaroglu (1968)***						
			ρ =	998.8 kg/m^3		Ss =	2.65		
S_f =	0.0005		d_{50} =	***0.00030*** m		ρ_s =	2650 kg/m^3		
1	**2**	**3**	**4**	**5**	**6**	**7**	**8**	**20**	**21**
h	R_h	***U***	***Q***	Ψ_A	Φ_A	C_s	Q_s	G_s	G_s
(m)	**m/s**	**m/s**	**m^3/s**				**m^3/s**	**kg/s**	**N/s**
0.52	0.506	0.49	3.00	1.956	1.92	1.62E-04	4.85E-04	1	13
0.6	0.591	0.66	5.00	1.675	2.83	1.52E-04	7.59E-04	2	20
0.68	0.704	0.88	8.10	1.407	4.40	1.48E-04	1.20E-03	3	31
0.72	0.739	0.99	10.00	1.340	4.97	1.42E-04	1.42E-03	4	37
0.76	0.788	1.10	12.00	1.257	5.84	1.41E-04	1.69E-03	4	44
0.81	0.831	1.25	15.00	1.192	6.68	1.34E-04	2.02E-03	5	52
0.85	0.859	1.37	18.00	1.152	7.27	1.29E-04	2.32E-03	6	60
0.88	0.924	1.45	20.00	1.071	8.73	1.36E-04	2.73E-03	7	71
0.95	0.982	1.62	25.00	1.009	10.17	1.34E-04	3.34E-03	9	87
1.01	1.189	1.76	30.00	0.833	16.48	1.65E-04	4.94E-03	13	128
1.23	1.562	2.19	50.00	0.634	32.81	2.00E-04	1.00E-02	27	261
1.63	1.562	2.84	100.00	0.634	32.81	1.55E-04	1.55E-02	41	402
1.97	1.879	3.21	150.00	0.527	52.26	1.81E-04	2.72E-02	72	706

Table 5.8:Explanations of Expressions in the Formula of Graf et Acaroglu (1968)

Column	Symbol	Explanation	Expression
1	h	Flow depth	
2	R_h	Total Hydraulic Radius	
3	U	Average velocity	
4	Q	Liquid discharge	
5	ψ_A	Shear stress intensity parameter	$\psi_A = \frac{(s_s - 1)d_{50}}{S_f R_h}$
6	Φ_A	Transport parameter	$\Phi_A = 10.39\psi_A^{-2.52}$
7	C_s	Concentration by volume	$C_s = \Phi_A \frac{\sqrt{(s_s - 1)g d_{50}^3}}{UR_h}$
8	Q_s	Solid discharge, as total load, by volume	$Q_s = C_s Q$
9	G_s	Solid discharge, as total load, by mass	$G_s = Q_s \rho_s$
10	G_s	Solid discharge, as total load, by weight	$G_s = Q_s \rho_s g$

Table 5.9: Computation Sheet for Stage-Solid Discharge Curve from Ackers et White (1968)

Computation Sheet for determining the stage-***Solid*** -dischage curve, Using the method of ***Ackers et White (1973)***									
ρ_s =	2650 kg/m^3		ρ =	998.8 kg/m^3		Ss =	2.65	v =	1.08E-06
S_f =	0.0005		d_{35} =	***0.00025*** m		d_* = $(g(Ss-1)/v^2)^{1/3}d_{35}$ =			6.00
n_w =	1-0.56logd_*	0.564		m_w =	9.66/d_* + 1.34 =	2.95			
A_w =	0.23/$d_*^{0.5}$ +0	0.23		C_w =	$10^{(2.86\log d_* - (\log d_*)^2 - 3.53)}$ =	0.0123			

1 h (m)	2 u_* m/s	3 U m/s	4 Q m^3/s	5 F_{gr}	6 G_{gr}	7 C_s	8 Q_s m^3/s	20 G_s kg/s	21 G_s N/s
0.52	0.158	0.49	3.00	1.009	4.2155E-01	3.84E-04	1.15E-03	3	30
0.6	0.170	0.66	5.00	1.193	7.8963E-01	7.07E-04	3.53E-03	9	92
0.68	0.186	0.88	8.10	1.413	1.4519E+00	1.28E-03	1.04E-02	28	270
0.72	0.190	0.99	10.00	1.504	1.8094E+00	1.59E-03	1.59E-02	42	414
0.76	0.197	1.10	12.00	1.599	2.2411E+00	1.95E-03	2.34E-02	62	608
0.81	0.202	1.25	15.00	1.712	2.8312E+00	2.44E-03	3.67E-02	97	953
0.85	0.205	1.37	18.00	1.795	3.3279E+00	2.86E-03	5.14E-02	136	1337
0.88	0.213	1.45	20.00	1.876	3.8593E+00	3.24E-03	6.47E-02	172	1683
0.95	0.219	1.62	25.00	1.996	4.7545E+00	3.87E-03	9.66E-02	256	2512
1.01	0.241	1.76	30.00	2.179	6.3619E+00	4.83E-03	1.45E-01	384	3767
1.23	0.277	2.19	50.00	2.568	1.0895E+01	7.11E-03	3.56E-01	943	9246
1.63	0.277	2.84	100.00	2.844	1.5149E+01	8.64E-03	8.64E-01	2290	22466
1.97	0.304	3.21	150.00	3.137	2.0737E+01	9.96E-03	1.49E+00	3957	38823

Table 5.10: Explanations of the expressions in the formula of Ackers et White (1973)

Column	Symbol	Explanation	Expression
1	h	Flow depth	
2	u_*	Total (friction) shear velocity	
3	U	Average velocity	
4	Q	Liquid discharge	
5	F_{gr}	Parameter of mobility	$F_{gr} = \frac{(u_*^{n_w})}{\sqrt{(s_s - 1)gd_{35}}}[\frac{U}{\sqrt{32}\log(10h/d_{35})}]^{(1-n_w)}$
6	G_{gr}	Transport parameter	$G_{gr} = C_w(\frac{F_{gr}}{A_w} - 1)^{m_w}$
7	C_s	Concentration by volume	$C_s = G_{gr}\frac{d_{35}}{h}(\frac{U}{u_*})^{n_w}$
8	Q_s	Solid discharge, as total load, by volume	$Q_s = C_s Q$
9	G_s	Solid discharge, as total load, by mass	$G_s = Q_s \rho_s$
10	G_s	Solid discharge, as total load, by weight	$G_s = Q_s \rho_s g$

Figure 5.6: Rating Curves for Stage-Liquid Discharge and Stage-Solid Discharge Using Empirical Formulas

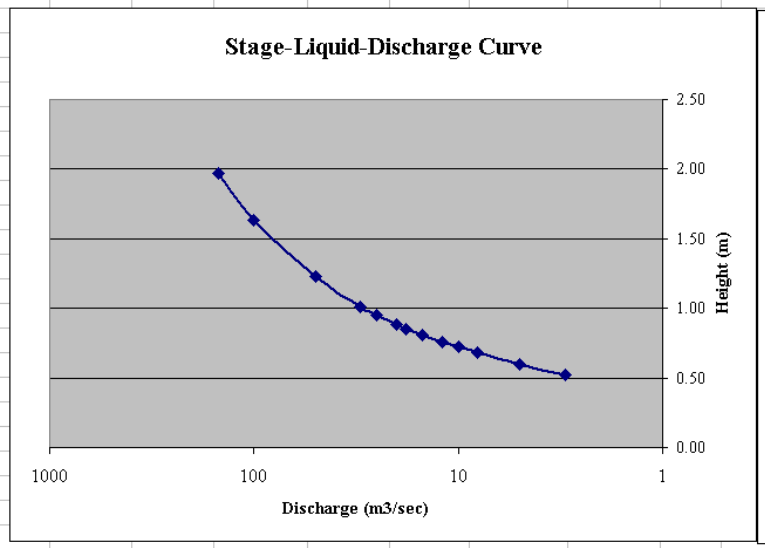

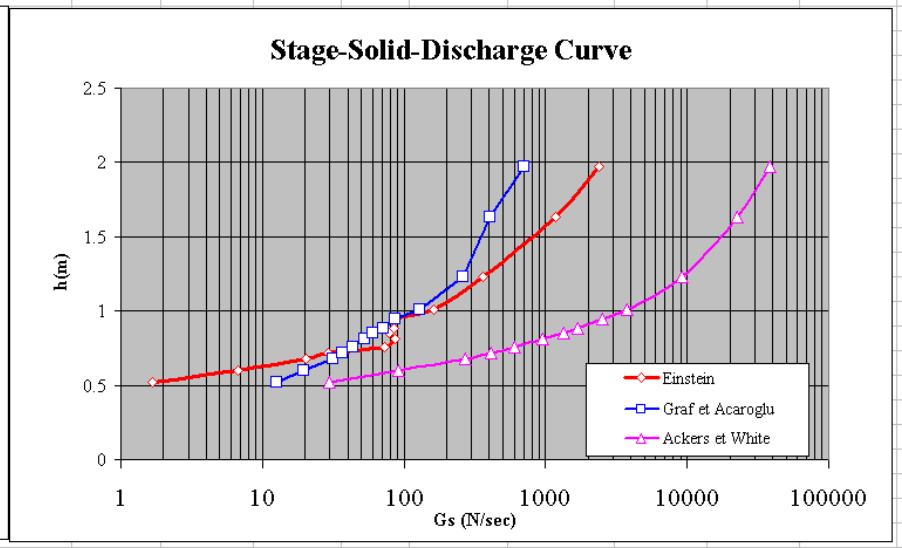

Figure 5.7: Bed Load and Suspended Load from Einstein's Formula

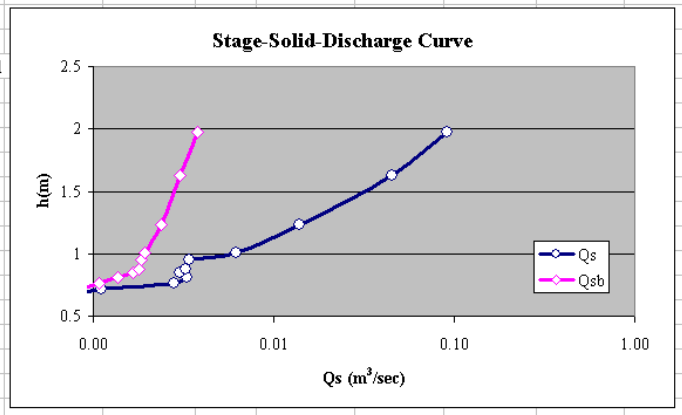

The results obtained from three methods do not give the same values for the solid discharge. Reasons could be:

- Most formulae developed for the capacity of sediment transport are only valid for such watercourses, which pass through their own alluvium, namely in a bed being made up of material, which was also transported and can again be transported.
- Even though assumed that the simplified conditions of uniform granulometric conditions and non-cohesive sediments, bed forms may form, the granulometric distribution may be non-uniform and cohesion may exist. Estimated values for representative granulometry could have contributed errors. Also it becomes evident that granulometric samples taken insitu – if armouring takes place- have to be interpreted with great care.
- Developed stage height-discharge relationship for fixed bed conditions are applied to predict the bed-load transport assuming mobile bed conditions.

Therefore, even though such formulae are of great value for the hydraulic engineering, they must be applied within hydraulic conditions under which they have been established. It is important however to remind that the formulae for the sediment transport can only give an idea about the order of magnitude of the solid discharge that one should reasonably expect in a particular flow situation (Graf, 2001). It is difficult to determine a reliable bed load transport to be used in the field because of the lack of reliable data from streams. According to literature, the procedure developed by Einstein is still the most comprehensive one available. Ackers and White's equation has received increasing attention and should always be checked as a reference (Maidment, 1992).

The formulae, developed for the quantitative determination of the transport of sediments, are based on experimental results, being often limited, and thus should be used with much caution (Graf, 2001). In Engineering practice, one compares several formulas with field observations to select the most appropriate equation at a given field site. Out of the results obtained from three methods Einstein's equation appears to give better intermediate results for the particular location compared to other two formulae.

5.2 EXPLANATORY ANALYSIS OF RIVER GILGIL SEDIMENT FLUX

5.2.1 River Gilgil – Time Series of Discharge

The average annual flow in Gilgil river during the period 1962-1980 is about 24 x 10^6 m^3, which is equal to one seventh of Malewa. Highest annual flow to be expected in 100 years is 121 x 10^6 m^3 and

the highest actual flow during the investigated period is 49 x 10^6 m^3. These values correspond very well with the results from the investigation made by Brind and Robertson (1958), and their computation indicates a maximum recurrent 100 years flow of 111 x 10^6 m^3, and an actual annual high flow of 71 x 10^6 m^3 from the investigated period 1941-1946.

Even though, Monthly time series of discharge data in Gilgil is available from 1932 to 1997 unfortunately, daily discharge has not found in the Gauging Station 2GA1. Monthly time series of discharge are shown in the Figure 5.8.

Figure 5.8: Monthly Discharge at 2GA1, Gilgil

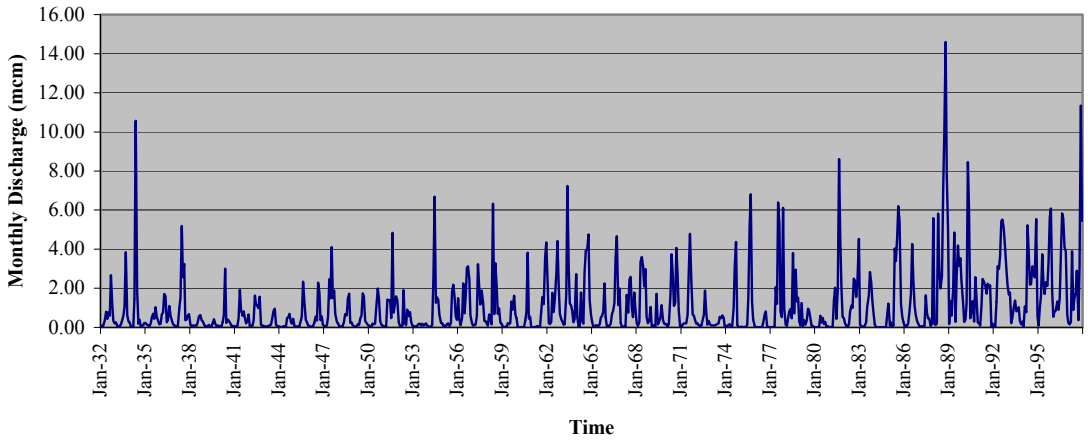

5.2.2 Available Sediment Data

Only few past records of sediment measurements in Gilgil at gauging station, 2GA1 are found. Also in Gilgil, other Gauging stations (2GA3 & 2GA6), very few number of sediment data available. But, subsequent daily discharge data is not available while monthly discharge series is available as the sediment measurements were done during 1950's.

5.2.3 Estimation of Annual Sediment Load

5.2.3.1 Direct Estimation Using Measured Sediment Data

As mentioned in Chapter (4.0), Field Data Collection and Analysis, sediment concentrations were measured in few locations in Gilgil River. These data is used to estimate the direct daily sediment load to the lake. Figure 5.9, shows the calculated daily sediment load to the lake through Gilgil from an instantaneous measurement.

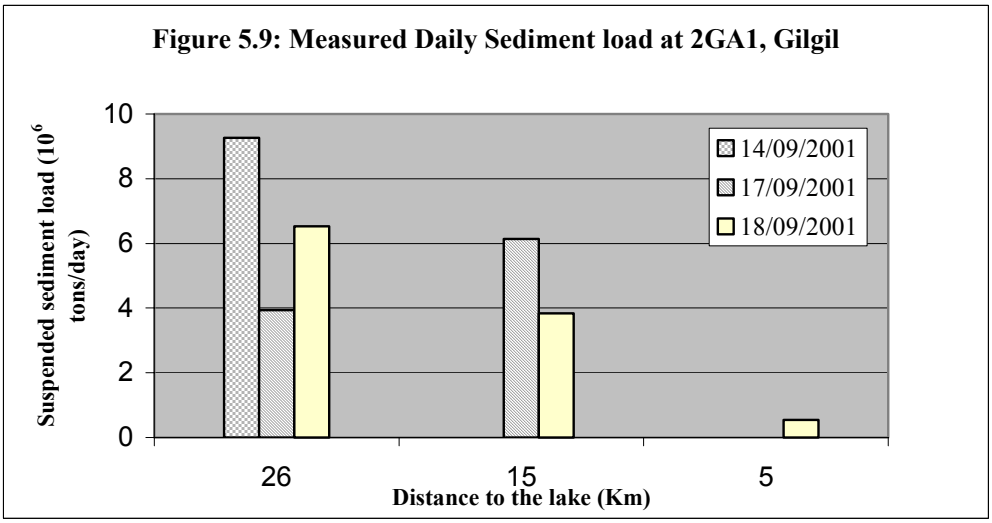

From the graph, it shows that the Gilgil carries a fair amount of sediment towards the lake. But very close to lake (5 Km), a low amount of suspended sediment load is observed. This is due to very low downstream discharge from Gilgil. From the field observation, it is clear that the Gilgil discharge is diverted to farms and finally only very little amount flows towards the lake. In consequence, important deposition of sediment takes place. This indicates, during recent years only small-suspended sediment load enters the lake through Gilgil compared to the Malewa river suspended sediment load.

5.2.3.2 Sediment Rating Curve

Recent field observations convinced that only very little amount of water enters to the lake through Gilgil even though considerable discharge flows towards the lake in upstream of Gilgil. But, past monthly records at 2GA1 indicates (Figure 5.6) that reasonable discharge flows through Gilgil especially during flood season. As similar to Malewa, Sediment Rating Curve is developed for Gilgil Gauging Station 2GA1 with the available sediment data. But as some of the subsequent daily discharge data is not found, average daily discharge is estimated from the monthly data for calculations. Regression Analysis using the natural logarithm was applied and Figure 5.10 shows the developed power model for the data.

The power equation obtained for the sediment-rating curve for Gilgil at 2GA1 is,

$$Y = 31.995X^{1.2457} \quad \text{.....Equation (5.2)}$$

Where,

Y = Daily Suspended Sediment Load in tons/day

X = Daily discharge in m^3/sec

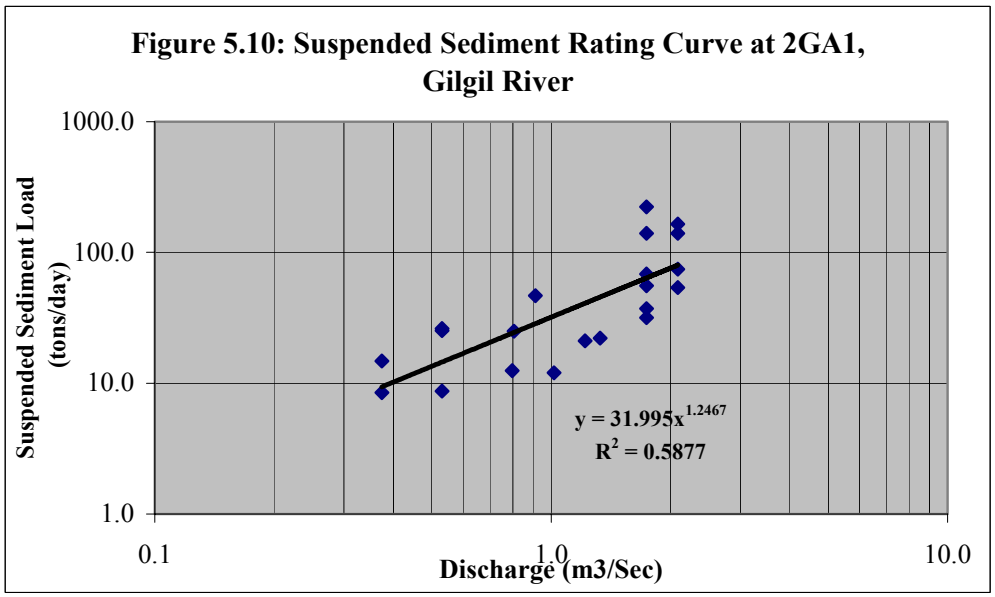

Number of observation used for the regression model is only 21 records. Summary output of Regression Analysis shows that the correlation (R^2 =0.58) between data is not so good. Also the model doesn't cover the range of discharge to estimate the suspended sediment load. Therefore, it is not a very good model to estimate the long-term suspended sediment load.

But, the developed regression power model equation is applied for the available daily discharge data to get an idea about the suspended sediment load through Gilgil. Anyhow, it is not possible to estimate the annual suspended sediment load, as daily discharge data at 2GA1 gauging station is not continuously available.

5.2.3.2.1 Bias Correction

Following results (Table 5.11) obtained for the periods considered after applying correction factors similar to Malewa for the regression model estimated results.

Table 5.11: Results out of three Bias correction Methods

Time Period	Discharge (10^6 m^3)	Sediment (tons)	Bias Correction		
			QMLE	SE	MVUE
07/25/58 - 10/11/58	9.38	3945.7	4838.55	4750.56	4824.668
08/6/59 - 29/08/60	11.30	4142.2	5079.63	4987.27	
09/10/60 - 28/11/60	9.38	4049.7	4966.18	4875.87	
11/17/66 - 29/12/66	18.02	7756.9	9512.21	9339.25	

According to results the average suspended sediment concentration of Gilgil at 2GA1 guaging station is about 0.50 kg/m^3. Compared to Malewa, even though this is a high concentration, it does not represent a long-term average value, as the data is not continuous. Out of the measured values during the field observations in 2001, the average concentration is about 0.99 kg/m^3 along the Gilgil River. This is based on 9 measurements on different locations in Gilgil.

It is evident that the Malewa sediment-rating curve is a supply-limited sediment-rating curve. The case of supply-limited rating curves is characterized by low concentrations and high variability (Julian, 1995). Sediment transport is limited by the supply of sediment, usually washload, which varies with the location and intensity of rainstorms on the watershed, seasonal variation in temperature, weathering, vegetation, and type of precipitation. The source of sediment includes upland erosion, stream bank erosion, and point sources.

Hysteresis effects between discharge and concentration, seasonal variation, inaccuracies in flow and sediment measurements, and variability in the suspended load may explain the scatter of points on the suspended sediment transport graph. Better results are sometimes achieved, provided that sufficient data are available, by setting individual sediment rating curves for each month. At a given discharge, higher sediment concentrations are generally observed during the rising limb of the hydrograph (Julian, 1995).

The regression power function used in this study is in the form of;

$$C = aQ^b \quad \text{.....Equation 5.1}$$

Where, C is the suspended sediment concentration in mg/l, Q is the discharge in m^3/sec, a and b.

Peters-Kummerly (1973) and Morgan (1995) as reported by Rebeca, (2001) state that the "*a"* coefficient represents an index of erosion severity. High "*a"* value indicates intensively weathered materials, which can easily be transported. According to Peters-Kummerly (1973), the "*b"*coefficient represents the erosive power of the river, with large values being indicative for rivers where a small increase in discharge results in a strong increase in erosive power of the river.

Malewa and Gilgil regression modelling gave, the "*a"* coefficient as 1.4661 and 31.995 respectively indicating that Malewa has less erosive capacity while Gilgil indicates high erosive capacity compared to Malewa. Further, Malewa and Gilgil, "*b"*coefficients are 1.8082 and 1.2467 respectively. This shows low erosive power of both rivers.

In Malewa, long-term average annual sediment concentration is 0.23 Kg/m3 and 0.26 kg/m3 from 1932-1990 and 1957-1990 respectively. Compared to other river basins in the world this is a low concentration. As an example, for the Missouri and Colarado Rivers in the United States, the annual average sediment concentrations are respectively, 3.54 and 27.5 kg/m3. The Yello River in China is the greatest sediment-carrying stream in the world. Its annual average sediment concentration has reached 911 kg/m3 (Maidment, 1992).

5.3 LAKE NAIVASHA SEDIMENTATION RATE

5.3.1 Lake Geo-referenced Sonar Bathymetric Depth Survey

The volume of sediment accumulated in the lake is computed by the difference between the present water capacity of the lake and a known water capacity from 1957 survey. The total volume of sediment is converted to dry weight of sediment on the basis of the average specific weight of deposits.

5.3.1.1 Lake Stage-Surface Area Relationship for 2001 and 1957

Using the bathymetric map developed in Chapter (4), lake surface area is calculated for each elevation in ILWIS software. This is done in histogram statistics, pixel information. Pixel size of the 2001 and 1957 bathymetric maps is 30 meter and within this accuracy lake surface area calculation has been carried out up to the lake level of 1886.67 masl. Appendix 5.6 shows the detailed calculations.

2001 and 1957 surface areas are plotted in the same graph as shown in Figure 5.11. To have a comparison with earlier studies, lake surface area calculated by Ase et al. (1986), based on the 1927 survey was plotted on the same graph.

Figure 5.11: Lake Stage-Surface Area Curves based on surveys 2001, 1957 & 1927

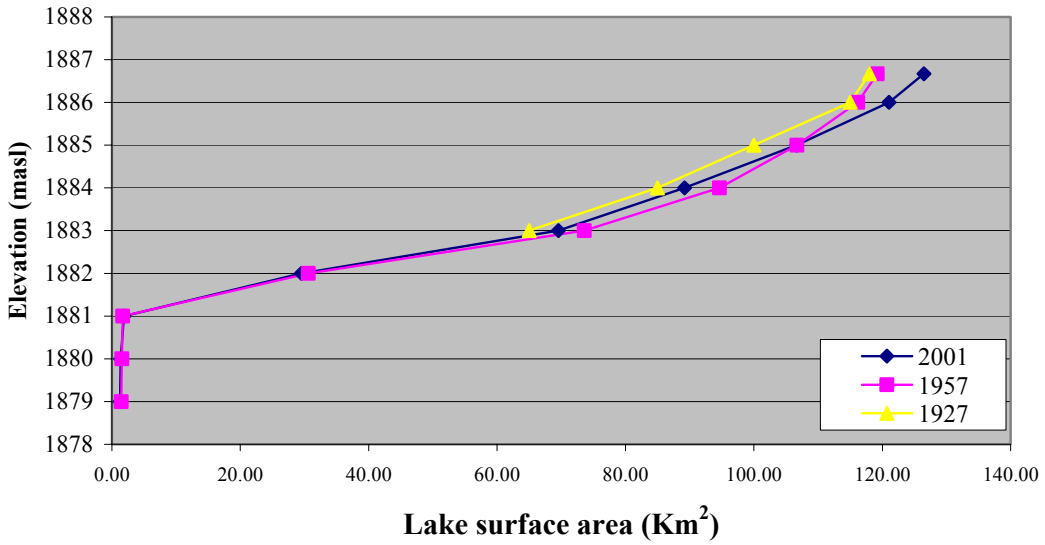

From the stage area curves of 1957 and 2001, it shows that the two data sets represent very close figures up to the elevation 1882 and after that 1957 surface area was high compared to 2001. Below 1882 elevation figures mainly represent the Crescent Lake while above 1883-elevation shows main lake area. Therefore, even though differences between 1957 and 2001 surface area in the Crescent Lake it does not represent in the same scale with the main lake. But in the detailed calculation sheet it shows differences in surface area even in the Crescent Island during 1957 and 2001.

If there is sediment accumulation in the lake, surface area and volume in 1957 should be higher than the 2001 surface area and volume. But, it is interesting to notice that after the elevation 1885, lake surface area of 1957 has reduced while 2001 surface area has been increased occupying larger figures. This may be due to the loss of papyrus area along the lakeshore line and also increase of human activities around the lakeshore from 1957 to 2001. This reasoning can be further justified with the visual inspection of 1957 analogue map of the lake that most of the shoreline covered by the papyrus swamp during 1957 is now under water. The boat route used during the 2001 bathymetric survey to enter the main lake from Crescent lake harbor was under the papyrus belt in 1957. During the lake survey in 1957 (5th July, 1957), lake level was 1886.95 masl (6191.1 ft); while the lake level during the 2001 survey (24th September, 2001) was 1886.38 masl. On the other hand this is an indication of data reliability and accuracy of digital data processing.

5.3.1.2 Lake Stage-Volume Relationship for 2001 and 1957

Lake volume calculations were carried out for 2001 as well as 1957 surveys in order to estimate the sediment accumulation during the period. ILWIS software was used to calculate the volume based on the pixel information (Pixel size is 30 m). For this calculation, for a particular fixed lake level, depth for each pixel was calculated. Then, on the basis of pixel wise, volume was calculated by multiplying pixel area and depth and cumulative was calculated for each elevation. Similar to stage area curves, both data sets were plotted in the same graph as shown in Figure 5.12 in order to make comparison as well as stage volume relationship.

Figure 5.12: Lake Volume from 1927, 1957 and 2001 Surveys

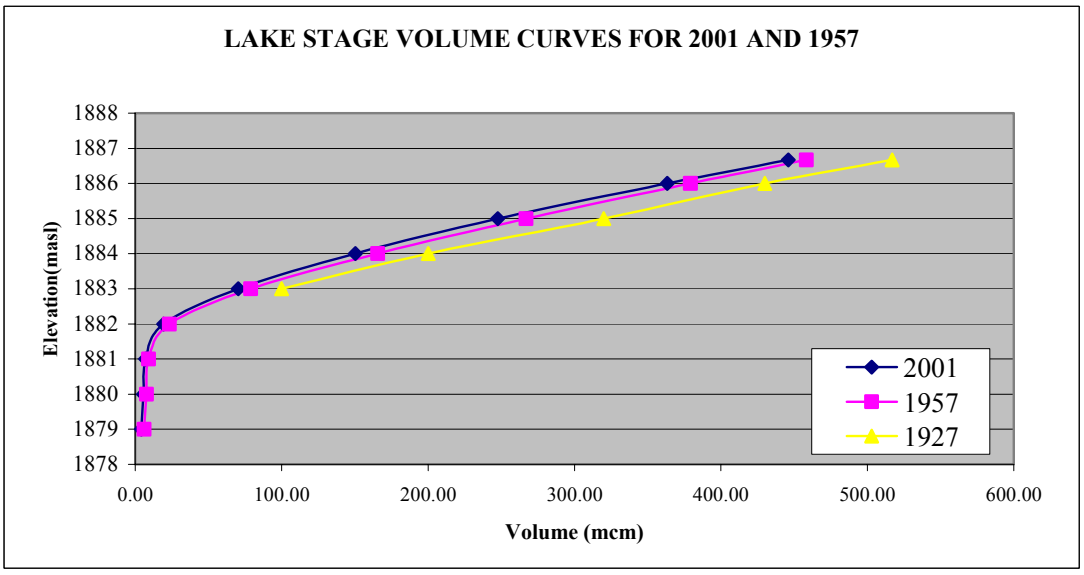

From the calculation it shows that the lake volume is 445.95 mcm in 2001 while in 1957 that was 458.338 mcm for the lake level of 1886.67 masl. Also at the lake level of 1885, lake volume is 247.52 mcm in 2001 while 266.833 mcm in 1957.

Calculated lake volumes and surface areas were compared with the earlier volume calculations done by Mmbui(1999) as well as Ase et al., (1986). The volumes calculated by Ase et al., (1986) based on

the 1927 survey is included on the same graph to compare. Their figures are in a little higher side compared to these figures. Reasons may be due to the different methodologies used for calculations; different data acquiring systems or most probably now lake has filled with sediment.

5.3.1.3 Volume of Sediment in the Lake from 1957 to 2001

Lake sediment volume calculation has done by differencing 1957 and 2001 volume for each elevation. Similar calculations have done for surface area. It is noticed that due to the higher surface area in 2001 after 1885 masl elevation, differences are negative values in higher elevations. This is due to the erosion along the shoreline rather than accumulation and higher water spread area. As this has counter effect for the volume calculations that is the reduction of cumulative volume differences between 1957 and 2001 after the elevation 1885 masl (In 1886 and 1886.67 masl). Detailed calculations are provided in Appendix. 5.6.

Therefore, sediment volume is calculated by considering the cumulative differences up to the elevation 1885 masl. Accordingly,
Volume of suspended sediment accumulation in the lake during 1957 to 2001 = 19.31 mcm

5.3.1.4 Unit Weight of Sediment after T years of Compaction

The bulk characteristics of sediments, which are of particular concern in reservoir sedimentation problems, are the grain size distribution and the specific weight of deposited sediment (Chow, 1964). As stated in Chapter (2)-Background Theory, dry mass estimation of sediment deposition into the reservoirs required determining reservoir bottom sediment bulk density (Specific weight). Specific Weight is calculated by using the collected undisturbed sediment samples and results of analysis are presented in Chapter (4). Grain size distribution of the core samples has done as stated in Chapter (3)-Materials and Methods and results has included in Chapter (4).

Different methods used to estimate the Unit Weight of sediment after 44 years (1957 to 2001) of compaction as described in Chapter (2), Background Theory. This has done using the analyzed grain size distribution of deposits. Results are shown below while detailed calculations are given in the Appendices 5.7 to 5-9.

According to the **Lane and Koelzer** (in Chow, 1964) as presented in the Chapter (2), Equation (2.3),

Table 5.12: Dry density calculation using equation 2.1

Sample No.	ID	%Clay p_c	%Silt p_m	%Sand p_s	Dry density after 44 years	
					(lb/ft3)	*(Kg/m3)*
1	M-1	73.38	25.31	1.31	61.35	982.73
2	S-1	35.49	57.77	6.75	69.22	1108.80
3	S-2	60.10	39.03	0.87	63.67	1019.90
4	S-3	45.21	41.36	13.43	68.70	1100.47
5	S-4	37.70	51.23	11.07	69.62	1115.21

After Miller (In Chow, 1964) further refined the data of Lane and Koelzer to determine average unit weight of deposits as mentioned in the Chapter 2.0. According to his equations, Unit Weight of Sediment after 44 years is as follows.

Table 5.13: Dry density calculation Equation by Miller (In Chow, 1964)

Sample No.	ID	%Clay p_c	%Silt p_m	%Sand p_s	Dry density after 44 years	
					(lb/ft3)	*(Kg/m3)*
1	M-1	73.38	25.31	1.31	55.97	896.56
2	S-1	35.49	57.77	6.75	58.83	942.37
3	S-2	60.10	39.03	0.87	58.83	942.37
4	S-3	45.21	41.36	13.43	64.78	1037.68
5	S-4	37.70	51.23	11.07	65.96	1056.58

From Table 2.3, according to the relationship of specific weight to grain-size distribution and reservoir operation used by the U.S. Soil Conservation Service, for Clay and silt mixes under permanently submerged conditions,

Specific Weight = 40 – 65 lb/ft3 = 640.74 - 1041.20 Kg/m3

= 0. 640 – 1.041 g/cm^3

According to the Julian (In Maidment, 1992), as described in Chapter 2.0,
Where, W_0 is the initial specific weight and K_0 is a factor given by the Table 2.4, Chapter 2.0.

Table 5.14: Dry Density Calculations using Equations 2.2 & 2.3

Sample No.	ID	p_cW_c *Clay*	p_mW_m *Silt*	p_sW_s *Sand*	W_0 (Kg/m3)	W_{T1} (g/cm3)
1	M-1	305.28	283.42	20.31	609.01	1.04
2	S-1	147.62	647.01	104.55	899.18	1.33
3	S-2	250.01	437.17	13.44	700.63	1.13
4	S-3	188.06	463.23	208.22	859.51	1.29
5	S-4	156.83	573.73	171.65	902.21	1.33

Table 5.15: Comparison of Dry density measured & obtained from different equations

Sample No.	ID	*Measured* (g/cm3)	Lane and Koelzer(g/cm^3)	Miller (g/cm3)	*David (1992)* (g/cm3)	*U.S.Soil* Survey (g/cm3)
1	M-1	0.497	0.98	0.90	1.04	0.64-1.04
2	S-1	0.474	1.11	0.94	1.33	
3	S-2	0.240	1.02	0.94	1.13	
4	S-3	0.153	1.10	1.04	1.29	
5	S-4	0.255	1.12	1.06	1.33	

The specific weight of sediment must be predicted in order to estimate the storage space, which will be displaced by sediment in a given period of time (Chow, 1964). The arrangement of particles has considerable bearing on the voids ratio, particularly in fine-grained sediments.

The effect of thickness of deposits is greatly influenced on the dry weight. Analysis of the dry weight of sediment deposits in this study has been based on samples obtained from the upper strata of deposits. These samples were taken with the sediment core sampler with a cutting edge. Consequently, they do not reflect the true average dry density of sediment where substantial thick nesses of superincumbent strata are involved.

An experimental result of one core sample shows the variation of the dry density with the increase of depth (Chapter 4.0). Therefore, experimental results obtained for the dry density for core samples in this analysis shows very low values compared to the other sources from literature. Due to limitations in the field, lengths of core samples were around the range of 0.3 to 0.57 m. On the other hand, as shown in the sampling location map in Chapter (4), almost all the samples obtained close to the lakeshore (Boat couldn't stand due to action of waves), which has great potential to disturb the sediments by movement of the Hippo families. Therefore, it is obvious that the core samples could not give maximum dry density expected after 44 years according to the formulas (in literature), due to the fact of inadequate sampling.

Furthermore, the variation of dry density in measured samples (0.153 to 0.497 g/cm^3) implies that the sampling of 5 locations is not enough to represent the entire lake sediment dry density variations. Therefore, to have a better picture of this variation, it is essential to do the sampling according to a well-designed sampling scheme.

5.3.2 Lake Naivasha Sedimentation Rate

Volume of total sediment accumulation in the lake during 1957 to 2001 = 19.31 million m^3
From the measured dry density and % Organic matter, neglecting lowest reading as an outlier,
Average dry density of the sediment deposition = 0.3665 g/cm^3 (Chapter 4.0)
Average % of organic matter = 18.82% (Chapter 4.0)

Total dry weight of sediment = Total Volume of sediment x Average dry weight of deposits
= 19.31 x 10^{12} x0.3665 gram/44 years
= 7.077 x 10^6 tons / 44 year
= 160.84 x10^3 tons/year
Total inorganic sediment load = 7.07711 x (1.0 - 0.1882)
= 5.745 x10^6 tons/ 44 year = 130.56 x10^3 tons/ year
Total organic sediment load = 1.32 x10^6 tons/44 years = 30 x10^3 tons/year

Capacity in 1957 at 1885 m elevation = 266.833 mcm
Capacity at 2001 at 1885 m elevation = 247.52 mcm
% Capacity loss = {(266.833 – 247.52)/266.833} x 100
= 7.2 % for 44 years
= 0.0016 % per year

Life Expectancy Rate of Lake Naivasha

Following Depreciation Formula can be applied to calculate the lake volume depreciation with time.

$$V_t = V_0(1-r)^n$$

Where, V_t = Volume at any time

V_0 = Initial Volume, considered as in 1957 volume (266.83 mcm)

r = Rate of Sedimentation (0.00164% per year)

n = Number of years

Lake Volume after 44 years (in 2001) = 247.52 x 10^6 m^3

Figure 5.13: Lake Volume Depreciation with Time

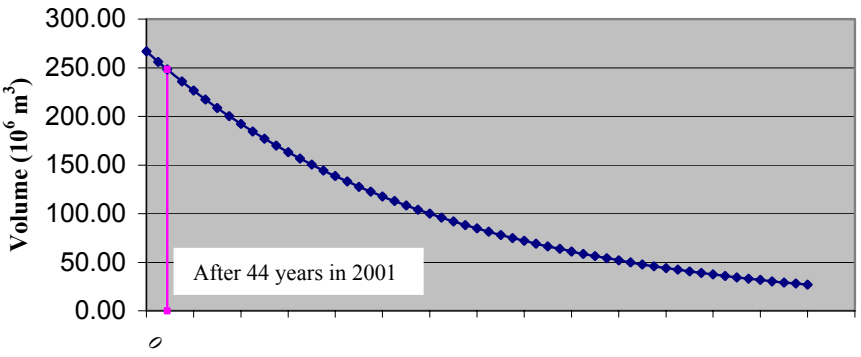

5.3.2.1 Trap Efficiency of the Lake

Although many factors may influence trap efficiency, the relative influence of each has not been evaluated to the extent that quantitative values can be assigned to individual factors (Chow, 1964).

To calculate the actual watershed sediment yield, the trap efficiency (the percentage of sediment input that is retained in the lake) must be estimated. Using data from over 40 U.S. reservoirs, Brune (1953, as reported by Rebecca in 2001) determined that the average trap efficiency for normally ponded reservoirs could be closely estimated using the ratio of lake capacity to the average annual inflow of water (C/I ratio). The resulting curves are the most frequently used trap efficiency estimate for reservoir and lake studies, although they tend to underestimate the percentage of coarse sediment retained and overestimate the percentage of fines (Heinemann, 1984 in Rebecca in 2001).

This kind of average annual relationship is unlikely to be accurate for the Naivasha Lake, as the lake doesn't have surface outlets. But many researchers pointed out that lake has significant seepage inflow and outflow. A rough estimate may be obtained by applying Brune's empirical relationship, but it is necessary to choose a representative lake capacity.

Therefore, assuming that the lake capacity at 1886.0 m. elevation is a representative value,

An annual average discharge at station 2GB1 = 153 x 10^6 m^3 (Ase et al.,)

Average annual flow from river Gilgil during the period 1962-1980 = 24 x 10^6 m^3(Ase et al.)

Lake capacity = 363.26 mcm (according to 2001 survey at the lake level of 1886.0 masl)

Therefore,

Capacity/Inflow Ratio = 2.05

According to the Brune's sediment trap efficiency curves (David R maidment, 1992), using the Envelope and Median curves for normal ponded reservoirs,
Percent sediment trapped in the lake = 98-95%

The value obtained for the trap efficiency is almost close to the 100% and considering the fact that the lake Naivasha has no surface outlet, trap efficiency value is estimated as 100%.

5.3.3 Estimation of Lake Water Shed Sediment Yield

The sediment yield from a watershed may be determined by measuring the accumulation of sediment in a lake/reservoir of known age and adjusting for losses over the spillway, or by periodic sampling of the stream flow (Chow, 1964).

Accordingly, mean annual sediment yield can be estimated as;

$$\text{Mean annual sediment yield} = \frac{\text{Accumulated sediment weight in the lake from 1957-2001}}{\text{Watershed drainage area x Time period considered}}$$

But, different active sediment input sources can contribute to the sediment accumulation in the lake except main rivers. Some of input sources could be the wind, shoreline erosion and human activities along the lakeshore especially southern part of the lake. Out of this sediment input sources, assuming major sediment input through main rivers ie. Malewa and Gilgil, long-term annual average sediment yield can be estimated for lake Naivasha catchment.

From 1957 to 2001, Lake Naivasha contains 19.0 million m^3 of sediment which, if spread evenly over the depositional area of lake bottom (89.23 km^2 at 1884 masl) would give an average thickness of 0.21 m. After 44 years from 1957-2001, the lake has only lost about 7 % of its capacity at 1885 m elevation. This corresponds to the sedimentation rate of 1 m /100 year which expressed by Dr. Verschuren, University of Kenya in oral communication during a seminar to Dr. Robert Becht.

From 1957 to 2001, accumulated sediment mass of 7.07×10^6 tons of in the lake contains 5.745×10^6 tons of inorganic sediment and 1.32×10^6 tons of organic sediment. Assuming that the lake trapped all the sediment that entered it and major sediment input through main rivers, the estimated long-term watershed sediment yield is about 39.5 tons/km^2/year of inorganic sediment considering the whole drainage basin. (Catchment area of the lake Naivasha = 3300 km^2 (Ase et al.,)). If these calculations made on the basis of total mass of sediment, long-term average annual sediment yield for whole drainage basin is about 48.0 tons/km^2/year.

But on the other hand, if there are another active major sediment inputs to the lake except main rivers, the estimated long-term annual average sediment yield could be less than the estimated watershed sediment yield based on the assumption i.e. major sediment input to the lake through main rivers. If calculations made considering only the hydraulically connected sub catchment areas of Malewa and Gilgil rivers (Malewa catchment 1730 km^2 and Gilgil 420 Km^2), the long-term annual average watershed sediment yield is about 74 tons/km^2/year.

Global minima for specific suspended sediment yield lie well below 2 tons/km^2/year. Maximum of 2000 tons/km^2/year for the Sulak River in the USSR and Fournier (1960) cites maximum values in excess of 10,000 t/km^2/year for the Lo Ho River in the People's Republic of China (Walling, 1985). Accordingly, the estimated watershed sediment yield of Naivasha catchment lie well below the maximum range, but very close to the low sediment yield values recorded so far.

CHAPTER 6.0 – REMOTE SENSING IMAGE ANALYSIS

6.1 Introduction

This chapter discusses the possibility of extracting water depth and water quality by interpretation of remotely sensed images. As the depth sounding and sampling of water quality parameters from boats are expensive and manpower consuming, especially when information over a large area is desired, an attractive alternative could be determination of the water depths and quality parameters by means of remote sensing techniques, i.e. through interpretation of satellite imagery (Hengel, 1988).

In case of lake Naivasha, due to large surface area of the lake, it is not an easy task to cover the entire lake by in-situ measurements. Also, wild animals and hippo population make access to the lake and adjacent area difficult, rendering research on mapping water quality parameters through satellite remote sensing. But this chapter covers only the literature survey of remotely sensed image analysis, due to limitations in time and lack of field data for calibration.

Remote sensing of coastal and inland waters has developed since the early seventies from an empirical based method producing qualitative water quality maps to more quantitative methods such as semi-empirical and analytical methods producing quantitative maps of water quality. The range of optical water quality properties that may be estimated by remote sensing has increased from suspended matter to include properties such as a chlorophyll contents (Dekker, 1998).

Multi-temporal images can be used to compute the number of tons of suspended matter and chlorophyll-a over the study area. However, most previous studies have not attempted to tackle the temporal comparison and change detection of the water quality parameters, mainly because of the difficulty associated with absolute radiometric calibration of the satellite images. From a monitoring point of view change detection, therefore calibration, is a critical aspect of ecosystem evaluation and management(Tassan,1993).

6.2 Literature review on published algorithms

6.2.1 Water Depth Mapping by means of Landsat TM

Daniel Spitzer et al.(1998), studied the possibility of extracting water depth by using satellite images. The proposed models comprises for the transmission of the solar radiance through the atmosphere, as well as the algorithms linking the water leaving radiance with the water depth using Landsat TM. They applied the algorithms for water depth mapping, developed by Spitzer and Dirks (1987).

According to them, models for the transmission of the solar radiance through the atmosphere, as well as algorithms linking the water leaving radiance with the water depth have to be developed for the

correct interpretation of the imagery. The approach proposed by the Strum (1981b) and Vanouplines (1986) is chosen for the atmospheric modelling. Algorithms, which link the water depth with the normalized water leaving radiance, were developed by Lyzenga (1978, 1985) and Spitzer & Dirks (1987) used by the Spitzer,D.et al.

6.2.2 Remote Sensing Algorithms for Water Quality

Moral & Gordon (1980), pointed out three approaches by which measurements of spectral (ir) radiance can be used to estimate concentrations of water constituents by processing remote sensing data:

- The empirical approach
- The semi-empirical approach
- Analytical approach

(a) The Empirical Method

In the empirical approach statistical relationships are sought between measured spectral values and measured parameters. The limitation of such an approach is that spurious results may occur, because casual relationships between the parameters are not necessarily implied.

Serwan (1993) studied the water quality parameters chlorophyll-a, total phophorus, Secchi disk depth, suspended solids, salinity and temperature in the Norfolk Broads using the Landsat TM data. An empirical approach of relating TM data with ground-referenced data for these parameters through regression analysis was employed and found that significant relationships between them.

(b) The semi-empirical Method

This approach may be used when the spectral characteristics of the parameters of interest are known. This knowledge can be included in the statistical analysis by focusing on well-chosen spectral areas and appropriate wavebands or combinations of wavebands are used as correlates. Quantitatively, the coefficients from any such relationship only apply to the data from which they derived. Each application must therefore be individually calibrated. This method is commonly used.

Brivio et al., (2001) determined the chlorophyll concentration changes in Lake Garda using an image-based radiative transfer code for Landsat TM images. They applied a completely image based atmospheric correction method by means of an inversion technique based on a simplified radiative transfer code (RTC) to investigate the water leaving radiances adequately, the contribution of the atmospheric path radiance reaching the sensor should be removed. Then, they derived chlorophyll maps by adopting a semi empirical approach of relating atmospherically corrected TM spectral reflectance to insitu measurements through regression analysis.

Pat (1998), studied of San Francisco Bay, using Landsat Thematic Mapper images and field spectral radiometer data. The field spectral radiometer has wavelengths identical to those on Landsat TM and its data were used with the water sample results to build relationships between spectral reflectance and both suspended particle matter (*SPM*) and chlorophyll-a concentrations. According to him, an advantage of using near-infrared spectral band is that because of its minimal water penetration most sub-bottom reflectance problems, especially in clear and shallow waters, are eliminated.

During this study he used spectral reflectance measurements made in the field during water sampling cruises, along with a satellite calibration and radiometric correction model to convert satellite digital numbers (DNs) to surface reflectances, allowing the mapping of desired water parameters on a temporal basis without the need for water sampling during each satellite overflight. Satellite radiometric correction model makes corrections for sensor gains and offsets, spectral irradiance, solar elevation, atmospheric scattering and absorption (additive and multiplicative effects), and Earth-Sun distance. The SPM and chlorophyll-a values computed from the water samples and the spectral reflectance measurements made in the field during the water sampling were used as input to regression analysis. The resulting relationship was used to transform the satellite surface reflectance images, which are generated using the radiometric calibration and correction model, into SPM and chlorophyll-a digital image maps.

Spectral Mixture Analysis:
Leal et. al.(1993), has estimated suspended sediment concentrations in surface waters of the Amazon River Wetlands from Landsat data based on a linear spectral mixture analysis of each image with end members derived from laboratory data of reflectance from water-sediment mixtures reported by Witte et al.(1981). Using these reference spectra, they applied a linear mixture analysis to multi-spectral images after accounting for instrument and atmosphere gains and offsets. Then sediment concentrations were estimated for individual pixels from the mixture analysis results based on a non-linear calibration curve relating laboratory sediment concentrations and reflectance to end member fractions. Accordingly, the methodology can be applied universally if the optical properties of water and sediment at the site are known, and it is, therefore, useful for the study of suspended sediment concentration in surface waters.

Satoshi et al., (2001), developed a new water turbidity index (WTI) based on multi spectral images and applied to Landsat TM images to monitor the turbid water at the Kushiro Mire, Japan. They used spectral mixture analysis (SMA) to produce a turbidity estimation model. The SMA “unmixes” a mixed pixel determining the fractions due to each spectral end member. The relative abundance of each end member was estimated based on this spectral information using SMA. Water Turbidity Index was calculated from the mixed spectrum of the test site and the regression curve for the relation between WTI and the actual turbidity was determined. Finally, this regression equation was used to derive a turbidity map from the WTI image.

Mayo et al.,(1995) used Landsat TM data and the high spectral resolution radiometric measurements in the range of 400 to 750 nm for estimating chlorophyll, suspended matter concentrations and secchi disk transparency in Lake Kinneret. According to them the radiometric data were used to create an algorithm for estimation of chlorophyll concentration from the TM data. It shows that the radiance in channel TM3 (620-690nm) was primarily dependent upon non-organic suspended matter concentration and (TM1-TM3)/TM2 was found to be a useful index for estimating chlorophyll concentration and the atmospherically corrected TM data were used for the calculations.

Tassan(1993), has developed an algorithm suitable for the determination of chlorophyll and suspended sediment concentrations in coastal waters from TM data through a numerical simulation. The composition has been carried out by a three-component model of sea colour derived from in-situ measurements performed in Gulf of Naples.

Dekker et al.,(1993) analysed Landsat TM images to assess the scope and limitations of their use for inland water quality detection. They mentioned the limiting factors in the quantitative determination of water quality parameters are in first instance the radiometric resolution and in second instance the spectral resolution. Combinations of spectral bands of the TM are discouraged for analysis purposes as long as a physical explanation of the result is lacking. They reported that under ideal circumstances the TM can be used to assess seston dry weight, sum of chlorophyll a and Secchi depth with limited accuracy.

(c)The analytical method

General approach of the analytical method described by Pasterkamp et al., (1999) for retrieval of suspended matter concentrations from SPOT images as follows.

In the (Forward) analytical method, inherent optical properties and concentrations of coloured water components are used to parameterise a bio-optical model, which unable to simulate the amount (expressed as radiance) of light that leaves the water in various portions of the spectrum. An important intermediate quantity used for relating this radiance measured by a sensor (somewhere above the water surface) to water quality parameters is the subsurface irradiance reflectance, R(0-). R(0-) is relatively incentive for light conditions; therefore it can be used as a robust optical estimator of water quality parameters.

The inherent optical properties are spectral absorption and backscatter per optical active water component. A suite of analytical approaches and inversion techniques can be used to invert the parameterised bio-optical model and retrieve concentrations of water constituents from the remotely sensed up welling light.

According to Pasterkamp et al., (1999), the forward bio-optical model and its inverse (water quality algorithm) model can be used for remote sensing of water quality. To establish algorithms in the "inverse water" compartment input from the "forward water" compartment, measured input parameters and inherent optical properties (IOPs) and corresponding concentrations is necessary. Determining concentrations from the satellite images requires the modules "inverse atmosphere" and "inverse water".

Figure 6.1 below illustrates the methodology outlined by the Pasterkamp et al., (1999) for estimating suspended sediment from remote sensing images using bio-optical modelling.

Figure 6.1: The forward and Inverse Bio-optical Model for Remote Sensing of Water Quality (Pasterkamp et al., 1999)

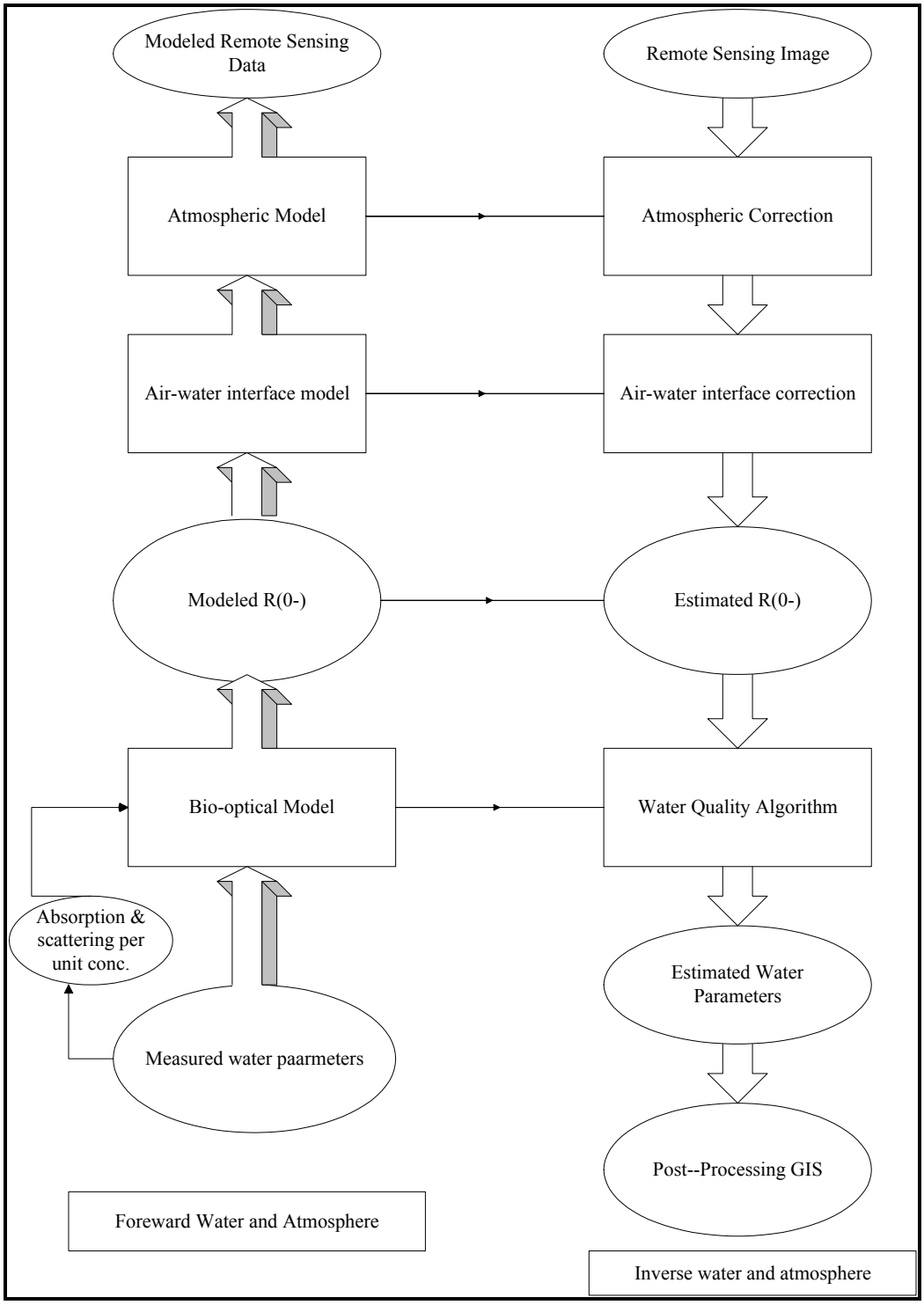

6.3 Limitations in Remote Sensing Image Interpretation

One of the constraints in use of remotely sensed images for extracting water depth and quality parameters is the application of atmospheric correction. This needs large calibration data sets in the field. Also as mentioned in the literature survey, to have the better results for water depth and quality parameters through interpretation of remotely sensed images, due attention should be paid for the factors discussed above.

A full remote sensing analysis of lake physical parameters (depth, turbidity, suspended matter) was not done because lack of a field spectrometer data to determine the optical water characteristics of that period.

CHAPTER 7.0 - DISCUSSION AND CONCLUSIONS

7.1 Discussion

It has been shown in this study the use of RS and GIS techniques are useful scientific tools for determining lake sedimentation. Planning and execution of geographically referenced lake bathymetric depth survey in combination with water and sediment sampling showed very feasible, and leading to accurate data. Spatial geo-statistical analysis was used to determine the spatial distribution of sediment in a particular water body, making ways to identify the causes / reasons for sedimentation. Use of a GIS environment made direct quantitative comparison with historical data possible. Prior comparison and selection of an appropriate geo-statistical gridding method is however recommended, to make best use of measured data. Further, it is evident from the literature that by interpreting remotely sensed images we can extract water depth, suspended sediment and water quality parameters if processed with field data. A full remote sensing analysis of lake physical parameters (depth, turbidity, suspended matter) was not done here because lack of a field spectrometer to determine the optical water characteristics of lake Naivasha in that period. Instead, more effort was spend on analyzing possible sediment transport mechanisms and inputs through the lower Malewa (and Gilgil) river systems.

According to our analysis, the sediment input in lake Naivasha in the period 1957 – 2001 was 19.0 million m^3 of sediment, which, if spread evenly over the depositional area of lake bottom (89.23 km^2 at 1884 m level m.a.s.l.) would give an average thickness of 0.21 m. The total mass of sediment accumulated in the lake was estimated at 7.07×10^6 tons for the 44 year period from 1957-2001. Out of this, 5.75×10^6 tons was determined as inorganic mineral matter and 1.32×10^6 tons of organic matter. Assuming that the lake trapped all the sediment (100% trapping efficiency) that entered it, the estimated long-term basin sediment yield is about 39.5 metric tons/km^2/year of inorganic sediment. However, this estimate uses the whole Naivasha lake basin as sediment supply area (including also the southern parts, who are not directly connected to the lake by surface drainage or river network). If we exclude, these sub-basin areas from the sediment yield estimate, we obtain 74.0 metric tons/km^2/year as a long-term average sediment yield for the Malewa – Turasha and Gilgil river basins. The sediment input in the lake (between 1957-2001) represents only a 7 % reduction of its volume capacity (volume estimate based on the 1985 m. m.a.s.l. level).

Sediment transport plays an important, if not the most important role in all problems of fluvial hydraulics. This phenomenon is very complex and consequently a theoretical study can only be performed in simple or simplified cases. During the analysis for estimating sediment fluxes to the lake through the main rivers, the complexity of the problem can be illustrated i.e., by the different results from the three formulas for bed load transport, which we used. Numerous sediment transport formulas have been proposed in the past, and subsequent modifications of original formulations have been

prescribed. Although significant progress has been made, none of the existing sediment transport formulas truly fulfils its task and equations and approaches have to be compared (Julian, 1995).

It is difficult to determine a reliable bed load because of the lack of reliable field data from natural streams (Maidment, 1992). Many bed load relationships have been developed from experimental flume data. For given stream flow conditions, a sediment transport equation can only predict the sediment transport capacity of a given bed sediment mixture. The formulae, developed for the quantitative determination of the transport of sediments, are based on experimental results, being often limited, and thus should be used with much caution (Graf, 2001). In engineering practice, one compares several formulas with field observations to select the most appropriate equation at a given field site.

It is evident that the Malewa suspended sediment-rating curve is a supply-limited sediment-rating curve. The case of supply-limited rating curves is characterized by low concentrations and high variability (Julian, 1995). Hysteresis effects between discharge and concentration, seasonal variation, inaccuracies in flow and sediment measurements, and variability in the wash load may explain the scatter of points on the sediment rating curve. Better results are sometimes achieved, provided that sufficient data are available, by setting individual sediment rating curves for each month. At a given discharge, higher sediment concentrations are generally observed during the rising limb of the hydrograph (Julian, 1995). Therefore, even though, estimated loads using suspended sediment-rating curves corrected statically to compensate these effects, daily data might not anticipated the inherent stochastic nature of flow.

According to the estimated results, Malewa River supplies long-term suspended sediment concentration of 0.23 kg/m^3 from 1932 to 1990 while 0.26 kg/m^3 considering the period from 1957 to 1990. Measured concentrations during the 2001 fieldwork, shows that the average suspended sediment concentration along the Malewa River is 0.21 kg/m^3 (based on a limited number of nine sample dates & measurements). Long-term annual average suspended sediment concentration of Malewa is about 42.8x10^3 tons and 55.9 x10^3 tons for the period of 1932-1990 and 1957-1990 respectively. Based on the latter figure, suspended sediment flux to the lake through Malewa from 1957 to 2001 can be estimated at 2.46x10^6 tons.

Further, long-term average annual Gilgil river sediment flux couldn't estimated to correlate with lake sedimentation, due to lack of reliable daily data in gauging station 2GA1, even though a sediment rating curve has been developed for 2GA1, gauging station. This makes correlation difficult with lake sedimentation with river fluxes. Reservoir sedimentation surveys give, in general, much more accurate data than the sediment estimations based on the measured suspended load and the estimated bed loads from empirical formulae.

We also screened three approaches for bedload transport of the lower Malewa river i.e., Einstein method, the Graf-Acaroglu formula and the Ackers & White equation (Graf, 2001). We were able to establish as such the total load solid discharge – rating curves for this river sector.

Except main rivers sediment input, we are aware of potential other sources of sediment, which may introduce sediment to the lake such as shoreline erosion, wind erosion – dry dust deposition, and certain human activities around the lakeshore. Spatial distribution of sediment in the lake shows high

accumulation of the sediment along some places on the shoreline, which in part supports this idea. However, also resuspension and in-lake transport of suspended sediment by wind-driven currents can in part explain these sediment accumulations.

7.2 Conclusions

Based on this study following conclusions have been drawn.

- Application of GIS and RS techniques in combination with GPS-based lake monitoring techniques can be used conveniently for assessing lake sedimentation processes can be a good management tool as it provides advantages over traditional methods.

- Long-term mean annual sediment yields of Malewa and Gilgil rivers are low compared to the global scale.

- Estimated sediment fluxes to the lake through main rivers, is low compared to the measured sediment accumulation in the lake. Of course, depositional processes in the river reaches between the surveyed river sections (2GB1, 2GA1, Dairy Training school section) and the lake, can explain these differences. Also other facts to support this difference are the difficulties in sampling and estimating bed load transport, as well the sources which may introduce sediment into the lake (wind, human activities around the lake shore etc.,).

7.3 Future Research

Analysis and remote sensing images and application of the optical remote sensing approach for depth, suspended sediment and water quality parameters through bio-optical modelling as discussed in Chapter (6) is recommended.

Further analysis for improving sediment-rating curves for both suspended and bed-load transport in Malewa and Gilgil by incorporating more field data is recommended.

REFERENCES

- **Ase, L.E., Sernbo, K. and Syren, P.(1986)**: Studies of Lake Naivasha, Kenya, and its Drainage Area: Naturgeografiska Institutionen, Stockholms University, 63, 1-75.

- **Asselman, N.E.M.(2000):** Fitting and Interpretation of Sediment Rating Curves, Journal of Hydrology 234 (2000) 228-248.

- **Brivio, P.A., Giardino, C. and Zilioli, E.(2001)**: Determination of chlorophyll concentration changes in Lake Garda using an image-based radiative transfer code for Landsat TM images: International Journel of Remote Sensing, Volume 22, No.2&3, 487-502.

- **Chow, Ven Te (1964)**: Handbook of Applied Hydrology.

- **David, P. Mau. and Victoria G. Christensen(2001):** Reservoir Sedimentation Studies to Determine Variability of Phosphorus Deposition in Selected Kansas Watersheds: Website: http://ks.water.usgs.gov/Kansas/pubs/reports/mau.fisc.html

- **Dekker, A.G. and Peters, S.W.M.(1993):** The use of Thematic Mapper for the analysis of eutropic lakes: a case study in the Netherlands. Internal J.Remote Sens. 14, 779-821.

- **Dekker, A.G., Malthus, T.J. and Hoogenboom, H.J. (1995):** The Remote Sensing of Inland Water Quality. In: Danson, F.M.,Plummer, S.E.(Eds.) Advances in Remote Sensing. Chichester: John Wiley and Sons (1995) pp.123-142.

- **Dekker, A.G. and Hoogenboom, H.J. (1997):** Operational Tools for remote sensing of water quality: A prototype toolkit, NRSP-2, 96-18, ISBN 90 5411 215 8 .

- **Gauget, J.J. and John, M.M. (1981):** Major Ion chemistry in a tropical African lake basin: Freshwater Biology, Vol.11, pp.309-333.

- **Gert, A.Schultz. and Edwin T. Engman (Eds.).,(19..):** Remote Sensing in Hydrology and Water Management, ISBN 3-540-64075-4.

- **Gonima, L.(1993):** Simple algorithm for the atmospheric correction of reflectance images, Internal J.Remote Sens. 14, No.6, 1179-1187.

- **Graf, W.H. and Altinakar, M.S.(2001):**Fluvial Hydraulics: ISBN 0-471-97714-4, 2001

- **Harry H. Barnes (1849):** Roughness Characteristics of Natural Channels, Geological Survey Water Supply Paper.

- **Hardy, R.J, Bates, P.D. and Anderson, M.D.(2000):** Modelling suspended sediment deposition on a fluvial floodplain using a two-dimensional dynamic finite element model, Journal of Hydrology 229, Pg. 202-218.

- **Harper, D.M., Geoff, P., Alison, C., Nzula K. and Kenneth M. (1993):** Eutrophication prognosis for Lake Naivasha, Kenya.

- **HEC-RAS User Manuel, Version 2.2 (1998):** Developed by the U.S. Army Corps of Engineers.

- **ILWIS User Manuel, Version 3.0 (2000):** Developed by the International Institute for Geo-information Science and Earth Observation.

- **Jack Lewis and Rand Eads (2001):** Automatic Real-Time Control of Suspended Sediment Sampling Based Upon High Frequency in situ Measurements of Nephelometric Turbidity: Website: http://water.usgs.gov/osw/techniques/sedtech21/lewis.html.

- **Joseph, M. M. (1991):** Vegetation Response to Climatic Change in Central Rift Valley, Kenya, Quaternary Research 35, pp.234-245.

- **Julien, Pierre Y. (1995):** Erosion and Sedimentation by Cambridge University Press (1995)

- **Keith, P.B.T., Robert K. L. and Sander C. C.,(1973):** Remote Sensing and Water Resources Management, American Water Resources Association, Urbano, Illinois.

- **Leal, A.K.M., Milton, O.S. and John, B.A.(1993):** Estimating Suspended Sediment Concentrations in Surface Waters of the Amazon River Wetlands from Landsat Images: Journel of Remote Sensing of Environment, 43, Pg281-301.

- **Litterick, M.R., Gaudet, J.J., Kalff, J. and Melack, J.M. (1979)**: The Limnology of an African Lake Naivasha, Kenya: Report prepared by the University of Nairobi, McGill University, Montreala and University of California, Santa Barbara.

- **Maidment, D. R. (1992):** Handbook of Hydrology: ISBN 0-07-039732-5

- **Mmbui, S.G. (1998):** Study of Long-term water balance of Lake Naivasha, Kenya: Master of Degree Thesis, ITC, The Netherlands.

- **Mayo, M., Gitelson, A., Yacobi, Y.Z. and Ben-Averaham, Z.,(1995):** Chlorophyll distribution in Lake Kinneret determined from Landsat Thematic Mapper data, Internal J.Remote Sens. Vol.16, No.1, pp.175-182.

- **Noha, S.D. (1998):** Integration of GIS and Computer Modelling to Study the Water Quality of Lake Naivasha, Central Rift Valley, Kenya: M.Sc Degree Thesis, ITC, The Netherlands.

- **Patrick, M. (2001):** Spatial Analysis of Water Quality and Eutropication Controls in Lake Naivasha, Kenya: M.Sc Degree Thesis, ITC, The Netherlands.

- **Parker, R.S. (2001):** Bias Correction – Retransformation Website: http://webserver.cr.usgs.gov/sediment/bias.frame.html

- **Pasterkamp, S., Peters, S.W.M., Rijkeboer, M. and Dekker, A.G.(1999)** : RESTWES: Retrieval of Total Suspended matter concentrations from SPOT images, Report number W-99/33, September,1999.

- **Rebecca, K.R.A. (2001):** Using the sediment record in western Oregon flood-control reservoir to assess the influence of storm history and logging on sediment yield, Journal of Hydrology 244, pp. 181-200.

- **Remconsult Engineering Surveyors (1998):** Report on lake depth survey under the Water Resources Assessment and Planning Project (WRAP), Ministry of Water Resources, Nairobi, Kenya.

- **Lake Naivasha Riparian Owners Association (1993):** Report on a Three Phase Environmental Impact Study of Recent Developments around Lake Naivasha, Kenya.

- **Satoshi, K., Yoshiki, Y., Futoshi, N. and Masami, K.(2001):** Development of WTI and Turbidity estimation model using SMA – Application to Kushiro Mire, Eastern Hokkaido, Japan; Journal of Remote Sensing of Environment, 77, pp.1-9.

- **Serwan, M.J. B. (1993):** Detecting water quality parameters in the Norfolk Broads, U.K., using Landsat imagery, Internal J.Remote Sens. 14, No.7, pp.1247-1267.

- **Schultz, G.A.(1993):** Hydrological modeling based on remote sensing information. Adv.Space res., Vol.13, No.5, pp 149-166.

- **Tassan, S. (1993):** An improved in-water algorithm for the determination of chlorophyll and suspended sediment concentration from Thematic Mapper data in coastal waters, Internal J.Remote Sens. 14, No.6, 1221-1229 (1993)

- **Van Hengel, W. and Spitzer, D. (1998):** Water Depth Mapping by means of Landsat TM: Report bcrs-88-12, Final report project 4512/OP-1.4

- **Van Reeuwijk, L.P. (1995):** Procedures for Soil Analysis, Technical Paper No. 09, Food and Agriculture Organization for the United Nations, 5th Edition.

- **Viak Report (1974):** Naivasha Water Supply Project, Ministry of Agriculture, Kenya.

- **Walling, D.E., Hadley, R.F., Lal, R., Onstad, C.A. and Yair, A. (1985):** Recent Developments in Erosion and Sediment Yield Studies, International Hydrological Programme, United Nations Educational Scientific and Cultural Organization, Paris.

- **Pat S. Chavez. (1998):** Mapping Suspended Sediment Using Remotely Sensed Satellite Images: San Francisco Bay, Proceedings, Federal Interagency Workshop, http://water.usgs.gov/osw/techniques/sedtech21/lewis.html.

Appendix 4.1

Appendix 4.2

- Natural Neighbour Method
- Minimum Curvature Method

Appendix 4.3

Bathymetric Map Using Moving Average Method

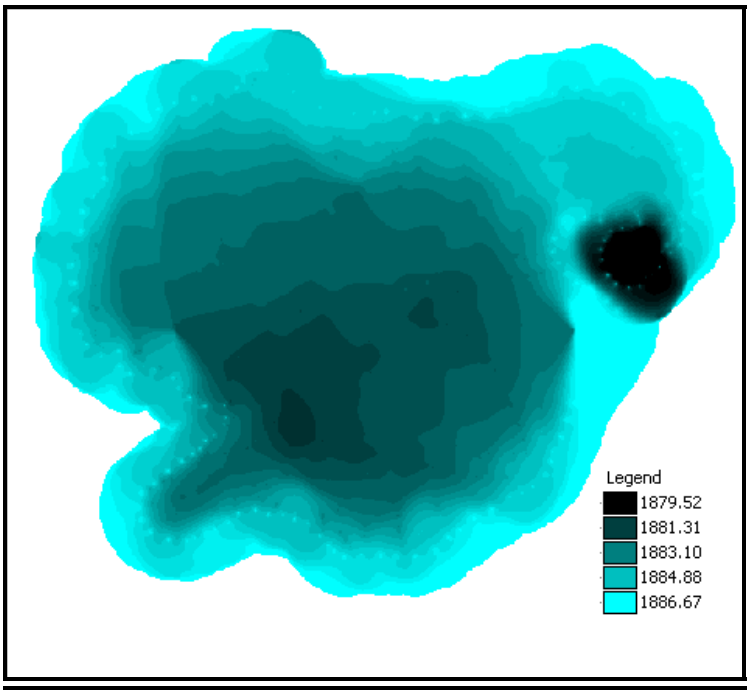

APPENDIX – 4.4

METHODOLGY FOR THE TRANSFORMATION OF CASINI CO-ORDINATE SYSTEM TO UTM SYSTEM

A segment map of 1957 contour survey was created using ILWIS software. For this a new geo-reference and co-ordinate system was created within the ILWIS software with the following specifications as stated by Mr. Jan Hendrikse in ILWIS Department at ITC (Reference printed from Mr. Data attached herewith).

In the ILWIS programme file "Datum.def", under the section, "Arc 1960" following details were entered.

"Naivasha=-206, 67,-99,Lake Naivasha"

After that coordinate system was created using following specifications.

Casini Projection

Type = Projection
Projection = cassini
Datum = Arc 1960
Datum Area = Naivasha

Specifications of the projection

False Easting = 0.000000
False Nothing = 0.000000
Central Meridian = 37.000000
Latitude of true scale = 0.000000
Scale Factor = 1.000000

With this Casini coordinate system, a segment map was digitised using the available contour maps in units meter system. Then co-ordinate transformation was done using the vector operations in ILWIS. This was verified by using the two-bench mark survey carried out recently.

Contd..Appendix – 4.4

Datum shifts by Jan Hendrikse, ITC, ILWIS development - Extracted from Mr. Data

Given 5 points in two co-ordinate systems:
3D GEOCENTRIC WGS84 CO-ORDINATES: X, Y, Z
(WGS84 ellipsoid is exactly known)
3d local 'Cassini' co-ordinates: East, North, Orthom height
(approximating ellipsoid is probably Clarke 1880, but datum shifts are unknown)

With the so-called Bowring_method I have converted the geocentric co-ordinates to
ellipsoidal Phi, Lam, Height (on the WGS84) (*)

With an ILWIS Co-ordinate System having a Cassini projection with CM = 37E and the Clarke 1880 ellipsoid, I have converted the Cassini E,N co-ordinates back to LatLons on the Clarke ellipsoid (**)

ILWIS can handle the (Molodensky) transformation between two ellipsoidal systems, i.e., to change from a WGS84 Latlon to a Latlon on any other (local) ellipsoid, given the shifts (without rotation) between the two ellipsoids.
The missing rotation parameters cause errors of less than a meter (planimetric) in an area of 500 by 500 km.
For each Datum the shifts dX,dY,dZ (of each ellipsoid relative to WGS84) are listed and stored in ilwis\system\datum.def

I wrote a program "Inverse_Molodensky", that assumes the knowledge of 3 points (LatLonHeight) in two different Ellipsoidal systems,
one of them being the WGS84 ellipsoid, the other one being a Local system for which we know only the ellipsoid but not its Datum shift.
The inversion of the Molodensky equation requires the input of a, 1/f , da, df , N, M parameters of the Local ellipsoid and phi, lam and h on both ellipsoids.
The inversion produces dX, dY and dZ, the shifts between the two ellipsoid origins.
This result can be used to define a new Datum shift in the file datum.def

Applying Inverse_Molodensky to the data (*) and (**), I obtained the following results, and inserted them in datum.def:
Under the section [Arc 1960]
Naivasha=-206,67,-99,Lake Naivasha

After defining the cassini ("Cas37plu") projection co-ordinate system in ILWIS with the following specifications,
Type=Projection
Projection=cassini
Datum=Arc 1960
Datum Area=Naivasha

[Projection]
False Easting=0.000000
False Northing=0.000000
Central Meridian=37.000000
Latitude of True Scale=0.000000
Scale Factor=1.000000

I can transform the WGS84 LatLons to both cassini latlons and cassini projected E,N co-ordinates
The points can, if needed, also be converted to UTM37South co-ordinates, assuming we know a datum shifts for these.
Comparing the columns cassE, cassN with cassXplu, cassYplu and notice a max error .5m in E and 3m in N.
These errors could be caused by for instance wrong ellipsoid assumption, or using orthometric heights combined with plane (projected) co-ordinates.

APPENDIX 4.5

Malewa Reach (1) – Details of Calculations

HEC-RAS Plan: Malewa2GB1 River: Malewa Reach: D/S of GB2 Relo

Reach	River Sta	Q Total	Min Ch El	W.S. Elev	Crit W.S.	E.G. Elev	E.G. Slope	Vel Chnl	Flow Area	Top Width	Froude # Chl
		(m3/s)	(m)	(m)	(m)	(m)	(m/m)	(m/s)	(m2)	(m)	
D/S of GB2	5	0.50	1948.15	1950.68		1950.69	0.000012	0.06	8.49	4.69	0.01
D/S of GB2	5	2.00	1948.15	1950.98		1950.98	0.000122	0.20	9.89	4.91	0.05
D/S of GB2	5	8.00	1948.15	1951.60		1951.62	0.000925	0.61	13.10	5.38	0.12
D/S of GB2	5	15.00	1948.15	1951.99		1952.04	0.002231	0.98	15.30	6.02	0.20
D/S of GB2	5	25.00	1948.15	1952.40		1952.50	0.004258	1.39	17.99	7.11	0.28
D/S of GB2	5	50.00	1948.15	1953.17		1953.39	0.008217	2.06	24.27	9.19	0.40
D/S of GB2	4	0.50	1948.77	1950.68		1950.69	0.000030	0.09	5.82	4.17	0.02
D/S of GB2	4	2.00	1948.77	1950.97		1950.98	0.000280	0.28	7.07	4.45	0.07
D/S of GB2	4	8.00	1948.77	1951.58		1951.61	0.001851	0.80	9.97	5.24	0.19
D/S of GB2	4	15.00	1948.77	1951.94		1952.02	0.004080	1.25	12.01	5.95	0.28
D/S of GB2	4	25.00	1948.77	1952.31		1952.47	0.007431	1.74	14.39	7.06	0.39
D/S of GB2	4	50.00	1948.77	1953.04		1953.33	0.012490	2.40	20.83	9.90	0.53
D/S of GB2	3	0.50	1949.21	1950.68		1950.68	0.000154	0.14	3.51	4.56	0.05
D/S of GB2	3	2.00	1949.21	1950.97		1950.98	0.000961	0.41	4.85	4.92	0.13
D/S of GB2	3	8.00	1949.21	1951.55		1951.60	0.003978	1.01	7.92	5.87	0.28
D/S of GB2	3	15.00	1949.21	1951.88		1951.99	0.008363	1.47	10.17	7.85	0.41
D/S of GB2	3	25.00	1949.21	1952.23		1952.42	0.011405	1.92	13.03	8.45	0.49
D/S of GB2	3	50.00	1949.21	1952.92		1953.25	0.016388	2.55	19.61	11.36	0.62
D/S of GB2	2	0.50	1949.84	1950.68		1950.68	0.000828	0.26	1.96	4.59	0.12
D/S of GB2	2	2.00	1949.84	1950.95		1950.97	0.002903	0.61	3.28	5.19	0.24
D/S of GB2	2	8.00	1949.84	1951.50		1951.57	0.007779	1.21	6.59	7.75	0.42
D/S of GB2	2	15.00	1949.84	1951.83		1951.95	0.011081	1.57	9.54	10.05	0.51
D/S of GB2	2	25.00	1949.84	1952.20		1952.37	0.011516	1.85	13.52	11.47	0.54
D/S of GB2	2	50.00	1949.84	1952.93		1953.18	0.010428	2.19	22.88	13.88	0.54
D/S of GB2	1	0.50	1950.19	1950.64	1950.57	1950.67	0.029005	0.81	0.62	3.64	0.63
D/S of GB2	1	2.00	1950.19	1950.86	1950.78	1950.94	0.028990	1.25	1.61	4.89	0.69
D/S of GB2	1	8.00	1950.19	1951.35	1951.21	1951.51	0.029026	1.79	4.48	7.86	0.76
D/S of GB2	1	15.00	1950.19	1951.63	1951.50	1951.87	0.029003	2.20	6.81	8.64	0.79
D/S of GB2	1	25.00	1950.19	1951.93	1951.79	1952.28	0.029018	2.62	9.54	9.10	0.82
D/S of GB2	1	50.00	1950.19	1952.54	1952.34	1953.08	0.029006	3.27	15.30	10.17	0.85

Details for Cross-Section No. 02 – Reach (1)

Plan: Malewa2GB1 River: Malewa Reach:D/S of GB2 Riv Sta: 2 Profile: PF 1

			Left OB	Channel	Right OB
E.G. Elev (m)	1950.68	Element			
Vel Head (m)	0.00	Wt. n-Val.		0.060	
W.S. Elev (m)	1950.68	Reach Len. (m)	4.00	4.00	4.00
Crit W.S. (m)		Flow Area (m2)		1.96	
E.G. Slope (m/m)	0.000828	Area (m2)		1.96	
Q Total (m3/s)	0.50	Flow (m3/s)		0.50	
Top Width (m)	4.59	Top Width (m)		4.59	
Vel Total (m/s)	0.26	Avg. Vel. (m/s)		0.26	
Max Chl Dpth (m)	0.84	Hydr. Depth (m)		0.43	
Conv. Total (m3/s)	17.4	Conv. (m3/s)		17.4	
Length Wtd. (m)	4.00	Wetted Per. (m)		5.05	
Min Ch El (m)	1949.84	Shear (N/m2)		3.15	
Alpha	1.00	Stream Power (N/m s)		0.80	
Frctn Loss (m)	0.01	Cum Volume (1000 m3)		0.01	
C & E Loss (m)	0.00	Cum SA (1000 m2)		0.02	

APPENDIX 4.6

Malewa Reach (2) – Details of Calculations

HEC-RAS Plan: Reach 2 River: Malewa River Reach: Reach 2

Reach	River Sta	Q Total	Min Ch El	W.S. Elev	Crit W.S.	E.G. Elev	E.G. Slope	Vel Chnl	Flow Area	Top Width	Froude # Chl
		(m3/s)	(m)	(m)	(m)	(m)	(m/m)	(m/s)	(m2)	(m)	
Reach 2	5	1.00	1917.49	1918.01		1918.02	0.000237	0.24	4.22	10.99	0.12
Reach 2	5	8.00	1917.49	1918.42		1918.46	0.001506	0.87	9.19	13.49	0.34
Reach 2	5	12.00	1917.49	1918.54		1918.61	0.002110	1.10	10.87	14.37	0.41
Reach 2	5	18.00	1917.49	1918.69		1918.79	0.002796	1.37	13.09	15.37	0.48
Reach 2	5	25.00	1917.49	1918.84		1918.97	0.003365	1.62	15.45	16.28	0.53
Reach 2	5	50.00	1917.49	1919.26		1919.51	0.004417	2.19	22.79	18.55	0.63
Reach 2	4	1.00	1917.77	1917.97		1918.00	0.012738	0.80	1.25	10.61	0.74
Reach 2	4	8.00	1917.77	1918.36		1918.43	0.006022	1.21	6.62	17.10	0.62
Reach 2	4	12.00	1917.77	1918.47		1918.57	0.005960	1.40	8.56	17.45	0.64
Reach 2	4	18.00	1917.77	1918.61		1918.75	0.005848	1.62	11.12	17.90	0.66
Reach 2	4	25.00	1917.77	1918.76		1918.93	0.005721	1.81	13.80	18.36	0.67
Reach 2	4	50.00	1917.77	1919.20		1919.46	0.005352	2.27	22.06	19.69	0.68
Reach 2	3	1.00	1917.40	1917.84		1917.86	0.005129	0.71	1.41	7.01	0.50
Reach 2	3	8.00	1917.40	1918.31		1918.37	0.004970	1.09	7.31	18.53	0.56
Reach 2	3	12.00	1917.40	1918.42		1918.51	0.004866	1.27	9.44	18.76	0.57
Reach 2	3	18.00	1917.40	1918.57		1918.68	0.004713	1.47	12.27	19.07	0.58
Reach 2	3	25.00	1917.40	1918.73		1918.86	0.004594	1.65	15.19	19.38	0.59
Reach 2	3	50.00	1917.40	1919.17		1919.39	0.004363	2.08	24.08	20.65	0.61
Reach 2	2	1.00	1917.23	1917.80		1917.82	0.002471	0.58	1.72	6.67	0.36
Reach 2	2	8.00	1917.23	1918.21		1918.28	0.007248	1.18	6.78	20.37	0.65
Reach 2	2	12.00	1917.23	1918.32		1918.41	0.006573	1.34	8.96	20.56	0.65
Reach 2	2	18.00	1917.23	1918.46		1918.57	0.005969	1.52	11.84	20.82	0.64
Reach 2	2	25.00	1917.23	1918.60		1918.74	0.005513	1.68	14.87	21.05	0.64
Reach 2	2	50.00	1917.23	1919.04		1919.26	0.004608	2.06	24.24	21.66	0.62
Reach 2	1	1.00	1917.40	1917.68	1917.68	1917.75	0.020616	1.18	0.85	5.67	0.97
Reach 2	1	8.00	1917.40	1917.98	1917.98	1918.13	0.017787	1.71	4.69	16.03	1.01
Reach 2	1	12.00	1917.40	1918.07	1918.07	1918.26	0.016612	1.96	6.14	16.19	1.01
Reach 2	1	18.00	1917.40	1918.19	1918.19	1918.44	0.015119	2.22	8.11	16.41	1.01
Reach 2	1	25.00	1917.40	1918.31	1918.31	1918.62	0.014191	2.46	10.15	16.63	1.01
Reach 2	1	50.00	1917.40	1918.68	1918.68	1919.15	0.012563	3.06	16.31	17.29	1.01

Details for Cross Section No. 01-Reach (2)

Plan: Reach 2 River: Malewa River Reach:Reach 2 Riv Sta: 1 Profile: PF 1

			Left OB	Channel	Right OB
E.G. Elev (m)	1917.75	Element			
Vel Head (m)	0.07	Wt. n-Val.		0.034	
W.S. Elev (m)	1917.68	Reach Len. (m)			
Crit W.S. (m)	1917.68	Flow Area (m2)		0.85	
E.G. Slope (m/m)	0.020616	Area (m2)		0.85	
Q Total (m3/s)	1.00	Flow (m3/s)		1.00	
Top Width (m)	5.67	Top Width (m)		5.67	
Vel Total (m/s)	1.18	Avg. Vel. (m/s)		1.18	
Max Chl Dpth (m)	0.28	Hydr. Depth (m)		0.15	
Conv. Total (m3/s)	7.0	Conv. (m3/s)		7.0	
Length Wtd. (m)		Wetted Per. (m)		5.74	
Min Ch El (m)	1917.40	Shear (N/m2)		29.86	
Alpha	1.00	Stream Power (N/m s)		35.23	
Frctn Loss (m)		Cum Volume (1000 m3)			
C & E Loss (m)		Cum SA (1000 m2)			

APPENDIX 4.7

Malewa –Reach (4) – Close to the Lake at Italian Premises

HEC-RAS Plan: Plan 01 River: Malewa Reach: Reach_4

Reach	River Sta	Q Total	Min Ch El	W.S. Elev	Crit W.S.	E.G. Elev	E.G. Slope	Vel Chnl	Flow Area	Top Width	Froude # Chl
		(m3/s)	(m)	(m)	(m)	(m)	(m/m)	(m/s)	(m2)	(m)	
Reach_4	5	1.00	1896.43	1897.00		1897.00	0.000245	0.19	5.15	14.64	0.10
Reach_4	5	2.00	1896.43	1897.09		1897.09	0.000460	0.31	6.53	14.97	0.15
Reach_4	5	5.80	1896.43	1897.31		1897.33	0.001002	0.58	9.97	15.40	0.23
Reach_4	5	10.00	1896.43	1897.52		1897.54	0.001254	0.76	13.08	15.65	0.27
Reach_4	5	15.00	1896.43	1897.72		1897.76	0.001430	0.92	16.24	15.90	0.29
Reach_4	5	20.00	1896.43	1897.88		1897.94	0.001571	1.06	18.93	16.05	0.31
Reach_4	5	50.00	1896.43	1898.61		1898.75	0.002182	1.63	30.73	16.31	0.38
Reach_4	4	1.00	1896.61	1896.99		1896.99	0.001627	0.34	2.94	14.98	0.24
Reach_4	4	2.00	1896.61	1897.07		1897.08	0.001968	0.47	4.27	15.47	0.28
Reach_4	4	5.80	1896.61	1897.29		1897.32	0.002545	0.76	7.61	15.78	0.35
Reach_4	4	10.00	1896.61	1897.48		1897.53	0.002499	0.93	10.71	15.90	0.36
Reach_4	4	15.00	1896.61	1897.68		1897.74	0.002464	1.08	13.85	16.01	0.37
Reach_4	4	20.00	1896.61	1897.84		1897.92	0.002506	1.21	16.51	16.10	0.38
Reach_4	4	50.00	1896.61	1898.56		1898.72	0.002948	1.78	28.16	16.50	0.43
Reach_4	3	1.00	1896.65	1896.88	1896.88	1896.93	0.035669	1.02	0.98	9.66	1.02
Reach_4	3	2.00	1896.65	1896.94	1896.94	1897.01	0.032188	1.16	1.72	12.79	1.01
Reach_4	3	5.80	1896.65	1897.19		1897.26	0.008835	1.16	4.98	13.83	0.62
Reach_4	3	10.00	1896.65	1897.39		1897.47	0.006259	1.27	7.86	14.25	0.55
Reach_4	3	15.00	1896.65	1897.59		1897.69	0.005403	1.40	10.72	14.65	0.52
Reach_4	3	20.00	1896.65	1897.75		1897.87	0.005203	1.52	13.12	14.97	0.52
Reach_4	3	50.00	1896.65	1898.44		1898.66	0.005515	2.09	23.90	16.37	0.55
Reach_4	2	1.00	1896.37	1896.78		1896.79	0.002222	0.40	2.49	12.47	0.29
Reach_4	2	2.00	1896.37	1896.89		1896.90	0.002282	0.52	3.82	13.04	0.31
Reach_4	2	5.80	1896.37	1897.15		1897.18	0.002334	0.78	7.43	13.86	0.34
Reach_4	2	10.00	1896.37	1897.36		1897.41	0.002401	0.97	10.33	13.98	0.36
Reach_4	2	15.00	1896.37	1897.56		1897.63	0.002533	1.14	13.11	14.09	0.38
Reach_4	2	20.00	1896.37	1897.72		1897.80	0.002730	1.30	15.37	14.18	0.40
Reach_4	2	50.00	1896.37	1898.38		1898.59	0.003819	2.01	24.93	14.55	0.49
Reach_4	1	1.00	1896.41	1896.68	1896.68	1896.75	0.032026	1.13	0.89	6.92	1.01
Reach_4	1	2.00	1896.41	1896.76	1896.76	1896.85	0.028467	1.36	1.47	7.85	1.01
Reach_4	1	5.80	1896.41	1896.95	1896.95	1897.13	0.023824	1.87	3.10	8.99	1.02
Reach_4	1	10.00	1896.41	1897.12	1897.12	1897.35	0.020926	2.15	4.64	9.85	1.00
Reach_4	1	15.00	1896.41	1897.28	1897.28	1897.57	0.019620	2.36	6.35	11.13	1.00
Reach_4	1	20.00	1896.41	1897.41	1897.41	1897.74	0.019233	2.55	7.84	12.00	1.01

APPENDIX 4.8

Gilgil Reach (01)

HEC-RAS Plan: Reach1 River: Gilgil River Reach: Reach1

Reach	River Sta	Q Total	Min Ch El	W.S. Elev	Crit W.S.	E.G. Elev	E.G. Slope	Vel Chnl	Flow Area	Top Width	Froude # Chl
		(m3/s)	(m)	(m)	(m)	(m)	(m/m)	(m/s)	(m2)	(m)	
Reach1	4	0.10	1961.82	1961.92	1961.92	1961.95	0.015825	0.78	0.13	2.09	1.00
Reach1	4	0.40	1961.82	1962.07		1962.10	0.004719	0.85	0.47	2.65	0.64
Reach1	4	0.75	1961.82	1962.20		1962.24	0.002897	0.87	0.86	3.16	0.54
Reach1	4	2.00	1961.82	1962.49		1962.54	0.002153	1.04	1.93	4.30	0.49
Reach1	4	10.00	1961.82	1963.15		1963.34	0.003200	1.93	5.18	5.56	0.64
Reach1	4	15.00	1961.82	1963.34		1963.63	0.004191	2.39	6.26	5.82	0.74
Reach1	4	20.00	1961.82	1963.54		1963.90	0.004556	2.67	7.49	6.28	0.77
Reach1	3	0.10	1961.59	1961.66	1961.66	1961.69	0.016403	0.75	0.13	2.31	1.00
Reach1	3	0.40	1961.59	1961.87		1961.88	0.001465	0.55	0.72	3.04	0.36
Reach1	3	0.75	1961.59	1961.95		1961.98	0.002019	0.76	0.98	3.13	0.44
Reach1	3	2.00	1961.59	1962.10		1962.20	0.004266	1.36	1.47	3.29	0.65
Reach1	3	10.00	1961.59	1962.64	1962.64	1963.08	0.009569	2.95	3.39	3.86	1.01
Reach1	3	15.00	1961.59	1962.96	1962.96	1963.48	0.009213	3.20	4.68	4.49	1.00
Reach1	3	20.00	1961.59	1963.27	1963.27	1963.78	0.008416	3.19	6.27	5.97	0.99
Reach1	2	0.10	1961.32	1961.66		1961.66	0.000041	0.10	1.04	4.54	0.06
Reach1	2	0.40	1961.32	1961.87		1961.87	0.000081	0.18	2.17	5.70	0.10
Reach1	2	0.75	1961.32	1961.96		1961.97	0.000151	0.28	2.69	5.99	0.13
Reach1	2	2.00	1961.32	1962.14		1962.15	0.000400	0.53	3.78	6.56	0.22
Reach1	2	10.00	1961.32	1962.70		1962.78	0.001159	1.25	7.98	8.06	0.40
Reach1	2	15.00	1961.32	1962.94		1963.05	0.001374	1.51	9.92	8.39	0.44
Reach1	2	20.00	1961.32	1963.10		1963.26	0.001661	1.77	11.33	8.62	0.49
Reach1	1	0.10	1961.35	1961.58	1961.58	1961.64	0.015546	1.07	0.09	0.80	1.01
Reach1	1	0.40	1961.35	1961.76	1961.76	1961.86	0.012900	1.42	0.28	1.39	1.01
Reach1	1	0.75	1961.35	1961.88	1961.88	1961.95	0.012940	1.19	0.63	4.39	1.01
Reach1	1	2.00	1961.35	1962.01	1962.01	1962.12	0.010735	1.47	1.36	6.05	0.99
Reach1	1	10.00	1961.35	1962.44	1962.44	1962.73	0.008288	2.40	4.16	7.07	1.00
Reach1	1	15.00	1961.35	1962.64	1962.64	1963.00	0.007743	2.66	5.64	7.74	0.99
Reach1	1	20.00	1961.35	1962.82	1962.82	1963.21	0.007750	2.74	7.29	9.57	1.00

APPENDIX 4.9

Gilgil River Reach (02)

HEC-RAS Plan: Plan 01 River: Gilgil River Reach: Reach 2

Reach	River Sta	Q Total	Min Ch El	W.S. Elev	Crit W.S.	E.G. Elev	E.G. Slope	Vel Chnl	Flow Area	Top Width	Froude # Chl
		(m3/s)	(m)	(m)	(m)	(m)	(m/m)	(m/s)	(m2)	(m)	
Reach 2	5	0.10	1921.86	1921.99		1922.00	0.001168	0.31	0.32	4.24	0.35
Reach 2	5	0.46	1921.86	1922.08		1922.10	0.001995	0.65	0.72	4.45	0.52
Reach 2	5	0.80	1921.86	1922.13		1922.17	0.002573	0.86	0.93	4.56	0.61
Reach 2	5	2.00	1921.86	1922.24		1922.34	0.004059	1.38	1.45	4.81	0.80
Reach 2	5	4.00	1921.86	1922.35	1922.35	1922.55	0.005918	1.99	2.01	5.07	1.01
Reach 2	5	5.00	1921.86	1922.42	1922.42	1922.65	0.005695	2.11	2.37	5.23	1.00
Reach 2	5	12.00	1921.86	1922.79	1922.79	1923.16	0.005147	2.70	4.44	6.06	1.01
Reach 2	4	0.10	1921.76	1921.98		1921.99	0.000687	0.25	0.39	4.54	0.27
Reach 2	4	0.46	1921.76	1922.07	1922.00	1922.08	0.001543	0.55	0.84	5.39	0.45
Reach 2	4	0.80	1921.76	1922.11	1922.04	1922.14	0.001995	0.74	1.09	5.50	0.53
Reach 2	4	2.00	1921.76	1922.22		1922.29	0.002993	1.17	1.71	5.78	0.68
Reach 2	4	4.00	1921.76	1922.33		1922.48	0.004731	1.73	2.31	6.03	0.89
Reach 2	4	5.00	1921.76	1922.35	1922.35	1922.56	0.006009	2.02	2.47	6.10	1.01
Reach 2	4	12.00	1921.76	1922.69	1922.69	1923.03	0.005222	2.58	4.65	6.93	1.01
Reach 2	3	0.10	1921.86	1921.97		1921.98	0.000748	0.23	0.43	6.07	0.28
Reach 2	3	0.46	1921.86	1922.05		1922.06	0.001355	0.48	0.98	7.37	0.42
Reach 2	3	0.80	1921.86	1922.10		1922.12	0.001546	0.61	1.32	7.55	0.47
Reach 2	3	2.00	1921.86	1922.22		1922.26	0.001800	0.89	2.24	8.03	0.54
Reach 2	3	4.00	1921.86	1922.34		1922.42	0.002199	1.22	3.28	8.54	0.63
Reach 2	3	5.00	1921.86	1922.38		1922.48	0.002520	1.38	3.63	8.70	0.68
Reach 2	3	12.00	1921.86	1922.60	1922.57	1922.82	0.004574	2.09	5.75	11.55	0.94
Reach 2	2	0.10	1921.90	1921.96		1921.96	0.003435	0.36	0.27	6.35	0.55
Reach 2	2	0.46	1921.90	1922.02		1922.04	0.004296	0.69	0.67	6.84	0.71
Reach 2	2	0.80	1921.90	1922.05		1922.09	0.005240	0.90	0.89	7.11	0.81
Reach 2	2	2.00	1921.90	1922.13	1922.13	1922.22	0.006888	1.36	1.47	7.76	1.00
Reach 2	2	4.00	1921.90	1922.25	1922.25	1922.38	0.006296	1.61	2.49	9.53	1.01
Reach 2	2	5.00	1921.90	1922.30	1922.30	1922.44	0.006088	1.66	3.00	10.67	1.00
Reach 2	2	12.00	1921.90	1922.62		1922.76	0.002866	1.67	7.18	14.32	0.75
Reach 2	1	0.10	1921.81	1921.88	1921.88	1921.90	0.012490	0.59	0.17	4.94	1.01
Reach 2	1	0.46	1921.81	1921.94	1921.94	1921.98	0.009377	0.84	0.56	7.73	0.99
Reach 2	1	0.80	1921.81	1921.98	1921.98	1922.02	0.008565	0.98	0.82	8.38	1.00
Reach 2	1	2.00	1921.81	1922.06	1922.06	1922.15	0.007474	1.33	1.50	8.70	1.02
Reach 2	1	4.00	1921.81	1922.16	1922.16	1922.30	0.006393	1.64	2.44	9.13	1.01
Reach 2	1	5.00	1921.81	1922.21	1922.21	1922.36	0.006044	1.75	2.86	9.31	1.01

APPENDIX 5.1

Past Records of Suspended Sediment Measurements - Malewa 2GB01

Note: Sediment Data obtained from the original file " RIVER DATA"

Relevent discharge data obtained from the Mr. Data daily flows

Date	Sediment Load ppm	Discharge m3/sec	Date	Sediment Load ppm	Discharge m3/sec
6-Feb-1956	36	3.86	5-May-52	204.8	9.87
13-Feb-56	17.8	2.28	6-May-52	315.5	11.85
20-Feb-56	343.2	7.27	12-May-52	293.7	25.81
27-Feb-56	58.2	2.8	14-May-52	137.2	22.45
3-Mar-56	32.7	1.96	14-May-52	145.1	22.45
12-Mar-56	18.3	1.52	15-May-52	158.7	20.78
19-Mar-56	23.9	1.52	15-May-52	120.7	20.78
26-Mar-56	22.7	1.26	15-May-52	317.5	20.78
9-Apr-56	20.8	1.66	16-May-52	184.1	19.1
16-Apr-56	19.2	2.45	16-May-52	165.7	19.1
7-May-56	279.6	19.77	23-May-52	179.9	9.35
14-May-56	83.9	9.96	23-May-52	169.5	9.35
21-May-56	163.5	17.39	23-May-52	166.1	9.35
28-May-56	92.7	10.59	24-May-52	109.1	7.06
4-Jun-56	91.5	5.92	26-May-52	35.7	5.48
11-Jun-56	63.6	3.75	26-May-52	68.1	5.48
18-Jun-56	35.5	2.62	27-May-52	75.7	5.42
25-Jun-56	78.5	7.61	27-May-52	112	5.42
16-Jul-56	63.7	4.39	27-May-52	109.6	5.42
3-Sep-56	125.4	28.94	25-Jun-53	68.3	2.12
10-Sep-56	95.5	24.66	25-Jul-53	16.3	1.01
17-Sep-56	83.1	13.27	27-Jul-53	12.8	1.01
24-Sep-56	57.7	7.33	21-Sep-53	20.7	1.66
1-Oct-56	173.5	19.83	28-Sep-53	17.5	1.01
8-Oct-56	112.8	21.53	5-Oct-53	7.6	0.9
15-Oct-56	567.6	11.57	12-Oct-53	37.2	1.01
22-Oct-56	54.2	8.46	19-Oct-53	31.11	2.98
28-Jan-57	50.5	10.82	26-Oct-53	23.6	2.62
4-Feb-57	23.9	3.55	2-Nov-53	27.4	4.17
11-Feb-57	23.4	2.12	9-Nov-53	13.4	1.81
18-Feb-57	20	1.13	16-Nov-53	22.4	2.45
11-Jul-57	281.1	14.71	14-Dec-53	18.2	2
22-Apr-49	39.7	4.61	11-Jan-54	9.6	0.79
27-Apr-49	83.8	3.36	18-Jan-54	6.6	0.69
26-May-49	44.8	1.66	25-Jan-54	6.8	0.69
8-Jun-49	101.9	8.75	1-Feb-54	6	0.69
17-Jun-49	102.1	1.96	2-Feb-54	6.5	0.69
15-Jul-49	109.1	4.39	8-Feb-54	4.6	0.6

Date	Sediment Load ppm	Discharge m3/sec
16-Aug-49	66.8	3.75
19-Aug-49	47.8	6.54
31-Aug-49	39.5	17.13
4-Sep-49	35.4	14.71
8-Sep-49	19.8	9.05
20-Sep-49	91.7	14.35
27-Sep-49	20.9	8.46
26-Oct-49	21.3	1.96
17-Nov-49	20.8	2.45
1-Dec-49	16.5	1.52
12-Dec-49	23.8	1.39
28-Dec-49	20.8	2.28
26-Jan-50	7.8	1.26
10-Mar-50	2.5	1.13
11-Mar-50	7.8	1.13
24-Mar-50	3.2	1.81
29-Mar-50	6.3	1.26
12-Apr-50	26.2	1.52
13-Apr-50	19.5	2.8
14-Apr-50	60.4	3.75
15-Apr-50	73.7	3.96
18-Apr-50	280.4	6
20-Apr-50	33.9	4.39
22-Apr-50	58.4	2.8
1-May-50	45.1	1.66
3-May-50	59	1.66
5-May-50	34.6	1.39
11-May-50	63	1.81
12-May-50	44.2	1.66
16-May-50	20.2	1.81
19-May-50	37.3	2.12
2-Jun-50	64.6	1.52
8-Jun-50	55.6	1.81
14-Jun-50	61.3	2.12
17-Jun-50	134.3	4.61
23-Jun-50	151.4	4.39
27-Jun-50	120.6	2.62

Date	Sediment Load ppm	Discharge m3/sec
15-Feb-54	9.8	0.6
1-Mar-54	8.9	0.6
8-Mar-54	7.8	0.6
15-Mar-54	5.9	0.6
22-Mar-54	5.2	0.6
5-Apr-54	54.2	1.13
12-Apr-54	44.3	2.8
26-Apr-54	18.1	1.52
29-Apr-54	4.5	1.66
3-May-54	75.3	1.94
8-May-54	4.6	2.28
10-May-54	187.5	4.85
17-May-54	773.5	16.84
24-May-54	113.1	26.79
31-May-54	70.9	36.73
7-Jun-54	303.8	46.68
21-Jun-54	59.8	19.09
28-Jun-54	43.8	5.06
28-Jun-54	34.5	5.06
5-Jul-54	59.6	10.27
12-Jul-54	78.2	10.91
19-Jul-54	50.7	6.28
26-Jul-54	259.7	11.56
2-Aug-54	177.9	13.3
9-Aug-54	38.2	7.18
16-Aug-54	59.2	10.91
23-Aug-54	359.7	12.53
30-Aug-54	47.3	11.57
6-Sep-54	80.7	8.46
13-Sep-54	164.7	16.22
20-Sep-54	35.3	7.89
27-Sep-54	55.1	7.33
4-Oct-54	112.5	13.99
11-Oct-54	24.8	4.61
18-Oct-54	21.1	3.36
25-Oct-54	38.5	3.96
1-Nov-54	44.6	5.06

Contd.. Appendix 5.1

Date	Sediment Load ppm	Discharge m3/sec	Date	Sediment Load ppm	Discharge m3/sec
15-Jul-50	289.1	10.27	8-Nov-54	25.7	3.16
20-Jul-50	165.9	13.27	15-Nov-54	25.4	2.45
2-Aug-50	249.6	15.08	22-Nov-54	16.3	2.12
18-Aug-50	1168.4	19.41	29-Nov-54	13.1	2.28
28-Aug-50	151.5	13.7	6-Dec-54	21.9	5.06
29-Aug-50	428.6	16.17	13-Dec-54	25.3	2.28
6-Sep-50	1502.5	15.84	14-Dec-54	18.2	2.12
13-Sep-50	97.5	8.47	20-Dec-54	11.1	1.96
18-Sep-50	149.9	11.77	21-Dec-54	8.3	1.96
22-Sep-50	119.8	15.46	3-Jan-55	30.7	1.66
3-Oct-50	62.4	4.17	10-Jan-55	36.1	1.13
12-Oct-50	74.7	3.36	17-Jan-55	29	1.13
14-Oct-50	41.4	2.8	24-Jan-55	37	1.13
18-Nov-50	30.2	2.8	31-Jan-55	26	0.9
12-Dec-50	27.7	1.52	7-Feb-55	40.7	1.66
14-Dec-50	19.8	1.39	14-Feb-55	51	1.39
8-Jan-51	34	0.9	21-Feb-55	31.3	0.9
16-Jan-51	6.6	0.9	28-Feb-55	33.5	1.81
7-Feb-51	37	0.79	2-Mar-55	41.1	1.81
13-Feb-51	26	0.69	7-Mar-55	42.7	1.01
20-Feb-51	42.5	0.79	14-Mar-55	33.7	0.79
27-Feb-51	54	0.69	28-Mar-55	33.4	0.9
12-Mar-51	34.3	0.79	4-Apr-55	33.1	0.9
13-Mar-51	33.9	0.9	11-Apr-55	32.8	1.52
15-Mar-51	1.06	1.39	18-Apr-55	68.6	3.16
26-Mar-51	16	1.26	25-Apr-55	49.5	3.75
2-Apr-51	28.5	2.98	16-May-55	75.5	2.45
5-Apr-51	41	3.76	30-May-55	44.2	1.66
9-Apr-51	260.3	6.91	13-Jun-55	26.7	0.9
11-Apr-51	73.6	8.74	20-Jun-55	25	1.13
13-Apr-51	209.9	10.12	29-Aug-55	143.6	17.78
14-Apr-51	38.3	10.58	5-Sep-55	132.5	17.39
16-Apr-51	1609.5	11.51	19-Dec-55	83.1	8.22
19-Apr-51	218.9	12.9	2-Jan-56	253.6	20.67
24-Apr-51	603.2	15.23	9-Jan-56	60.2	4.17
25-Apr-51	289.7	15.69	16-Jan-56	33.3	2.62
25-Apr-51	267.6	15.69	23-Jan-56	59.1	7.06
27-Apr-51	274.9	16.62	30-Jan-56	70.4	10.59
2-May-51	196.5	18.95	2-Apr-48	6.2	0.69
3-May-51	186.6	19.41	20-Mar-49	25.2	0.69
23-Jun-51	42.1	5.78	14-Apr-49	45.6	1.26
2-May-52	211.9	6.36	17-Apr-49	52.3	2.45

APPENDIX 5.2

SEDIMENT RATING CURVE IN VIAK REPORT, MALEWA

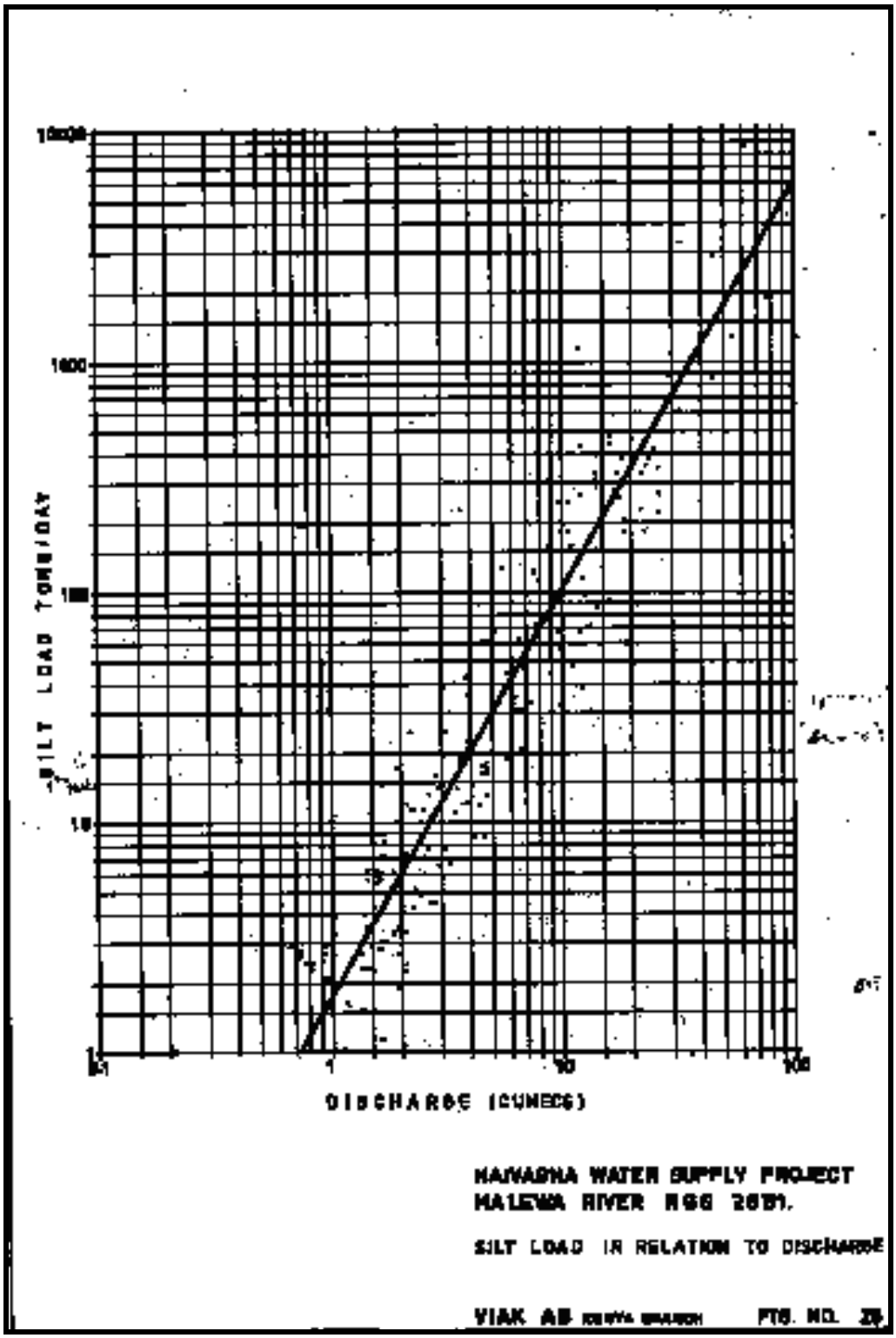

APPENDIX 5.3

Fortran Program Used to Compute Equations 2.13 to 2.16 (Ref: webserver.cr.usgs.gov)

```
C     This program computes the bias corrected load using MVUE
C
      INTEGER I
      REAL A,AA,ARG,B,QBAR,QSAVE,QSTAR,QVAR,S2,TEMP,UE,V,XM,XN
      WRITE(*,*)'This program reads the daily discharges from a file
     #called MVUE.IN'
      WRITE(*,*)'and writes the bias corrected loads to a file called
     #MVUE.OUT.'
      WRITE(*,*)'     The discharges in MVUE.IN can be in any format
     # but must be in the'
      WRITE(*,*)'first column.'
      WRITE(*,*)' '
      WRITE(*,*)'Enter a 1 to continue or any letter to quit. '
      READ(*,'(I5)',ERR=99)I
      IF(I.NE.1)GO TO 99
      OPEN (15,FILE='MVUE.IN',STATUS='OLD')
      OPEN (16,FILE='MVUE.OUT')
C  INPUT VARIABLES
C     XN   = Number of data pairs
C     QBAR = Mean of ln Q
C     QVAR = Sum of ((LN Q - LN Q MEAN)**2)
C     XM   = Number of degrees of freedom of residuals
C     S2   = Mean square error
C     A    = Exponentiated intercept of sediment load - discharge
C            relation
C     B    = Slope of sediment load - discharge relation
      XN = 7.
      QBAR = 3.7390
      QVAR = 3.45225
      XM = 5.
      S2 = 0.3465
      A = 0.020
      B = 2.76
C     Enter updated data
      WRITE(16,*)'Output of the MVUE program'
      WRITE(*,*)'Default (Number of data pairs) XN = ',XN
      WRITE(*,*)'Enter n to select default or enter new value- '
      READ(*,'(F9.0)',ERR=10)AA
      XN=AA
   10 WRITE(16,*)'  XN   (Number of data pairs)              = ',XN
      WRITE(*,*)'Default (Mean of ln Q) QBAR = ',QBAR
```

```
      WRITE(*,*)'Enter n to select default or enter new value- '
      READ(*,'(F9.0)',ERR=11)AA
      QBAR=AA
   11 WRITE(16,*)'  QBAR (Mean of ln Q)                    = ',QBAR
      WRITE(*,*)'Default [Sum of ((LN Q - LN Q MEAN)**2)] QVAR
     # = `, QVAR
      WRITE(*,*)'Enter n to select default or enter new value- '
      READ(*,'(F9.0)',ERR=12)AA
      QVAR=AA
   12 WRITE(16,*)'  QVAR [Sum of ((LN Q - LN Q MEAN)**2)]    = ',QVAR
      WRITE(*,*)'Default (No of degrees of freedom) XM = ',XM
      WRITE(*,*)'Enter n to select default or enter new value- '
      READ(*,'(F9.0)',ERR=13)AA
      XM=AA
   13 WRITE(16,*)'  XM   (No of degrees of freedom)         = ',XM
      WRITE(*,*)'Default (Mean square error) S2 = ',S2
      WRITE(*,*)'Enter n to select default or enter new value- '
      READ(*,'(F9.0)',ERR=14)AA
      S2=AA
   14 WRITE(16,*)'  S2   (Mean square error)               = ',S2
      WRITE(*,*)'Default (Intercept of Qs-Q relation) A = ',A
      WRITE(*,*)'Enter n to select default or enter new value- '
      READ(*,'(F9.0)',ERR=15)AA
      A=AA
   15 WRITE(16,*)'  A    (Intercept of Qs-Q relation)       = ',A
      WRITE(*,*)'Default (Slope of Qs-Q relation) B = ',B
      WRITE(*,*)'Enter n to select default or enter new value- '
      READ(*,'(F9.0)',ERR=16)AA
      B=AA
   16 WRITE(16,*)'  B    (Slope of Qs-Q relation)           = ',B
      QAVE=0.0
C  *********************
C  READ QSTAR (DISCHARGES AT WHICH LOADS ARE PREDICTED)
      WRITE(16,*)' '
      WRITE(16,*)' Obs  Daily      V eq 5     Arguement       gm
     #  L mvue'
      WRITE(16,*)' '
      I=0
   20 READ(15,*,END=30) QSTAR
        V=(1./XN + (((LOG(QSTAR)-QBAR)**2)/QVAR))
        ARG=((XM+1)/(2.*XM))*((1.- V)*S2)
        TEMP = GM(XM,ARG)
        UE=(A*(QSTAR**B))*TEMP
        I=I+1
```

```
      QAVE=QAVE+UE
      WRITE(16,901) I,QSTAR,V,ARG,TEMP,UE
  901 FORMAT(I5,G12.4,3G12.5,F12.0)
    GO TO 20
   30 CONTINUE
    WRITE(16,900)QAVE
  900 FORMAT(43X,'Total',3X,F14.0)
   99 CONTINUE
    END
    FUNCTION GM(XM,ARG)
C  ********
C    FUNCTION TO COMPUTE FINNEY'S GM(T)
C
C    AUTHOR.....TIM COHN
C    DATE.....OCTOBER 1, 1986
C
C    XM    R*4    NUMBER OF DEGREES OF FREEDOM OF RESIDUALS
C    ARG   R*4    ARGUMENT TO FINNEY'S FUNCTION
C
    DATA TOL/1.E-7/
    IF (ABS(ARG) .GT. 50.0) THEN
      PRINT *,' MAGNITUDE OF ARG IS TOO LARGE (GM)'
      GM = 0.0
      RETURN
    ENDIF
      GM = 1.0
      IF(XM .LE. 0.0) RETURN
      BT = ARG*XM**2/(2.0*(XM+1.0))
      TERM = 1.0
    DO 10 P=1,1000
      TERM = TERM * BT/((XM/2.0+P-1.0)*P)
      GM = GM+TERM
      IF(P .GT. 1.0 .AND. ABS(TERM) .LT. TOL) RETURN
   10 CONTINUE
       PRINT *, 'GM DID NOT CONVERGE'
       RETURN
    END
```

APPENDIX 5.4

SAMPLE CALCULATION SHEET FOR MVUE METHOD OF BIAS CORRECTION METHOD IN FORTRAN PROGRAM

Output of the MVUE program

XN	(Number of data pairs)	= 234.000000
QBAR	(Mean of ln Q)	= 1.335000
QVAR	[Sum of ((LN Q - LN Q MEAN)**2)]	= 280.418000
XM	(No of degrees of freedom)	= 232.000000
S2	(Mean square error)	= 5.961350E-01
A	(Intercept of Qs-Q relation)	= 1.446000
B	(Slope of Qs-Q relation)	= 1.808200

Obs	Daily	V eq 5	Arguement	gm	L mvue
1	1.390	.78804E-02	.29699	1.3436	4.
2	1.390	.78804E-02	.29699	1.3436	4.
3	1.260	.86191E-02	.29677	1.3433	3.
4	1.130	.95187E-02	.29650	1.3429	2.
5	1.130	.95187E-02	.29650	1.3429	2.
6	1.130	.95187E-02	.29650	1.3429	2.
7	1.130	.95187E-02	.29650	1.3429	2.
8	1.010	.10535E-01	.29620	1.3425	2.
9	1.010	.10535E-01	.29620	1.3425	2.
10	1.030	.10351E-01	.29625	1.3426	2.
11	1.050	.10173E-01	.29631	1.3427	2.
12	1.060	.10086E-01	.29633	1.3427	2.
13	1.080	.99174E-02	.29638	1.3428	2.
14	1.100	.97540E-02	.29643	1.3428	2.
15	1.120	.95958E-02	.29648	1.3429	2.
16	1.130	.95187E-02	.29650	1.3429	2.
17	1.260	.86191E-02	.29677	1.3433	3.
18	1.260	.86191E-02	.29677	1.3433	3.
19	1.390	.78804E-02	.29699	1.3436	4.
20	1.520	.72676E-02	.29718	1.3438	4.
21	1.520	.72676E-02	.29718	1.3438	4.
22	1.520	.72676E-02	.29718	1.3438	4.
23	1.520	.72676E-02	.29718	1.3438	4.
24	1.390	.78804E-02	.29699	1.3436	4.
25	1.390	.78804E-02	.29699	1.3436	4.
26	1.260	.86191E-02	.29677	1.3433	3.
27	1.260	.86191E-02	.29677	1.3433	3.
28	1.260	.86191E-02	.29677	1.3433	3.
29	1.130	.95187E-02	.29650	1.3429	2.
30	1.260	.86191E-02	.29677	1.3433	3.
31	1.260	.86191E-02	.29677	1.3433	3.
32	1.260	.86191E-02	.29677	1.3433	3.
33	1.260	.86191E-02	.29677	1.3433	3.
34	1.260	.86191E-02	.29677	1.3433	3.
35	1.260	.86191E-02	.29677	1.3433	3.

APPENDIX 5.5

SUMMARY OF SEDIMENT LOADS AFTER BIAS CORRECTIONS

Year	Annual Discharge (m^3/sec)	Sediment Load (Rating Curve)	Load after Bias Correction (metric tons)		
			QMLE	SE	MVUE
1932	1945	17084	23016	23000	22942
1933	1835	20026	26980	26962	22943
1934	2513	60514	81527	81471	80860
1935	1389	8198	11045	11037	11019
1936	2069	18451	24858	24841	24776
1937	3153	45432	61209	61167	60911
1938	993	4414	5947	5943	5935
1939	607	1902	2563	2561	2557
1940	1428	15547	20946	20931	20842
1941	1773	13809	18605	18592	18553
1942	1842	18285	24634	24618	24546
1943	925	5546	7472	7467	7453
1944	939	4993	6726	6722	6711
1945	1419	12407	16715	16704	16655
1946	1638	15179	20450	20436	20378
1947	2843	37736	50840	50805	50605
1948	1524	12680	17083	17071	17027
1949	1483	12157	16379	16368	16328
1950	1516	12914	17398	17387	17340
1951	3074	46112	62124	62082	61760
1952	1486	11617	15651	15641	15601
1953	617	1672	2252	2250	2247
1954	2874	50241	67688	67641	67255
1955	1818	17819	24006	23990	23919
1956	3471	46867	63142	63099	62856
1957	2568	31159	41979	41950	41794
1958	3316	63017	84900	84841	84230
1959	1559	11352	15294	15283	15250
1960	1249	7619	10265	10258	10239
1961	4424	181544	244585	244417	241577
1962	3878	85597	115321	115242	114328
1963	3684	100912	135953	135860	134606
1964	3780	65968	88875	88815	88343
1965	1015	5258	7084	7079	7066
1966	1976	24832	33455	33432	33294
1967	2421	37172	50079	50045	49754

1968	3844	94948	127919	127832	126649
1969	776	3704	4991	4987	4976
1970	2599	30897	41626	41597	41448
1971	2735	44622	60116	60075	59749
1972	1341	9643	12992	12983	12952
1973	1000	5224	7038	7033	7020
1974	2134	23083	31099	31078	30982
1975	2425	37776	50893	50858	50609
1976	1069	7943	10702	10694	10666
1977	3079	48196	64932	64888	64569
1978	3293	44632	60130	60089	59837
1979	2327	27041	36431	36407	36261
1980	1337	14215	19151	19138	19060
1981	3321	66316	89344	89283	88730
1982	1663	12921	17408	17396	17359
1983	2658	30803	41500	41471	41330
1984	613	2025	2728	2726	2721
1985	2185	20764	27974	27955	27883
1986	1582	18469	24883	24866	24729
1987	1101	5896	7943	7938	7923
1988	3783	77432	104320	104249	103550
1989	3381	54020	72778	72728	72344
1990	4039	85661	115407	115328	114512
Total 1932-1990		1892266	2549355	2547609	2528361
Annual Average		32072	43209	43180	42854
Total 1957-1990		1380662	1860097	1858822	1846341
Annual Average		41838	56367	56328	55950
Total 1957 - 2001		1840882	2480129	2478430	2461788
In million metric tons		**1.841**	**2.480**	**2.478**	**2.462**

APPENDIX *5.6*

LAKE NAIVASHA AREA AND VOLUME CALCULATIONS
COMPARISON OF 2001 AND 1957 SURVEYS

Contour	Bathymetric Survey 2001		Bathymetric Survey 1957		Difference between
(m)	Cum.Area(m2)	Cum Area (Km^2)	Cum.Area(m2)	Cum Area (Km^2)	1957-2001
1873	6269.9	0.01			
1874	126293.7	0.13	593850.0	0.59	0.468
1875	429936.0	0.43	883161.3	0.88	0.453
1876	845540.8	0.85	1048865.9	1.05	0.203
1877	1010349.6	1.01	1226214.6	1.23	0.216
1878	1133060.5	1.13	1357882.6	1.36	0.225
1879	1244127.3	1.24	1435808.6	1.44	0.192
1880	1346237.1	1.35	1554041.1	1.55	0.208
1881	1870221.6	1.87	1681230.7	1.68	-0.189
1882	29493642.7	29.49	30589094.1	30.59	1.095
1883	69560156.0	69.56	73579173.3	73.58	4.019
1884	89226148.0	89.23	94636215.1	94.64	5.410
1885	106671698.3	106.67	106696833.2	106.70	0.025
1886	121066494.1	121.07	116193953.8	116.19	-4.873
1886.67	126498102.0	126.50	119210675.7	119.21	-7.287

Contour	Bathymetric Survey 2001		Bathymetric Survey 1957		Cum.Difference bet
(m)	Cum. Volume(m^3)	Cum Volume(mcm)	Cum. Volume(m^3)	Cum Volume(mcm)	1957-2001
1873	910.93	0.00			
1874	52463.91	0.05	369028.93	0.369	0.317
1875	289330.33	0.29	1141840.01	1.142	0.853
1876	980346.85	0.98	2146906.43	2.147	1.167
1877	1920125.61	1.92	3314363.49	3.314	1.394
1878	2992940.18	2.99	4604173.35	4.604	1.611
1879	4184563.27	4.18	6012215.78	6.012	1.828
1880	5479980.22	5.48	7527831.93	7.528	2.048
1881	6920209.67	6.92	9137765.44	9.138	2.218
1882	19265355.14	19.27	23201977.54	23.202	3.937
1883	70357675.92	70.36	78747639.15	78.748	8.390
1884	150248684.93	150.25	165435670.3	165.436	15.187
1885	247518033.08	247.52	266832549.7	266.833	19.315
1886	363256064.71	363.26	379260080.1	379.260	16.004
1886.67	445946581.85	445.95	458338089.7	458.338	12.392

Volume of Sediment accumulation = 19.31 mcm

APPENDIX 5.7

Calculation of Dry Specific Weight of Sediment Deposits From Lane and Koelzer Formula (Julian, 1995)

Sample No.	Size Class	Fraction *Ap*	r_{md1} *(lb/ft3)*	$Ap*r_{md1}$ *(lb/ft3)*	K *(lb/ft3)*	r_{md44} *(lb/ft3)*	$Ap*r_{md44}$ *(lb/ft3)*
M-1	Sand	0.01	93	1.22	0.0	93.00	1.22
	Silt	0.25	65	16.45	5.7	74.37	18.82
	Clay	0.73	30	22.01	16.0	56.30	41.31
		After one year =		***39.68***		After 44 yrs.	***61.35***
S-1	Sand	0.07	93	6.28	0.0	93.00	6.28
	Silt	0.58	65	37.55	5.7	74.37	42.96
	Clay	0.35	30	10.65	16.0	56.30	19.98
		After one year =		54.48		After 44 yrs.	69.22
S-2	Sand	0.01	93	0.81	0.0	93.00	0.81
	Silt	0.39	65	25.37	5.7	74.37	29.03
	Clay	0.60	30	18.03	16.0	56.30	33.83
		After one year =		***44.21***		After 44 yrs.	***63.67***
S-3	Sand	0.13	93	12.49	0.0	93.00	12.49
	Silt	0.41	65	26.88	5.7	74.37	30.76
	Clay	0.45	30	13.56	16.0	56.30	25.45
		After one year =		***52.94***		After 44 yrs.	***68.70***
S-4	Sand	0.11	93	10.30	0.0	93.00	10.30
	Silt	0.51	65	33.30	5.7	74.37	38.10
	Clay	0.38	30	11.31	16.0	56.30	21.22
		After one year =		***54.90***		After 44 yrs.	***69.62***

Summary of Calculations - Lane & Koelzer Formula

Sample No.	ID	%Clay p_c	%Silt p_m	%Sand p_s	r_{md1} *(lb/ft3)*	Dry density after 44 years *(lb/ft3)*	*(Kg/m3)*
1	M-1	73.38	25.31	1.31	39.68	61.35	982.73
2	S-1	35.49	57.77	6.75	54.48	69.22	1108.80
3	S-2	60.10	39.03	0.87	44.21	63.67	1019.90
4	S-3	45.21	41.36	13.43	52.94	68.70	1100.47
5	S-4	37.70	51.23	11.07	54.90	69.62	1115.21

Note: ***62.4 lb/ft3 = 9810 N/m3***
1 lb/ft3 = 16.0185Kg/m3

APPENDIX 5.8

Calculation of Dry Specific Weight of Sediment Deposits
Ref: Millers Formula (Julian, 1995)

Sample No.	Size Class	Fraction *Ap*	r_{md1} *(lb/ft3)*	Ap*r_{md1} *(lb/ft3)*	K *(lb/ft3)*	r_{md44} *(lb/ft3)*	Ap*r_{md44} *(lb/ft3)*
M-1	Sand	0.01	93	1.22	0.0	93	1.2
	Silt	0.25	65	16.45	5.7	72	18.2
	Clay	0.73	30	22.01	16.0	50	36.5
		After one year =		**39.68**		**After 44 years =**	**55.97**
S-1	Sand	0.07	93	6.28	0.0	93	6.3
	Silt	0.58	65	37.55	5.7	72	41.6
	Clay	0.35	30	10.65	16.0	50	17.7
		After one year =		***54.48***		**After 44 years =**	***65.55***
S-2	Sand	0.01	93	0.81	0.0	93	0.8
	Silt	0.39	65	25.37	5.7	72	28.1
	Clay	0.60	30	18.03	16.0	50	29.9
		After one year =		***44.21***		**After 44 years =**	***58.83***
S-3	Sand	0.13	93	12.49	0.0	93	12.5
	Silt	0.41	65	26.88	5.7	72	29.8
	Clay	0.45	30	13.56	16.0	50	22.5
		After one year =		***52.94***		**After 44 years =**	***64.78***
S-4	Sand	0.11	93	10.30	0.0	93	10.3
	Silt	0.51	65	33.30	5.7	72	36.9
	Clay	0.38	30	11.31	16.0	50	18.8
		After one year =		***54.90***		**After 44 years =**	***65.96***

APPENDIX 5.9

Calculation of Dry Specific Weight of Sediment Deposits

Ref: Handbook of Hydrology by David R Maidment Formula

Sample No.	Size Class	Fraction *Ap*	*W (Kg/m3)*	W_0 (Kg/m3)	K_0	W_{T1} (kg/m3)
M-1	Sand	0.01	1550	20.31	0.0	20
	Silt	0.25	1120	283.47	91.0	396
	Clay	0.73	416	305.26	256.0	621
				After 44 years		***1038***
S-1	Sand	0.07	1550	104.63	0.0	105
	Silt	0.58	1120	647.02	91.0	759
	Clay	0.35	416	147.64	256.0	464
				After 44 years		***1328***
S-2	Sand	0.01	1550	13.49	0.0	13
	Silt	0.39	1120	437.14	91.0	550
	Clay	0.60	416	250.02	256.0	566
				After 44 years		***1129***
S-3	Sand	0.13	1550	208.17	0.0	208
	Silt	0.41	1120	463.23	91.0	576
	Clay	0.45	416	188.07	256.0	504
				After 44 years		***1288***
S-4	Sand	0.11	1550	171.59	0.0	172
	Silt	0.51	1120	573.78	91.0	686
	Clay	0.38	416	156.83	256.0	473
				After 44 years		***1331***